THE SILVER-OXYGEN SYSTEM AT ELEVATED PRESSURES AND TEMPERATURES

A Thesis

presented for the

Degree of Doctor of Philosophy

in the University of London

by

Mohammed Ishaq Talukdar

Nuffield Research Group in Extraction Metallurgy

Royal School of Mines

Imperial College of Science and Technology

London

June 1968

Abstract

The previous work on the silver-oxygen system from the thermodynamicists' view point, has been reviewed. The design consideration of high pressure equipment in general, and of that used here in particular, have been discussed.

Fusion points of silver and silver oxide subjected to oxygen pressures ranging from 0.2 to 750 atm. have been determined to derive the pressure-temperature relation for the silver-oxygen system. The eutectic point crresponding to

$$Ag(s) \rightleftharpoons \text{liq.} \rightleftharpoons Ag_2O(s)$$

is found to be at 530°C and 530 atm.

Compositions of the silver-oxygen melts have been measured thermogravimetrically along the silver liquidus and on the isotherms at 950° and 1050°C in the all liquid region in the pressure range 1 to 100 atm. The extrapolated oxygen content at the eutectic point is 0.22 atom fraction. A phase diagram for the silver-silver oxide system has been constructed. Thermodynamic quantities for the process,

$$\tfrac{1}{2}O_2(g) \rightleftharpoons \underline{O} \text{ (liq. silver)}$$

have been derived.

Electrical conductivities of solid silver oxide as a function of temperature and pressure have been studied.

The effect of varying proportions of alloyed gold on the fusion point of silver in equilibrium with oxygen has been studied. Compositions of the Au - Ag - O system were measured at 1050°C and in the pressure range 1 to 60 atm. to evaluate the effect of gold concentration on the solubility of oxygen in silver and to derive thermodynamic quantities for the process,

$$\tfrac{1}{2} O_2 (g) \rightleftharpoons \underline{O} \text{ (Au-Ag alloy)}.$$

Ancillary studies were made to examine the effect of nitrogen pressure on the melting point of silver, and oxygen pressure on the melting point of gold.

Acknowledgements

The author is indebted to professor F. D. Richardson, F.R.S., Director of the Nuffield Research Group in Extraction Metallurgy, for providing him the facilities to work in the group and also for helpful advice and comments during the course of this study.

The author expresses his sincere gratitude to Dr. E.H. Baker whose unfailing interest in the project and constant guidance have been the sources of inspiration for the author throughout this work.

He thanks Professor C. B. Alcock, Dr. B. C. H. Steele, Dr. P. S. Rogers and Dr. G. R. Belton (Dept. of Metallurgy, University of Pennsylvania) for instructive discussions. Thanks are also due to Dr. D. A. Pantony and Mr. S. D. Brooks(Dept. of Mineral Technology) for permitting to use their Stanton Automatic Thermobalance and to Mrs. Ann Forster and Mr. Alan Forster, his colleague, for reading the manuscript of this thesis. He also acknowledges various help and cooperation of his other research colleagues and members of the research and technical staff of the group.

Finally the author thanks the Association of Commonwealth Universities for awarding him a scholarship, the British Council for their hospitality and the U.K. Science Research Council for additional finance.

Contents Page

Contents Page

Contents Page

Contents Page

CHAPTER I

INTRODUCTION

1. HISTORICAL BACKGROUND OF HIGH PRESSURE WORK

The earliest high pressure work may perhaps be attributed to the Florentine Academy who, in the early 18th century, attempted to find if water was compressible. Later experiments were carried out by Canton[1]. In 1762, he published experiments to prove that water is not incompressible. Hall[2] carried out a large number of experiments over a period of several years on the melting and crystallization of calcium carbonate under high pressure in order to verify Hutton's assumption that rocks exist in a fused state in the earth's interior and published his results in 1812. Perkins[3], using a cannon as the containing vessel, reached a pressure of 2000 kg/cm^2 in 1819. Amagat[4] started his sytematic work on the compressibilities of gases in 1869.

Work aimed at the synthesis of diamond has always attracted the imagination of men and can be said to have started as early as 1888 when Parsons[5,6] began his experiments on carbon at high temperatures and high pressures. Tammann[7] who moved in the field of high pressures after the termination of Amagat's activities in 1893, made an extensive study of solids under pressure, including the effect of pressures on the transition temperature of solids. Many other properties of materials such as the electrical resistance, thermoelectric power, viscosity, refractive index etc. were studied under pressures by these early workers.

The above examples were chosen to illustrate the manifold activities the early workers initiated in the field of high pressure.

Inheriting such a widely set stage for high pressure activities, the later workers were confronted with the task of developing correspondingly diverse techniques for carrying out fruitful investigations. The individual who proved himself up to this immense task was Professor P.W. Bridgman of Harvard University. Working relentlessly from 1906 to 1961, Bridgman[8] contributed to almost all the above mentioned branches of high pressure activities and carried the field of high pressure research to what it is to-day. His book, "The Physics of High Pressure", first published in 1931 (Bell and Sons, London), is considered to be a classic in the field. Starting with an extensive historical survey of the early high pressure researchers, the book covers the various aspects of high pressure activities and illustrates many novel high pressure techniques.

During the same period, many other researchers worked in the various high pressure research centres all over the world. By 1955, high pressure research reached its exciting peak when Bundy, Hall, Strong and Wentorf had their brilliant success in producing diamonds from graphite in a laboratory device. Other achievements in this field during the last six decades or so have enabled men to synthesize rocks and minerals in the laboratory and to have a better understanding of the geochemical structure of the earth's interior. Mechanical, thermal, electrical and optical properties of solids under pressures up to ca. 10^6 bars have also received extensive study[9]. These and many other developments in the field of high pressure research have been surveyed by Bradley[10] and published in the book titled "High

Pressure Physics and Chemistry". "In this book", to quote Bradley, the editor, "a group of international workers have combined to write a comprehensive and advanced study covering most major aspects of this field and including both theoretical and experimental work and static and dynamic pressures". In the concluding section of his article Bradley has also listed a number of leading books, review articles and symposia in the field of high pressure research.

Comparatively recent high pressure work, particularly in the field of metallurgy, constituted the proceedings of a symposium held at Dallas, Texas in February 1963 and has been published under the title, "Metallurgy at High Pressures and High Temperatures" [11]. Another recent publication in the field covering mostly the work in the field of polymer chemistry is due to Weale[12].

2. NOTE ON THE TITLE

The present work may not belong to the categories of the usual high pressure topics. However, high pressure did come into the picture as a means of introducing more and more oxygen into liquid silver and increasing the stability range of silver oxide. It was only by subjecting silver and silver oxide under high pressure oxygen (maximum pressure 750 atm.) that it was possible to study the system over the desired wide range of compositions (1-22 atom per cent of oxygen). This entailed the use of relevant high pressure techniques and equipment and this is what the title is intended to reflect.

3. A SURVEY OF PREVIOUS WORK ON THE SOLUBILITY OF OXYGEN IN COPPER, SILVER AND GOLD

The interaction of oxygen with some metals has been extensively studied in connection with the study of iron and steel making processes [13,14,15]. But relatively few studies of its interactions with noble metals such as copper, silver and gold - particularly, with reference to its solubility in these metals, have been made. The following statement of Smithells[16] accounts for such a situation

"Oxygen is soluble to some extent in most metals, an oxide phase also appears when the limit of solubility is exceeded. The solid solubility of oxygen in the common metals is usually considered as small in comparison with the total amount of oxygen which may be present in the metal. Many molten metals are capable of dissolving large quantities of oxygen (or of their oxides, which amounts to the same thing), but on freezing, the excess oxygen is precipitated as oxide. The solubility of oxygen in the solid metals is of the same order as that of hydrogen. It is, however, much more difficult to determine accurately".

A. Copper-Oxygen System

i) The Solubility of Oxygen in the Solid

The measurement of solid solubility of oxygen in copper was first attempted by Hanson, Marrayat and Ford[17] who placed the limit at less than 0.008 per cent oxygen at 1000° C. Vogel and Pocher[18] presented

microscopic evidence of the solid solubility and gave a saturation value of 0.08 per cent of oxygen at 950° C. Allen and Street[19] quoted the solubility limit as 0.005 per cent oxygen at 500° C. Rhines and Mathewson[20] determined the solubility of oxygen in copper between 600° C and 1050° C. Phillips and Skinner[21] also determined the solubility in the same temperature range, but used samples of copper from different sources. Both sets of solubility data are quoted below for comparison.

Table 1

Solubility of Oxygen in Copper

Rhines and Mathewson			Phillips and Skinner	
t° C	cm³/100 g.	wt.%	t° C	wt.%
600	5.0	0.0071	700	0.0022
800	6.6	0.0091	850	0.0025-0.0029
950	7.0	0.0100	900	0.0027-0.0035
1050	10.9	0.0156	1000	0.0044-0.0055
			1050	0.0072-0.0077

The difference between the two sets of data is attributed to the difficulties in experimental determination of small amounts of oxygen.

Clasing and Sauerwald[22] tried to determine oxygen solubility in copper in a different way. They pretreated sheet copper in hydrogen at 700°, embedded it with cupric oxide and then heated it at 375°. The cupric oxide decomposed into cuprous oxide and oxygen, the latter

saturating the copper metal. The absorbed oxygen was then determined by reducing the treated copper with hydrogen at 900° and weighing the H_2O formed. Their solubilities are: 0.0030% and 0.0091% at 600 and 900° C, respectively.

ii) The Solubility of Oxygen in the Liquid

The earliest investigations of the copper-oxygen system in the liquid range are due to Lucas[23] and Chevillot[24]. Lucas believed that liquid copper is capable of dissolving its oxide, but neither he nor Chevillot was able to furnish convincing proof of this property. Graham[25] definitely established the existence of such a solubility. Hamp[26] measured its extent and roughly outlined the copper-rich portion of the system. Heyn[27] published a temperature-composition diagram covering the range from 0 to 10 per cent cuprous oxide at atmospheric pressure. Within these limits of composition cuprous oxide was found to dissolve in 'liquid copper forming at 3.4 to 3.5 per cent, an entectic which melted at 1065° C. Slade and Farrow[28] extended these studies to mixtures of higher oxygen content. They observed that between 20 and 95 per cent of cuprous oxide, the metal oxide forms two liquid phases at a monotectic reaction temperature of 1195° C. Investigations by Roberts and Smith[29] and Vogel and Pocher supported the above results, but the latter authors placed the monotectic reaction temperature at 1200° C, with the concentration of two liquid layers at 1.5 and 10.2 per cent oxygen respectively.

Rhines and Mathewson presented a graphic summary of the results obtained by various investigators with the help of a copper-oxygen

equilibrium diagram. They also presented a provisional pressure-temperature diagram of the system copper-cuprous oxide; the dissociation pressure of cuprous oxide calculated by Sockdale[30] and data of Randall, Neilsen and West[31] were used for drawing the diagram. The temperature composition diagram is reproduced below.

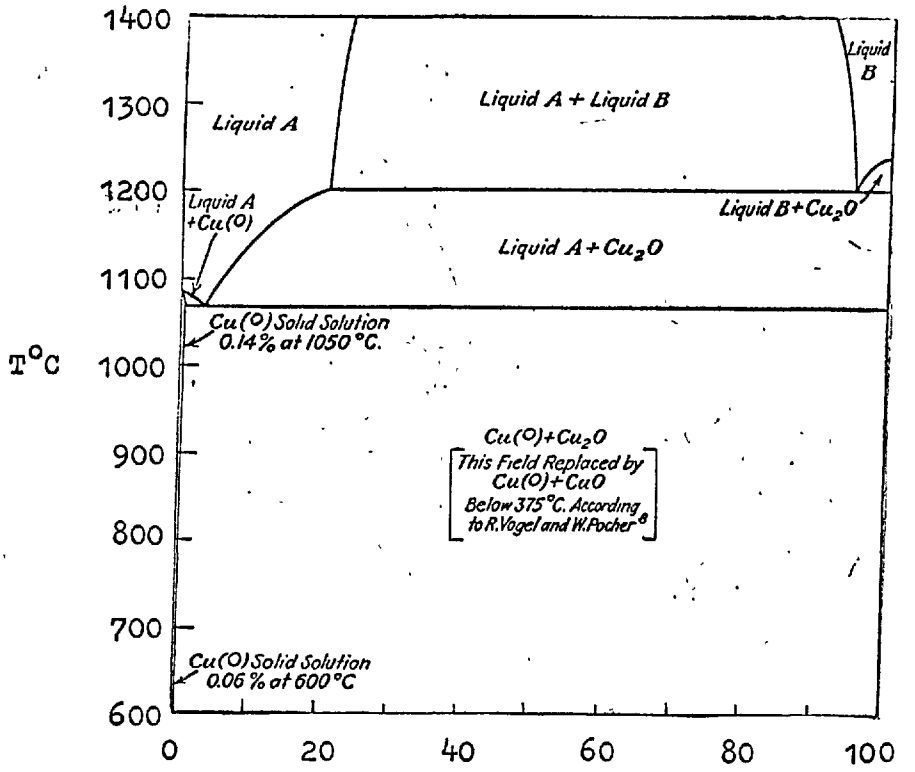

Fig.1. Copper-cuprous oxide constitutional diagram. (After Rhines and Mathewson).

By means of gas mixtures designed to give low oxygen potentials, the solubility of oxygen in molten copper has been studied in the low oxygen concentration range: Girardi and Siebert, (1090° -1300° C)[32],

Sano and Sakao (1115°-1256°)[33,34] and Tomlinson and Young (1085°-1500°)[35] have equilibrated liquid copper with CO/CO_2 gas mixtures. Toop (1300°-1600°)[36] levitated small copper beads in a stream of CO/CO_2 gas mixtures. Hofman and Schneider (1120°)[37] and Belton and Tankins[38] used H_2/H_2O gas mixtures in their equilibrium experiments. The results of all these authors are in reasonably good agreement with the exception of those of Girardi and Siebert which are lower and probably could be attributed to the loss of a significant amount of oxygen before being analysed, due to the quenching technique used.

Studies of Tomlinson and Young (and others) using CO/CO_2 gas mixtures were based on the reaction,

$$CO + \underline{O} = CO_2$$

for which the equilibrium constant K is given by

$$K = \frac{P_{CO_2}}{P_{CO} \times \text{atom \% } \underline{O} \times f_O}$$

where f_O is the activity coefficient of dissolved oxygen $\underline{O}$ and is based on the infinitely dilute solution as the standard state.

From their experimental results, Tomlinson and Young found that the liquid copper in the copper-rich end deviates positively from Raoult's law and that log f_o is independent of temperature and can be represented by the following relation:

$$\log f_O = -0.041 \text{ atom \% } \underline{O}$$

The standard free energy change for the reaction,

$$\tfrac{1}{2}O_2\ (g) = \underline{O}\ \text{(in liquid copper)}$$

is given by the relation,

$$\Delta G^0 = -46,440 + 18.6\,T \pm 150 \text{ cals.}$$

B. Silver-Oxygen System

The early silversmith observed that after silver had been melted in air and allowed to solidify, vigorous evolution of a gas took place with the accompaniment of severe "spitting" of the silver. He even used the degree of "spitting" as a rough measure of the purity of the silver. Another important phenomenon, which probably caused considerable trouble to the smith, was what he called "fire stain" [39]. Faced with the problem of improving the strength of the silver without loss of colour or ductility, the smith alloyed small quantities of copper with the silver. However he found that when such an alloy was heated in the air during working, it was left with some dull stains which were difficult to remove.

It is now well known that silver is unique, amongst metals, in its behaviour towards oxygen. Large quantities of oxygen dissolve readily in molten silver and most of it is expelled during solidification, causing the "spitting". Oxygen moves with great rapidity in silver, its rate of migration being very roughly equivalent to an apparent bulk diffusion coefficient as high as 10^{-3} to 10^{-4} cm^2/sec. As a result, when a sheet of the silver-copper alloy is annealed in the air, a large quantity of oxygen diffuses into the hot sheet and

copper is oxidized, both on and under the surface. Whilst the oxide on the surface can easily be dealt with by pickling in dilute acid, that below the surface remains as a dull stain.

"Spitting" and "fire stain", therefore, can easily be explained away in the light of the present knowledge. Nevertheless, these two phenomena are probably the earliest observations of the interaction of oxygen with silver.

i) The Solubility of Oxygen in the Solid

Following Dumas[40] observation in 1878 that silver, which has been melted in air, does not release all of its oxygen on solidification, several investigators subsequently studied the solubility of oxygen in solid silver. The solubility was shown to be proportional to the square root of oxygen pressure. Among the earlier publications, that of Steacie and Johnson[41] has been the subject of considerable discussion. This is because, their four isobaric solubility-temperature plots showed solubility minima at 400° C. Steacie and Johnson accounted for these minima on the assumption that, below 400° C the dissolved oxygen exists in the form of Ag_2O and above this temperature, as oxygen atoms, since Ag_2O dissociates. Simons[42] also has put forward similar views and suggested that the minimum is due to a balance between (1) increase in solubility of Ag_2O with increase in temperature and (2) increase in dissociation pressure of the oxide with increase in temperature.

Domanski[43] made a thermodynamic analysis of oxygen solubility in solid silver on the basis of the experimental data of Steacie and

Johnson. After discussing the three possible modes of the solubility of gases in metal, namely, dissolution in molecular form, in atomic form or through chemical combination, he indicated the possibility of oxygen dissolving in solid silver to give the chemical compound Ag_2O. On the basis of thermochemical data and taking into account the great quantitative superiority of silver over the dissolved oxygen, he ruled out the possiblity of Ag_2O_2 formation as well as the existence of free oxygen atoms not combined with the metal. He put forward a linear relation for the logarithm of the activity coefficient of Ag_2O:

$$\ln f_{Ag_2O} = b + mT$$

where f_{Ag_2O} is pressure-independent.

Eichenauer and Müller[44], while studying the diffusion of oxygen in solid silver proposed that surface adsorption might have been responsible for the solubility anomaly reported by Steacie and Johnson. Podgurski and Davies[45] studied the solid solubility of oxygen in silver and the thermodynamics of the internal oxidation of a silver-copper alloy. They particularly considered the solubility anomaly reported by Steacie and Johnson and concluded that the oxidation of trace impurities, like Cu present in the sample, were responsible for the solubility anomaly. In their view, Steacie and Johnson started with a dilute Ag-Cu alloy partially saturated with oxygen and that the reported degassing pretreatment of the silver sample at 500° C could not possibly remove all the oxygen associated with copper; at 800° C however, this oxygen could be removed from the dilute alloys.

Studies on the effects of oxygen on the grain-growth restraint in silver by Chaston[46] and Klein and Huggins[47] also support the above views.

Solubility relations advanced by various workers are given below.

a) Steacie and Johnson,

$$\log N_O = -1.03 - \frac{2650}{T} + \tfrac{1}{2} \log p,$$

where, N_O = atom fraction of oxygen

p = pressure of oxygen in atm.

b) Simons,

$$\log Z = 0.0034\ (t - 300),$$

where, Z = g. of Ag_2O per 1000g Ag

and t = ^0C.

c) Eichenauer and Müller,

$$\log S = -0.597 - \frac{2593}{T} + \tfrac{1}{2} \log p,$$

where, S = solubility of oxygen in cubic cm. (stp) per g. Ag and p is in torr.

d) Podgurski and Davies,

$$\log S = -0.840 - \frac{2250}{T} + \tfrac{1}{2} \log p,$$

where, S = solubility of oxygen in cu.cm. and p is in torr.

ii) <u>The Silver-Silver Oxide Equilibrium</u>

The solid reaction, $Ag_2O(s) = 2Ag(s) + \frac{1}{2} O_2$, has been extensively studied. As early as 1887, Le Chatelier[48]

showed that the dissociation of Ag_2O into Ag and O_2 was reversible. The pressure-temperature relationship for the reaction was studied by Lewis[49], Keyes and Hara[50], Benton and Drake[51] and Otto[52]. Lewis obtained three equilibrium points in the temperature range 302°-445° C, corresponding to equilibrium pressures of 20.5- 207 atm. Keyes and Hara determined six equilibrium values in the temperature range 374°-500° C, corresponding to the pressure range 74.3-388.3 atm. Combining their results with those of Lewis, Keyes and Hara gave an equation for dissociation pressure as,

$$\log p_{atm} = -\frac{2859}{T} + 6.2853.$$

Benton and Drake studied the reaction in the temperature range 173° - 191° C corresponding to pressure range 422 to 790 mm. Otto studied the reaction in the temperature range 171° -281° C corresponding to pressures 0.596 to 13.33 atm. Taking all these data into account, Otto computed several equations relating the dissociation pressure and temperature. From all the available thermal data, he also calculated the standard enthalpy and entropy of formation of the oxide. These are given in Table 2

Table 2

Standard Enthalpy and Entropy of Formation of Silver Oxide.

$$\Delta H^0_{298} = -7.35 \text{ kcal}$$

$$\Delta S^0_{298} = -15.96 \text{ cals.}$$

iii) The Solubility of Oxygen in the Liquid

Studies on the solubility of oxygen in molten silver may be traced back to Chevillot[53], who in 1820 found that 8 g. of molten silver saturated with air gave up 7.8 cc of oxygen on solidifying, and to Gay-Lussac[54], who in 1830 found that 1 vol. of molten silver evolved 22 volumes of oxygen on solidification. Accurate investigations probably started with the classical studies of Sieverts and Hagenacker[55] and Donnan and Shaw[56]. Sieverts and Hagenacker established that the solubility of oxygen in molten silver was proportional to the square root of pressure. Consequently it has been also established that oxygen dissolves in liquid silver in atomic form and the solution process can be represented by the following equation:

$$\tfrac{1}{2}\, O_2\,(g) \quad = [O]_{Ag(l)}$$

whence

$$K = {}^{N_O}/_{p^{\frac{1}{2}}}$$

where, N_O is the atom fraction of dissolved oxygen, p is the pressure of oxygen in the gas phase and K is the equilibrium constant. Their solubility measurements at 1 atm. oxygen pressure and at different temperatures are reproduced in Table 3.

Table 3

Solubility of Oxygen at 1 atm. in Molten Silver

t^0 C	973	1024	1075	1125
mg O/100 g.Ag	305	295	277	264
c.c. O_2/100 g. Ag	213.5	205.6	193.9	184.9
Atom fraction, N_O	0.02015	0.01942	0.01833	0.01750
Vol. O_2 : Vol. Ag	22.4	21.5	20.4	19.4
N_O. O atom/10^4 Ag atom	206	199	187	178

Donnan and Shaw, on the other hand, deliberated on the nature of the solute species in the solution, e.g., whether the oxygen dissolves atomically in the solution or in the form of Ag_2O. They showed that at low concentrations of oxygen, either picture will give a proportionality with the square root of oxygen pressure. They tended to believe that oxygen dissolved in molten silver exists as silver monoxide, Ag_2O. The following paragraph is quoted from their paper to present their conclusion.

"It is interesting to compare the solubility of oxygen in molten copper, silver and gold. In the case of copper the solid oxide Cu_2O can separate from the solution since the dissociation pressure of Cu_2O at the melting point of copper is quite low. In the case of silver, the solid phase Ag_2O cannot separate owing to its very great oxygen dissociation-pressure, although Ag_2O can probably exist in dilute solution in molten silver. Finally, in the case of gold, the affinity between this metal and oxygen has become so low that even a very dilute solution of oxide of gold in molten gold would correspond to an oxygen-pressure many times greater than that of the atmosphere."

Subsequent studies on the oxygen solubility in molten silver are due to Parlee and Sacris[57] and Diaz, Masson and Richardson[58]. The last authors in their study, int roduced an electrochemical cell of the type,

$$\text{stainless steel, Ag(l), } O_2\,(g,p') \,\big|\, ZrO_2 \cdot CaO \,\big|\, \text{Ag(l), } O_2\,(g,p=1 \text{ atm}) \text{ stainless steel,}$$

to measure the oxygen content in molten silver at various oxygen

pressure p'. The reversible e.m.f. of the cell is given by

$$E = \frac{RT}{4f} \ln \frac{N_O(1 \text{ atm})}{N_O(p'_{eq})}$$

where $N_O(1 \text{ atm})$ is the atom fraction of oxygen dissolved in the liquid silver of the reference half-cell under one atm. (barometric) oxygen pressure and $N_O(p'_{eq})$ is the equilibrium oxygen content of silver, in atom fraction, in the other half-cell under oxygen pressure p'. Solubilities obtained electrochemically agree well with those reported in the earlier publications and confirm that Sieverts' law is obeyed by dissolved oxygen up to at least 2 atom per cent; this composition corresponds to an oxygen pressure of about 1 atm. at 950° C.

In passing, it may be noted that the e.m.f. technique may be applied, in principle, to the study of silver-oxygen system at elevated pressure, but it may encounter some difficulties in practice. For example, it will be necessary to balance the pressures inside and outside of the lime-zirconia tube, which acts as the solid electrolyte, by introducing inert gas at high pressure in the reference electrode side, namely, 1 atm. oxygen pressure side. The difference in partial pressure may cause diffusion of gases which in turn may introduce uncertainty in the actual oxygen pressures. Besides, the electrochemical characteristics of the lime-zirconia tube, under elevated oxygen pressures, has not been established.

Diaz et al combined their data with those of other authors and derived the following equation:

$$\log \frac{N_O}{p^{\frac{1}{2}}} = \frac{737.6}{T} - 2.281$$

From this, the following heat and entropy for the process,

$$\tfrac{1}{2} O_2 (g) = \underline{O}_{Ag}$$

are obtained:

$$\Delta\bar{H} = -3380 \text{ cal per } \tfrac{1}{2} \text{ mole of } O_2$$

$$\Delta\bar{S} = -1.3 \text{ cal deg}^{-1} \text{ at 1 g. atom \%}$$

The standard free energy change is given by,

$$\Delta G^0 = -3380 + 10.44T \text{ cal.}$$

iv) The Solubility of Oxygen in Silver under Higher Oxygen Pressure

All the studies on oxygen solubility discussed so far were at pressure of 1 atm. or below. Studies at higher pressures have so far entailed measuring the freezing or melting point of silver as a function of oxygen pressure. The first study on the oxygen solubility in liquid silver at pressures above 1 atm. was done by Allen[59] in 1932. He measured the freezing points of silver up to a maximum pressure of 13.9 atm. by thermal arrest methods and represented the results by the equation,

$$T = 961 - 22.31\, p^{\frac{1}{2}}$$

where p is the pressure of oxygen in atm. This equation also shows that the depression of freezing point is approximately proportional to the $p^{\frac{1}{2}}$. Allen also pointed out that by extrapolation of the melting

point curve, the conditions under which molten silver can be in equilibrium with silver oxide could be found. For this he took Keyes and Hara's equation,

$$\log p = -\frac{2859}{T} + 6.285$$

for the reaction,

$$Ag_2O(s) = 2Ag(s) + \tfrac{1}{2} O_2(g)$$

and showed that it intersected with his extrapolated melting point curve at ca. 507^0 C and 414 atm. Allen, then suggested that the eutectic between the silver and silver oxide may be expected near this temperature.

On the basis of Allen's suggestion, Vacher[60] has put forward a tentative pressure-temperature diagram for the silver-oxygen system. Recently, Chaston[61] has reviewed the silver-oxygen system and suggested similar equilibrium diagrams. The equilibrium diagram suggested by Vacher is reproduced at page 28.

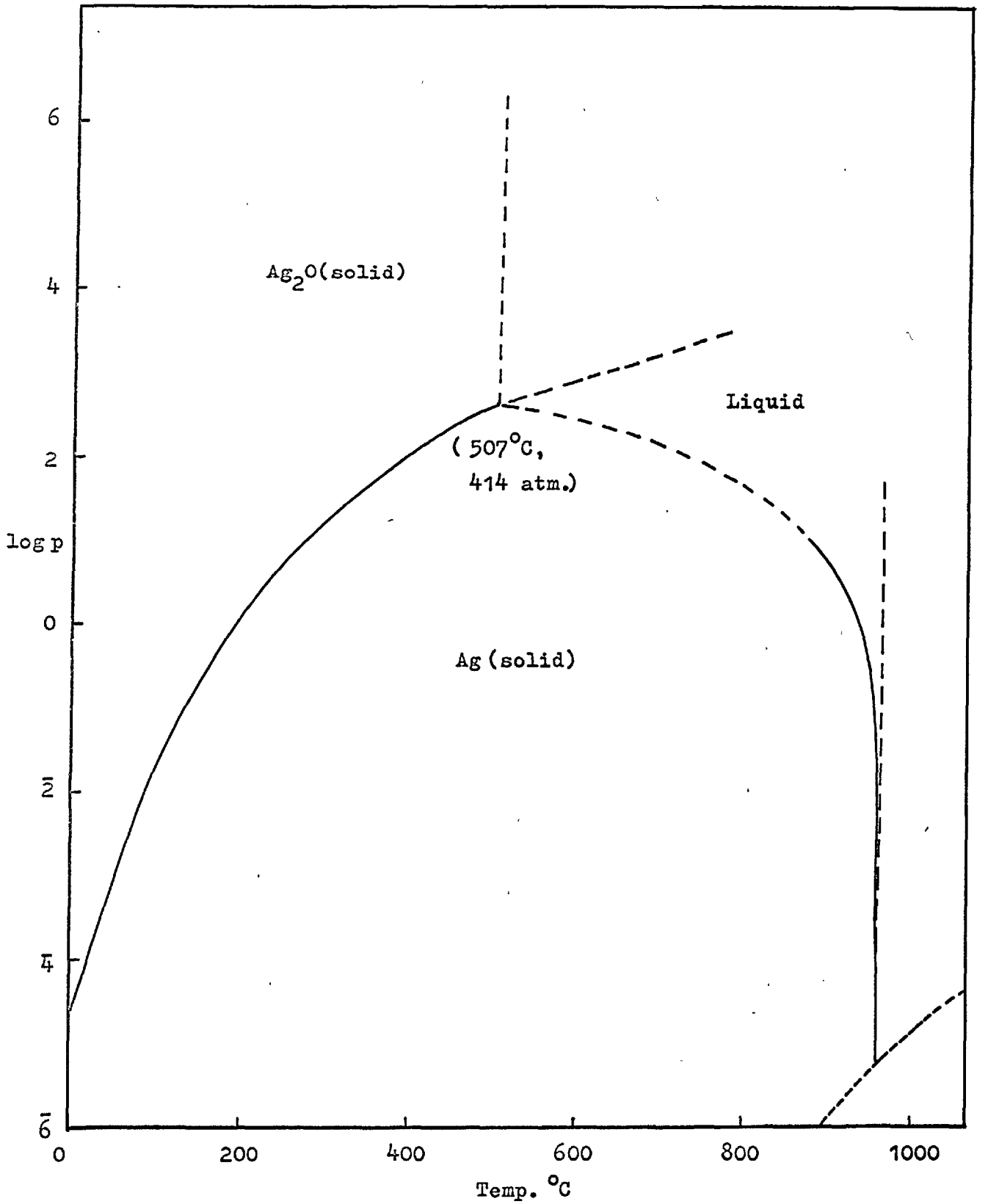

Fig. 2. Equilibrium diagram for Ag-Ag_2O system suggested by Vacher.

Baker and Johnstone[62] followed Allen and determined the melting point of silver under oxygen pressures up to 147.3 atm. Silver melts at 736° C under 147.3 atm. of oxygen pressure. This represents a melting point depression of 225° C and is indicative of high oxygen solubility. These authors pointed out that the freezing point depression versus square root of pressure plot showed linearity up to about 4 atm. only. In view of the fact that at higher pressures and corresponding higher oxygen concentrations, deviation from ideality is expected, this limit of linearity is quite reasonable.

Extrapolation of their fusion data, as would be expected, yields an approximate eutectic point near that given by Allen.

Gold-oxygen system : No data on the solubility of oxygen in gold have been reported.

4. SOME OF THE CONTRASTING FEATURES OF COPPER, SILVER AND GOLD.

The outer electronic configuration of copper, silver and gold may be represented as

np unoccupied

ns'

$(n-1)d^{10}$

where n equals, 4, 5 and 6 respectively. Apparently, it would be expected that the chemical behaviour of these elements would not be much divergent. But this expectation has not been borne out by facts. For example, while silver exhibits usually monovalency, copper exhibits both mono- and divalency, and gold exhibits relatively stable trivalency. This diversity in the chemistry of these elements has been explained away in terms of the varying degree of stability of the d electrons. This inherent diversity has been manifested in many instances. For example, if the solubility of these three elements in liquid iron is considered, it is seen that while both copper and gold are miscible with liquid iron, silver is completely immiscible. The solubility of oxygen in these elements provides another example of their contrasting behaviour. The solubility of oxygen in gold is too small to be measured. Both solid and liquid copper dissolve oxygen but to a limited extent. The copper-oxygen system shows a positive deviation from Raoult's Law in the liquid state; a miscibility gap exists. Liquid silver on the other hand dissolves a

large amount of oxygen and from the tremendous depression of the freezing point of silver due to the oxygen solubility, silver would hardly be expected to exhibit a positive deviation from Raoult's Law.

It is seen, therefore, that while the study of the phase equilibria and thermodynamics of the silver-oxygen system are important from the metallurgical point of view the difference in behaviour of silver from both copper and gold makes this study all the more interesting.

5. PROPOSED INVESTIGATION

In the present work, it has been proposed to conduct investigations broadly into the following aspects of silver-oxygen system:

(i) A study of the pressure-temperature relation for the silver oxygen system up to an oxygen pressure as high as possible and the establishment of the eutectic point for the system.

(ii) A study of the composition of the melt along the silver liquid and isothermally at 950° C and 1050° C and thus to obtain thermodynamic data such as activities, partial molal heats, and entropies.

(iii) A study of the effect of alloyed gold on the solubility of oxygen in silver.

CHAPTER II

Experimental Section 1

HIGH PRESSURE EQUIPMENT

1. GENERAL DESIGN CONSIDERATION OF HIGH PRESSURE EQUIPMENT

The following few pages are devoted to a brief discussion of some of the important aspects of high-pressure equipment and design consideration.

A. Materials of Construction

Plain carbon steels - both low and high carbon - may find high pressure applications at low temperatures (up to 400° C). A typical mild steel (low carbon steel) recommended to be used in the construction of gas cylinders for storage of liquifiable gases has the following chemical compositions and physical properties[63]

Chemical Composition:

Carbon	0.20-0.25 per cent
Manganese	0.45-0.75 per cent
Silicon	up to 0.2 per cent
Sulphur	up to 0.045 per cent
Phosphorus	up to 0.045 per cent

Physical Properties:

Yield point	Not less than 17 tons per sq. in.
Ultimate stress	28-33 tons per sq. in.
Elongation	Not less than 15%.

Higher carbon content causes an increase in tensile strength and decrease in ductility. In addition, high carbon steels are liable to unexpected variations in plasticity. And carbon steels in general

readily oxidize in air on heating and tend to undergo structural changes when kept for long periods over 400° C. As a result, alloy steels, such as nickel-chromium steels, are preferred to carbon steels for high-pressure equipment.

Addition of nickel improves the tensile properties of steel. For example, each one per cent addition of nickel (up to 5%) increases the tensile strength approximately 2-3 tons per sq. in. over that of the corresponding carbon steels. The addition of chromium increases the strength and hardness of steel without increasing the brittleness; it tends, however, to increase the susceptibility to brittleness on prolonged heating at high temperatures. The alloy steels are preferred also because of the fact that more uniform properties can be developed in them through heat treatment. The properties can be altered by adding different alloying elements in varying proportions. An alloy steel usually has a higher ratio of yield to ultimate tensile strength than is found with ordinary steels.

Nickel-chromium steels are suitable for laboratory experiments. While nickel appears to strengthen and toughen the ferrite matrix of the steel, chromium tends to toughen the carbide (cementite and pearlite) constituents. The optimum ratio of nickel to chromium is 2.5 to 1. The commercial high grade nickel-chromium steel contains 3.5 per cent nickel and 1.5 per cent chromium and low grade nickel-chromium steel contains 1.5 per cent nickel and 0.6 per cent chromium.

Other alloying elements such as titanium, vanadium, molybdenum and tungsten are also used in minor quantities in nickel-chromium steels.

Beside alloy steels, a number of other structural materials, known as "high duty" alloys are available in the market for the construction of very high-pressure equipment. These alloys have been marketed under various trade names such as "Monel", "Inconel", "Nimonic", "Rene 41"[64], "Carboloy" etc. Compositions of these alloys and some of their physical properties are listed in the appendix 2.

B. The Effect of Temperature upon the Properties of Carbon and Alloy Steel

Generally increase of temperature effects the elastic properties adversely and plastic properties favourably. Mild steel, for example, has a moderately high tensile strength and high ductility at room temperature; but it tends to become brittle at liquid air temperature and to lose most of its elastic strength when heated to about 500° C. Many stainless steels lose their corrosion resisting properties and undergo a coarsening of grain in the temperature range 500-850° C [65]. Besides an increase of temperature may help catalyse and accelerate the rate of some chemical reactions which have corrosive effects on the materials of construction. Carbon monoxide, for example, reacts with iron at elevated temperature and pressure to form the volatile iron carbonyls.

Furthermore, all metals exhibit the phenomenon of creep - the slow continuous distortion under constant load below that producing prompt fracture - at sufficiently high temperature; strength of the metals depends upon the time they are under stress, varying from a maximum

value approximately equal to the ultimate strength as given by the normal rate of loading, for short periods, to a minimum value approximately equal to the limiting creep stress, for a long period.

Another effect of temperature on the materials of construction is that it causes stresses to be set up in the walls of a vessel due to a temperature gradient. Comparatively large temperature gradients are established when the vessels are heated or cooled externally. When heat flow is from outside to inside, the effect of the temperature gradient alone is to decrease the hoop stress in the outer layers of the wall and increase it in the inner layers. The result is a higher hoop stress in the inside layers of the vessel under a given internal pressure than that without the temperature gradient and consequently a heavier wall must be used. When the heat transfer is from inside to the outside of the vessel, the reverse is the effect and consequently a thinner-walled vessel may be used.

Assuming a steady flow of heat through the walls, an expression may be derived for the temperature as a function of radius. Combining this expression with the usual stress-strain relation and the equations of equilibrium, expressions are obtained for the three principal stresses due to temperature. The expression for the tangential stress at the inside and outside surfaces are quoted below[67a]

$$S_{ti} = \frac{\alpha E \Delta t}{2(1-m)} \left(\frac{2K^2}{K^2-1} - \frac{1}{\ln K} \right) \qquad (1)$$

$$S_{to} = \frac{\alpha E \Delta t}{2(1-m)} \left(\frac{2}{K^2-1} - \frac{1}{\ln K} \right) \qquad (2)$$

where Δt is the temperature difference through the wall, α is the linear coefficient of expansion, K is the ratio of the outside to inside diameter, E is the efficiency of the weld or other joints (usually assumed to be equal to 1), m is the Poisson's ratio.

Equating the tangential stress at the inside with the yield strength, one may derive, in principle, an expression for the maximum temperature gradient a vessel can sustain without yielding at the bore from the expression (1). The expression is given by

$$\Delta t_y = \frac{(1-m)}{\alpha E} \cdot \sigma_y \cdot \left(\frac{K^2}{K^2-1} - \frac{1}{2 \ln K} \right)^{-1} \qquad (3)$$

For a medium sized pressure vessel the maximum permissible temperature gradient is about 150^0 C. It may be shown by approximate calculation that for a pressure vessel of 4 in. diameter and 1 in. wall thickness and with a furnace at 1000^0 C surrounded by refractory, the temperature gradient in the wall is 20^0 C. With this temperature gradient and with an internal pressure of 1000 atmospheres, the stress acting on the inner wall of the vessel is about 530 atmospheres which in effect doubles the safety factor.

C. Effect of Gaseous Atmosphere

The effects of reactive gases on the vessel wall are determined by pressure and temperature. Hydrogen for example, causes decarborization of steels, the rate increasing with the temperature and the partial pressure.

Oxygen, in the presence of moisture, tends to attack steels especially at high oxygen pressures and elevated temperatures. It is important, therefore, that dry oxygen be used in high pressure studies.

Alloying elements like chromium, nickel, vanadium, molybdenum and tungsten make steels more resistant to hydrogen and oxygen attack.

Nitrogen may combine with iron and with some of the other alloying elements in steels to form nitrides. Steels, therefore, are susceptible to nitrogen attack at elevated temperatures.

Carbon monoxide at high pressures and quite moderate temperatures attacks iron to form iron carbonyl, consequently, steel cylinders for carbon monoxide are often electroplated in the inside with copper.

Effects of various gases on metals have been extensively dealt with by Smithells[16].

D. Pressure Vessels and Yield Criteria

From the consideration of the properties of construction materials and from the theories of stress-strain distribution with a given geometry of structure various formulae relating the dimensions of the pressure vessel and properties of construction materials were put forward[66,67,67a]. In deriving these formulae the following assumptions were made:

(a) there is no temperature gradient in the walls of the vessel,

(b) the applied pressure is a static non-fluctuating one,

(c) there is no effect of scale, i.e., the stress depends on the ratio of the diameters rather than the diameter itself,

(d) the material is isotropic,

(e) there are no initial stresses in the material before the application of a pressure,

(f) temperatures are low enough so that creep can be neglected.

The following table reproduces some of the formulae relating the yield pressure, P, with the yield stress, f, of the wall material and the ratio K of the outer to inner diameter of the pressure vessel. In the case of thick-walled cylinders, substitution of the yield stress, f, by the ultimate tensile stress, is assumed to yield the bursting pressure in place of the yield pressure.

Table 4

Formulae of the Strength of Cylinders.[68]

Theory	Yield Pressure, P	Yield Pressure, P as $K \longrightarrow \infty$
1. Thin cylinders ($K < 1.20$)	$(K-1)f$	∞
Thick cylinders		
2. Maximum principal stress	$\frac{K^2-1}{K^2+1} f$	f
3. Maximum shear stress	$\frac{K^2-1}{2K^2} f$	$0.5f$
4. Maximum strain	$\frac{K^2-1}{1.25K^2+0.75} f$	$0.8f$
5. Maximum strain energy	$\frac{2(K^2-1)}{(10K^4+6)} f$	$0.63f$

The above quoted yield criteria are valid provided the assumptions mentioned earlier are also valid. But these formulae do not predict what would happen if the pressure is applied and released a great many times. One would expect, for example, fatigue to result from the cumulative effect of a large number of applications of stresses even though none of these reach the ultimate tensile strength; this would lead to the failures at much lower pressures than the cylinders will normally withstand.

E. Methods for Improving the Strength of Thick-Walled Cylinders.

When a thick-walled cylinder at a given uniform temperature is subjected to an internal pressure, the normal stress distribution across the wall is not uniform; the magnitude of the stress varies from point to point. As a result, the different layers of the metal are utilized to different extents and the outer layers of the metal are rather poorly utilized. The disadvantages of this non-uniform stress distribution have been overcome by special design of the pressure vessel. The four main types of vessels developed are described below.

i) Compound Vessels

These are made by thermally shrinking an outside cylinder onto an inner one. The shrinkage of the outside cylinder acts like an external pressure on the inner cylinder and the resulting hoop stresses on the inner and the outer cylinder are respectively compressive and tensional in character.

When a pressure is applied internally to such a compound cylinder, the tensional stress due to pressure is opposed by compressive stress due to shrinkage. The effect of the shrinkage, therefore, is to decrease the tangential stress in the inner layers and increase it in the outer layers and thus to achieve a more uniform distribution of stress.

In constructing a compound vessel, advantage may be taken of combining two different steels so as to achieve better tensile properties.

ii) Wire-Wound Vessels.

A different method of subjecting a cylinder to initial compressive stresses is to wind the cylinder with wire or ribbon at high tension. When an internal pressure is applied to such a cylinder the hoop stresses developed oppose, as before, the compressive stresses due to winding. The resulting stress distribution, as in the case of shrinkage, is more uniform throughout the wall than in the equivalent simple cylinder. Wire-wound vessels, however, differ from compound vessels in the respect that wire winding does not add to the longitudinal strength of vessels.

iii) Autofrettaged Vessels.

The third method, namely, the autofrettage method aims at developing initial compressive stresses in the wall of the vessel without the help of any external agency. Here, the metal is over-strained into the semi-plastic zone by applying a high internal

pressure. Usually, the overstrain extends only partly through the wall, the outer layers remaining in the elastic region. Upon release of the autofrettage pressure, various layers try to contract to various extents. The outer layers in the elastic zone, for example, tend to contract back to their original positions, but the inner layers in the semi-plastic zone cannot revert. This gives rise to residual compressive stresses in the inner layers and tensions in the outer layers. The net effect, therefore, is to even out the distribution of stresses due to an internal pressure.

From a knowledge of the stress-strain relationship for a given steel, it is possible to calculate the residual stresses set up by autofrettage[69]. Since the effect of overstrain is to reduce the elastic limit and increase the yield point, autofrettage may be carried out in several stages with a low temperature (200-400° C) heat treatment between the stages. This stabilizes the residual stresses and restores the elasticity of the overstrained metal.

The autofrettaged method finds more practical applications than the other two methods described above. This method is taken advantage of in the construction of gun-barrels. It may be mentioned here that both pressure-vessels used in the present work were made out of autofrettaged gun-barrels.

iv) Laminated-Wall Vessels

In this method, the vessel is constructed by starting with a relatively thin-walled cylinder and wrapping successive layers of sheet steel around it. Each layer is wrapped and tightened and the

longitudinal seam is welded before the next layer is put on. A complete pressure vessel is made by welding together as many of these multilayer cylindrical sections as are needed, and then welding heads on the ends.

The method has several additional advantages over the ones described above. For example, large vessels can be built up in the field from the wrapped sections; the site of the final vessel is not limited by the size of the largest available ingot; if failure does occur there is less fragmentation.

F. The Safety Factor and the Criteria of Failure

In the case of a thin-walled cylinder (ratio of outside diameter to inside diameter, $K < 1.20$) where the tensile hoop stress, S, is assumed to be uniformly distributed throughout the wall cross-section and the longtitudinal stress is half the hoop stress, the ratio of the internal pressure, P, to hoop stress, S, is given by

$$\frac{P}{S} = \frac{2(K_o - 1)}{K_o + 1} \qquad (4)$$

Now, when S equals the elastic limit as determined by the usual tensile test, elastic failure will begin. At higher pressure the wall will yield and show a permanent set. When S equals the ultimate strength as determined by the usual tensile test, failure by fracture of the wall will occur. In determining the necessary wall thickness for a given vessel and internal pressure, an allowable stress is chosen for S. This is some fraction of either the elastic limit or the

ultimate strength and the reciprocal of this fraction is called the safety factor. Common values for the safety factor are 2 to 2.5 based on the elastic limit and 4 to 5 based on the ultimate strength. The latter being in common use. For thick-walled cylinders, the relation,

$$\frac{P}{S} = \frac{K_o^2 - 1}{K_o^2 + 1} \tag{5}$$

is used to calculate the ratio of the internal pressure to hoop stress. Therefore,

$$S = P \cdot \frac{K_o^2 + 1}{K_o^2 - 1} \tag{6}$$

If σ is the ultimate strength of the wall material, the safety factor, F_s is given by

$$F_s = 1 \Big/ \frac{S}{\sigma} = 1 \Big/ \left(\frac{P}{\sigma} \cdot \frac{K_o^2 + 1}{K_o^2 - 1} \right)$$

$$= \frac{\sigma}{P} \cdot \frac{K_o^2 - 1}{K_o^2 + 1} \tag{7}$$

and for a pressure vessel with $K = 2$,

$$F_s = \frac{0.6\sigma}{P} \tag{8}$$

It may be noted that (8) does not take into account any deviation from perfectness of the welded or other joints nor the effect of factors like corrosion, fatigue etc.

G. Some Common Sources of Hazards and Corresponding Safety Measures

Recognition of hazards peculiar to work at high pressures is the pre-requisite to the adoption of proper safety precautions in the installation of a high pressure set-up. The sources of hazards and corresponding precautionary steps are, therefore, mentioned below.

i) Splitting of Bourdon Tubes

When a compressed inflammable gas rushes into a Bourdon tube containing air, an explosion may take place and the Bourdon tube may split; the metallic particles from the gauge can cause grave injuries. To permit the escape of gases, the case of a Bourdon Gauge is provided with large vent openings covered with paper for dust-protection. The danger from flying particles can be avoided if it is possible to remove the gauge glass and leave the face open or if the glass is replaced with Perspex as was done during the present work. Bourdon gauges should be placed above the eye-level and if possible placed behind a barrier. In the present experimental set-up, the 1000 atm. Bourdon gauge was shielded by a thick transparent Perspex wall. Check-valves are also installed to prevent the pressure from rising or falling too suddenly.

ii) When the metallic container ruptures, the frictional effect may cause very high local temperatures and the ignition of inflammable gases.

iii) In a flow line, various pressure relief devices such as safety valves or rupture discs are usually installed. The safety valve is

set to a pre-determined value depending on the operating pressure and the ultimate strength of the piping in question. The disadvantage with the rupture disc is that the entire contents of the pressure system are discharged.

iv) Oxygen cannot be compressed with safety in presence of oil. It has been found that when oxygen at high pressure is rapidly admitted into a space containing a bit of oil material, an explosion takes place. Oil, therefore, must be avoided in a high pressure set-up using oxygen.

v) It is desirable to have periodic inspections of the high pressure equipment, to ensure that they are in satisfactory working condition.

2. HIGH-PRESSURE EQUIPMENT USED IN THE PRESENT STUDY

Two high-pressure set-ups were used for the present study; one for the establishment of the pressure-temperature relation for the silver-oxygen system up to 750 atmosphere and the other for thermogravimetric measurements up to 100 atmospheres. The set-up for thermogravimetry is described more conveniently in Section 3. The pressure circuit (for the set-up used up to 750 atm.) is shown on page 47. The gas from the cylinder, C, passes through the filter, F_1, and the safety valve, S, to the compressor, P. After compression, the gas enters the pressure vessel, V, through a second filter, F_2.

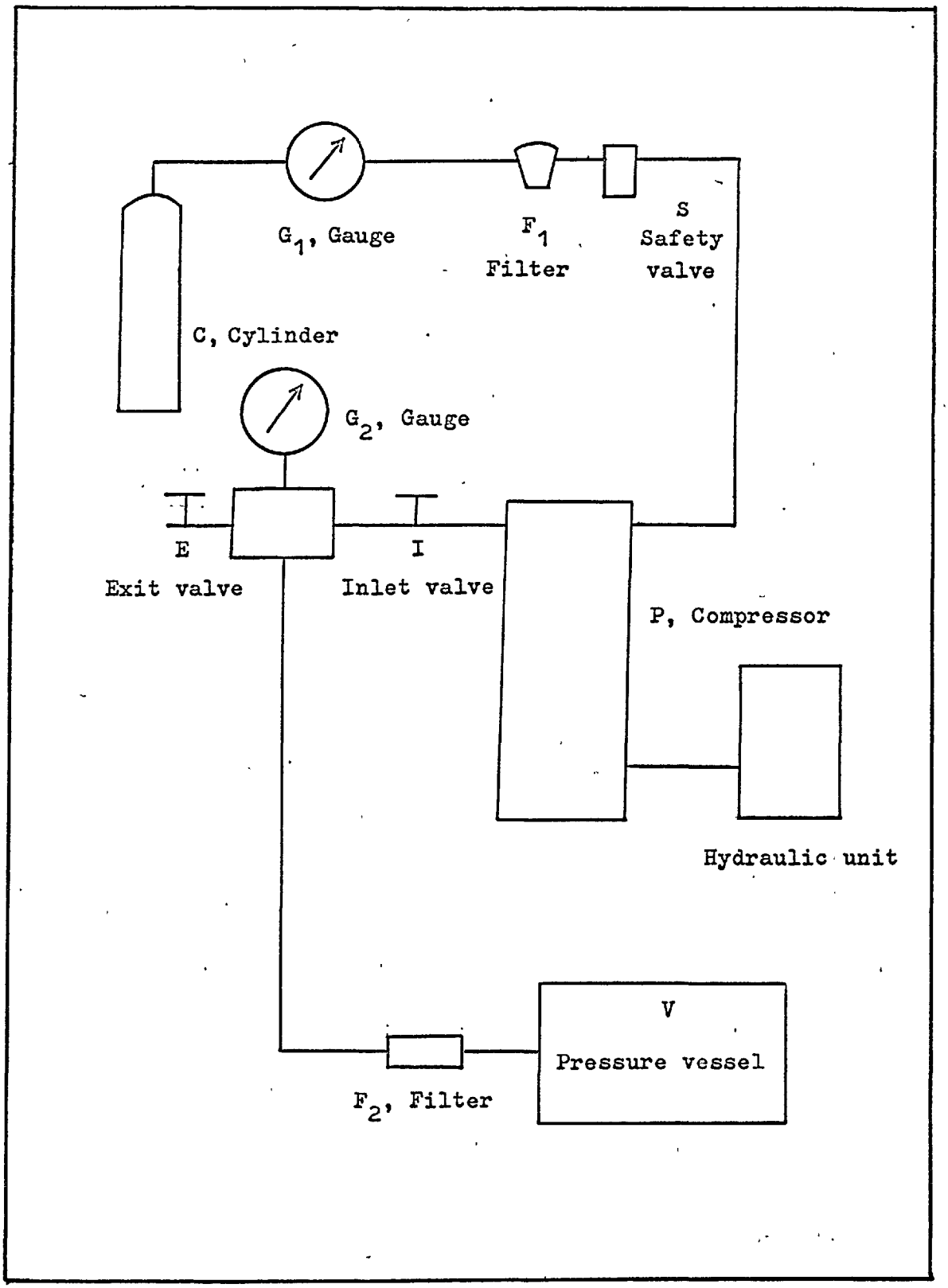

Fig. 3. Pressure circuit.

Pressure gauges, G_1 and G_2, read respectively the gas pressures before and after compression. I and E represent the inlet and exit valves respectively.

A photograph of the set-up is shown in the Plate No. 1 and the sectional view of the apparatus is shown in Fig. 4.

A. Ancillary Equipment

i) Gas-Compressor

The supply of oxygen at pressures below 140 atmospheres was obtained directly from the normal oxygen cylinders. Oxygen at pressures up to 250 atmospheres was obtained from specially built cylinders filled at 3600 p.s.i. Higher pressures were achieved by compression.

The compressor consisted of a single-stage intensifier operated hydraulically by a Vickers' pumping unit. The hydraulic fluid was a mixture of water and glycol. A magnetically operated directional valve regulated the suction and discharge of the fluid in the drive cylinder of the intensifier.

The intensifier-head ($\frac{1}{2}$" I.D.) was constructed of K-monel and was water-cooled. The piston was of bronze and pressure-sealing was accomplished by a Teflon-washer fixed to the top of the piston. The valve chamber above the head was also made of K-monel and incorporated poppet valves of the "Duo-Seal" type; the Teflon "O" rings on the poppets insured pressure-tight seals.

The stroke-length was $2\frac{1}{2}$" and the number of strokes per min. was 20. It took about 15 min. to compress the gas from 250 atm. to 750 atm.

ii) Filters

Solid particles in the gas stream can cause severe abrasive damage to valve seats. Filters, therefore, were incorporated in the set-up. The first filter, F_1, was placed in the low pressure side of the circuit and prevented dust particles from entering the compressor. This filter, supplied by I.V. Pressure Controllers Ltd. (M del 433/1) was made of high tensile brass, and the filter element, of sintered bronze with a pore-size of 5 microns. The filter element was removable for cleaning or for replacement. It could operate up to a maximum pressure of 6000 p.s.i.

The second filter, F_2, was incorporated to prevent alumina dust from the pressure vessel from getting into the pipelines. It was a Poroloy line filter, supplied by PPI Ltd. (Type, F-112-30), with a pore-size of 20 microns.

iii) Safety Valve

Any gas leaking from the high-pressure side of the set-up via the compressor inlet valve, would flow back into the low-pressure copper piping and inlet pressure gauge. In view of the comparatively low volume of the copper piping, the pressure developed by the back-flow of gas would be great enough to cause severe straining of the piping and damage the inlet pressure gauge considerably. To eliminate this hazard, a safety valve was incorporated in the low-pressure pipe-

line. This valve was a spring-loaded type supplied by Hale Hamilton Ltd. (Model R.V.3), and was set to relieve the pressure to the atmosphere at a pressure of 3800 p.s.i.

iv) Connecting Pipes, Control Valves and Pressure Gauges

In both the experimental set-ups, cold-drawn seamless piping was employed. For pressures up to 250 atm. copper piping with an external diameter of $\frac{1}{4}$ in. and a bore of $\frac{1}{8}$ in. was used. Taking the ultimate tensile strength of annealed copper as about 15 tons per sq. in., the bursting pressure for this piping becomes 1200 atm. by the formula

$$P_B = \sigma_{ultimate} \frac{K^2 - 1}{K^2 + 1} \qquad (9)$$

where, K is the ratio of the outer to inner diameters. This corresponds to a safety factor of 4 at a working pressure of 300 atm.

For higher pressure, i.e., up to 750 atm., "Monel" piping of external diameter $\frac{3}{8}$ in. and bore $\frac{1}{8}$ in. was used. Again taking the ultimate tensile strength of annealed 'Monel" as 30 tons per sq. in., the bursting pressure of this piping calculated from the above formula is found to be 3200 atm. which gives a safety factor of 4 at a working pressure of 800 atm.

The bursting pressures calculated on the basis of the above formula are very approximate and can only be taken as a rough guide. Nevertheless, they give the approximate safety factor of 4 which is considered adequate for the laboratory pressure set-up.

The inlet and outlet valves (I and E on page 47) were supplied by Charles S. Madan and Co. Ltd. and were of high tensile bronze; they were of the captured needle type. The standard working pressure for these valves is 25,000 p.s.i. while the test pressure is 40,000 p.s.i.

Bourdon test gauges with scales, 25 cm. in diameter calibrated within $\pm$ 0.25% were employed for pressure measurement. Four gauges, with ranges up to 4 atmospheres, 50 atmospheres, 300 atmospheres and 1000 atmospheres were employed.

B. Pressure Vessel

As shown in fig. 2, the pressure vessel was mounted horizontally. The vessel was made of a cylindrical section cut from an autofrettaged gun-barrel. The section was 13.3 in. in length and had inner and outer diameters 1.9 in. and 4.3 in. respectively. Both ends of the section were threaded outside over a length of 2 in. (8 t.p.i.) to enable two flanges of 7.5 in. outer diameter to be fitted. Nine $\frac{3}{4}$ in. B.S.F. bolts of the "Unbrako" type having an ultimate tensile strength of approximately 90 tons per sq. in. were used to bolt each lid to the body of the vessel. The pressure-tight seals were achieved by means of "O" rings sealed in the grooves of the lids. A water jacket was fitted on to the flanges and water-tight seals were also provided by "O" rings.

Taking the ultimate tensile strength of the autofrettaged steel as 60 tons per sq. in. and applying the maximum principal stress criterion

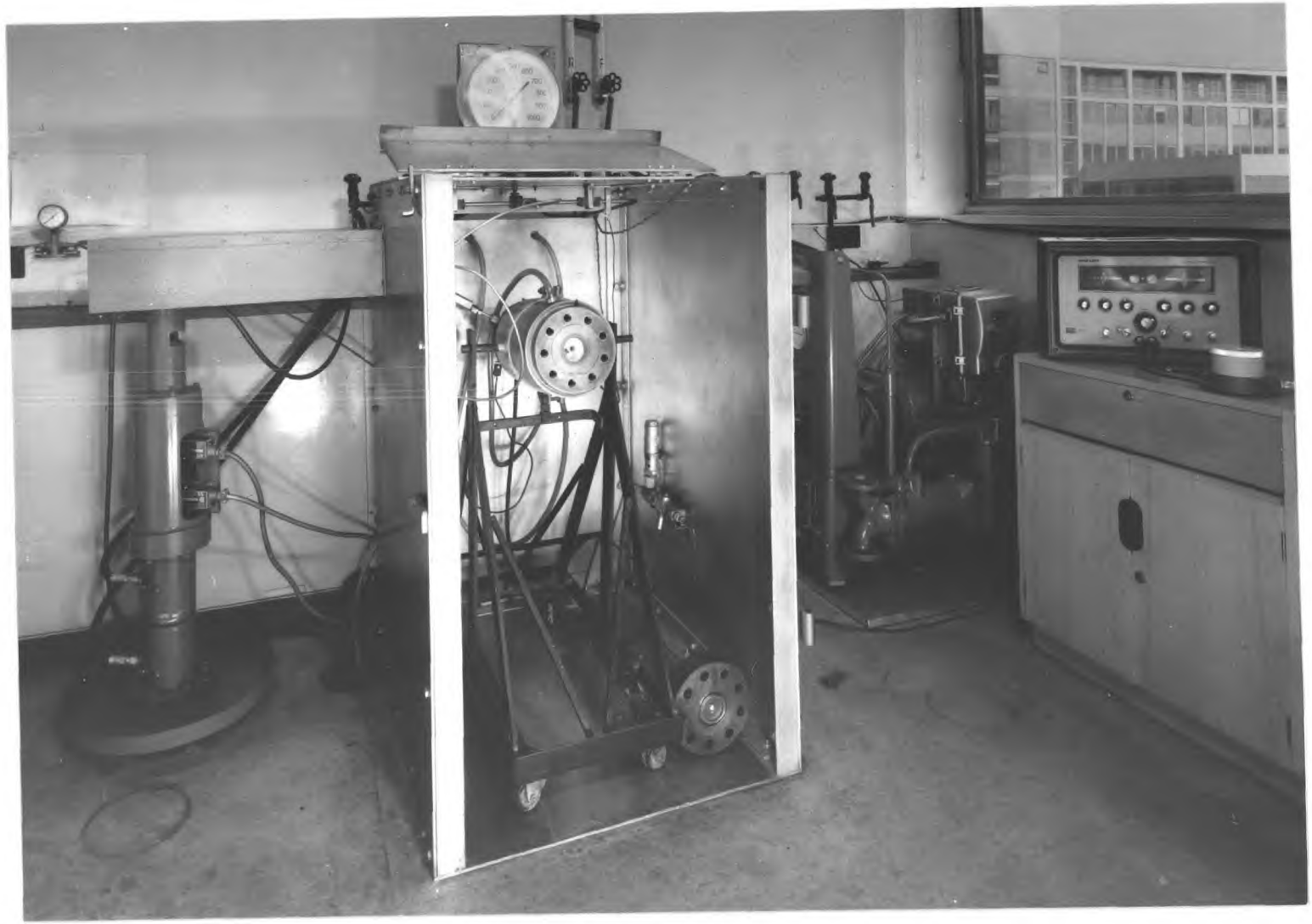

Plate No.1. A view of the high pressure set-up.

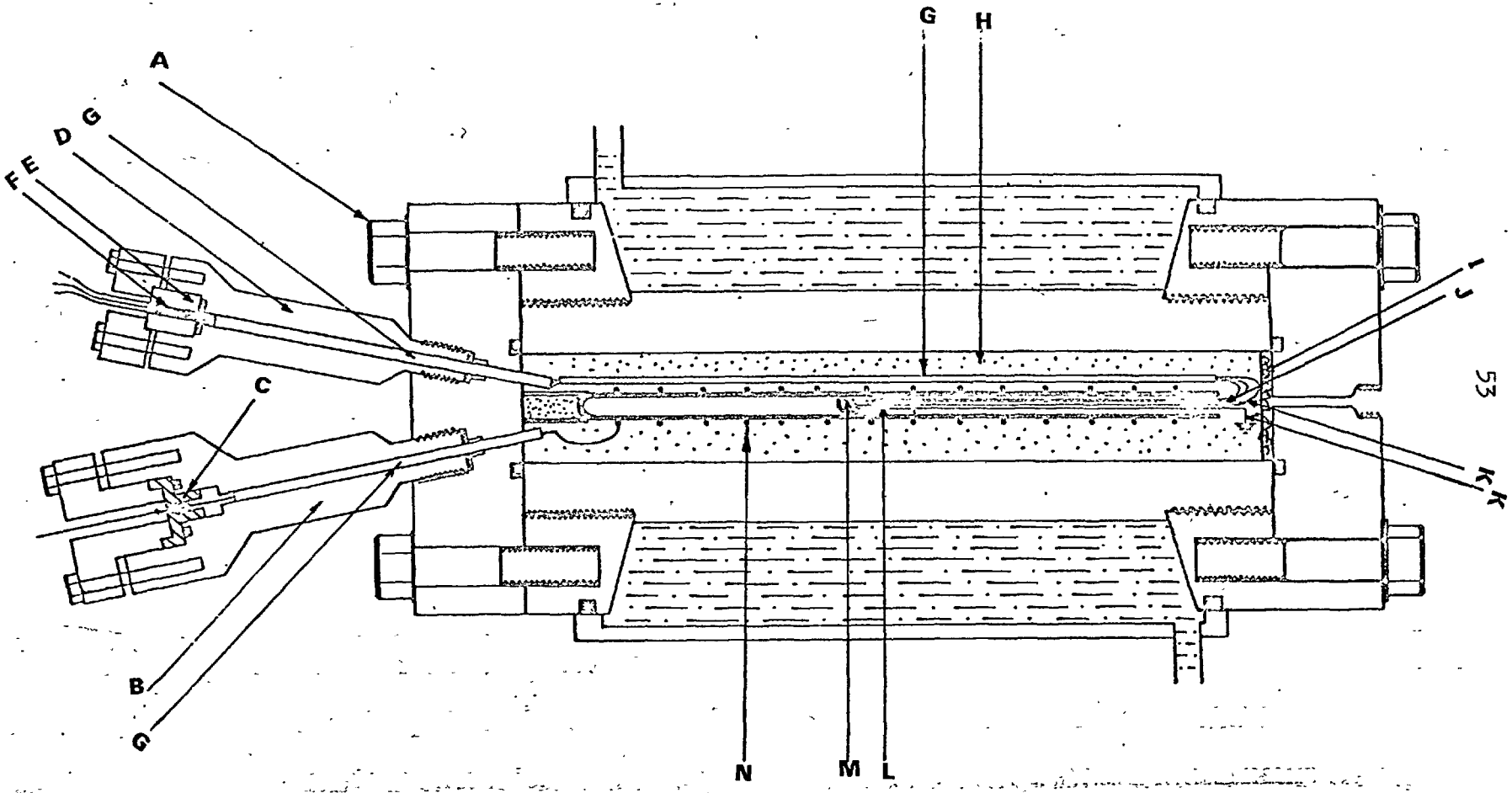

Fig. 4 . A sectional view of the high pressure vessel and furnace assembly.

Legends of Figure 4

A. 'Unbrako' bolt 3/4" B.S.F. (9 per lid).

B. Phosphor-bronze assembly for power input (2).

C. Metal-ceramic seal (Consolidated Electrodynamics type 41 - 901 - 0006).

D. Phosphor-bronze assembly for thermocouple wires and electrical leads.

E. Brass Block.

F. Araldite resin.

G. Alumina sleeve.

H. Alumina powder (100 mesh).

I. Asbestos wool.

J. Alumina thermocouple sheath.

K. Gold connecting leads.

L. Alumina boat.

M. Silver oxide sample.

N. Nichrome furnace element.

for the bursting pressure, namely

$$P_B = \sigma_{ultimate} \frac{k^2-1}{k^2+1}$$

is found to be approximately 5120 atm. This gives a safety factor of greater than 5 at a working pressure of 1000 atm.

i) Introduction of Furnace Leads

Methods of introducing insulated leads into high-pressure vessels have been described by various workers[70,71,72,73]. These devices, though they differ in detail, have in common a steel or other strong alloy plug (which is screwed onto the vessel wall) into which an insulated electrode is inserted. Insulators of plastic, glass or ceramic are used.

The design of devices for introducing power leads into a vessel containing high pressure oxygen demands additional precautions, particularly since ferrous metals, when overheated, can burn away in oxygen at high pressures. The first power terminal used here incorporated a single brass electrode in a steel plug; one end of the furnace element was earthed on the vessel. However, at a pressure of 600 atm. an electrical breakdown occurred between the electrode and the steel around , the latter burnt away in the escaping gas whilst the stream of molten metal and oxygen burnt a hole through the ¼" steel protective cabinet in about 20 seconds. Part of the burnt steel plug is shown in Plate No. 2 , the brass electrode having disintegrated.

As a consequence of this hazard improved devices were used to introduce power leads into the pressure vessel. To achieve electrical

Plate No. 2. A photograph of the burnt away electrode (×2).

isolation from the vessel, two separate electrode assemblies were used. (One of these is shown in Fig. 4.) The device consisted of a phosphor bronze plug into which was inserted a standard high temperature hermetically sealed "header" (Type No. 41-901-006, supplied by Bell and Howell Ltd.). Both the body of the "header" and the electrode pin are made of Inconel X. The electrode is insulated from the body with a special glass-ceramic material. The device can stand a pressure greater than 1500 atm. and is recommended for continuous operation up to a temperature of 300° C. The sealing between the plug and the header was achieved through an "O" ring. An extra length of copper rod, sufficient to protrude outside the plug, was soft-soldered on to the electrode pin and was insulated with alumina tubing.

ii) Introduction of Thermocouple Leads

When a number of thermocouple wires or other connecting wires are required for entry into the pressure-vessel through a single opening, arrangements must be made such that the opening is sealed pressure-tight and that the wires themselves are kept insulated from each other. The resin Araldite has been found to be successful for such seals up to a pressure of 5000 atmospheres[74,75], and is used by many workers. Some workers[76,77] use another resin, Stycast , in place of Araldite. Stycast is known to have better properties than Araldite at elevated temperatures.

In the device shown in fig. 4 the platinum and platinum-rhodium wires for temperature and electrical measurements were of

0.3 m.m. diameter and were sealed by Stycast into holes of 0.6 m.m. diameter bored in the brass block.

ii) "O" Rings and Gaskets

The "O" ring seals used in the pressure vessel were of acrylic rubber (P 90 type) and the gasket material was Klingerite 661. These proved themselves quite satisfactory at all pressures.

C. Furnace

Factors that are usually taken into account in constructing an ordinary tube furnace are: (1) the maximum temperature to which the inside of the tubular element is to be heated, (2) probable thermal losses at the maximum temperature, (3) the size of the tube, (4) the length of the hot-zone required, (5) the effect of gases both on the rate of heat losses and on the winding element, (6) the insulating refractories and (7) whether the furnace is vertical or horizontal.

High-pressure brings in additional factors, because high-pressure gases not only increase the rate of heat loss through convection but also cause displacement of the hot-zone.. In a vertical furnace the hot-zone shifts upwards[78]. Besides this, the power required to attain a given temperature increases with pressure; although no formal relationship is known, Smyth and Adams[78] found that a furnace which required 10 amps at 22 volts to attain a temperature of 1400° C at 1 atm. required 30 amps at 75 volts for the same temperature at 1200 atm.

The furnace tube used in the present pressure vessel (Fig. 4) was of recrystallized alumina. The tube was 29 cm. in length with

an inner and outer diameter of 1.2 and 1.6 cm respectively. The furnace was wound linearly on a lathe at 8 turns of wire per inch. The winding length was 25 cm. The windings were held in position with alumina cement.

For temperature below 900° C, Nicralloy wire (80/20 Ni-Cr) of 20 S.W.6 was used; for higher temperatures, 10% Rh-Pt alloy of the same gauge was used. The resistances of the Nicralloy and platinum alloy windings were 8 ohms and 2 ohms respectively at room temperature. The constant-temperature zone of both furnaces was about 2 cm. Since the vessel was mounted horizontally, the constant-temperature zone would not be affected significantly by pressure.

The free space between the furnace tube and the wall of the pressure vessel was filled with dry alumina powder (100 mesh).

D. Temperatures Measurement and Control Gear

The electrical circuit for controlling the temperature of the furnace is shown in Fig. 5. Manual control of the furnace temperature is carried out with the Variac E_1, the voltage being fed into the isolation transformer, P_1, which has a step-down ratio of 2:1. The temperature controller, C, and the ballast resistance, B.R., were meant for automatic control of temperature; this, however, was hardly ever employed.

The second Variac, E_2, and the isolation transformer, P_2, were used for controlling the temperature of the additional (booster) winding in the furnace of the thermogravimetric apparatus.

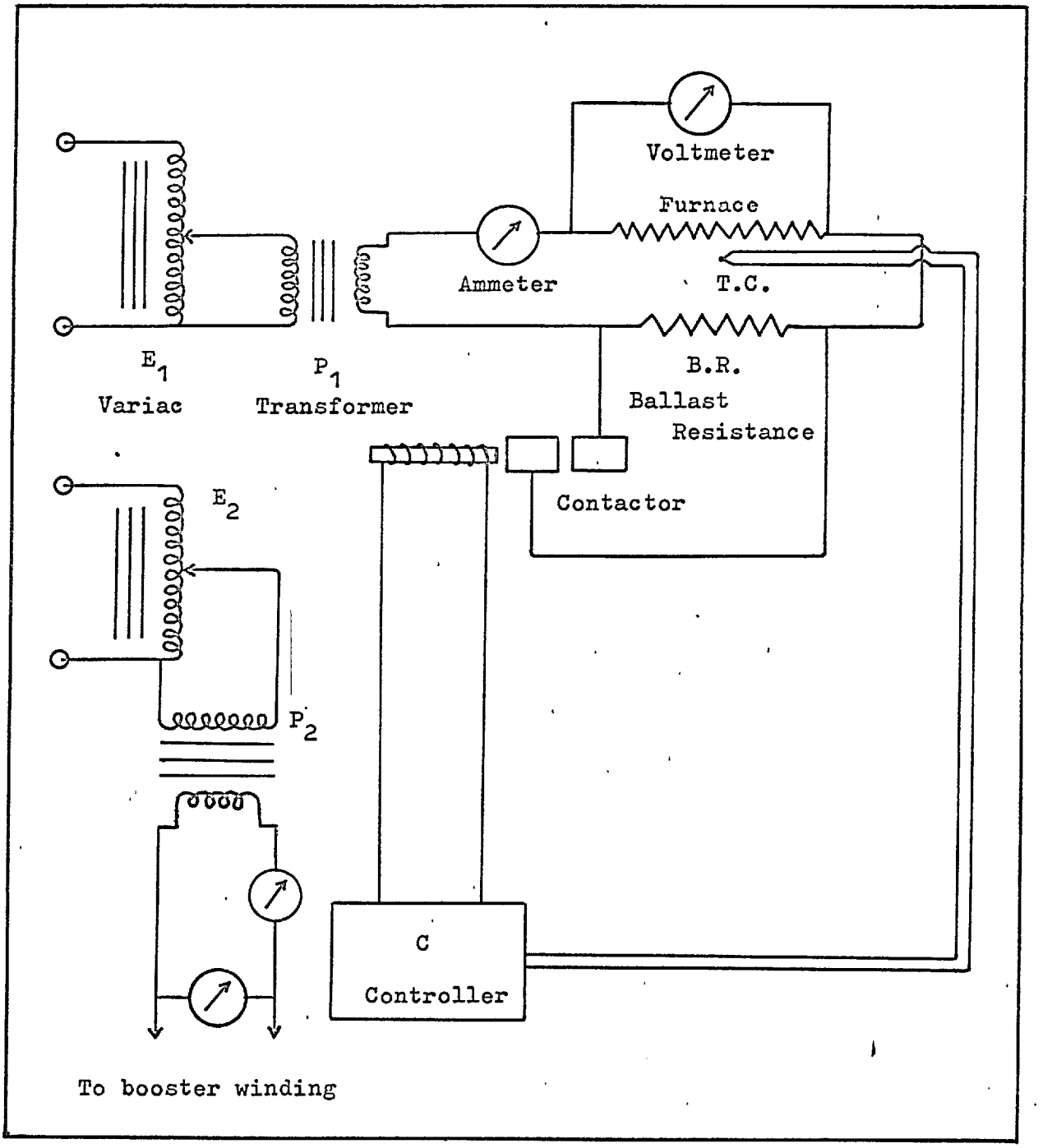

Fig. 5. Electrical circuit for temperature measurement and control.

Temperature was measured by means of a platinum-platinum + 13% rhodium thermocouple, the e.m.f. of which was fed into a two channel Honeywell recorder. The range of the recorder was 0-1 m.v. so that a biasing unit was necessary with the instrument. The recorder in conjunction with the biasing unit, could also be employed to measure differential e.m.f.'s when gold-point calibrations were necessary.

Temperature calibration of the recorder scale was made by means of a thermocouple potentiometer (Croydon Precision Instrument Co.). The maximum accuracy of temperature measurement was 0.5^{0} C.

CHAPTER III

Experimental Section 2

MEASUREMENTS AND PROCEDURE

1. DETERMINATION OF THE PRESSURE-TEMPERATURE RELATION FOR THE SILVER-OXYGEN SYSTEM.

A. Materials

Thin silver foils of thickness 0.052 mm and of purity 99.99+ and "Specpure" silver oxide were used in the determination of the fusion points. These materials were supplied by Johnson and Matthey. The gold wires of 0.5 mm diameter, used for the conduction electrodes, and the gold foil of thickness 0.076 mm used for checking the thermocouples were also "Specpure"; the metallic impurities like iron, silver, copper, palladium, etc. did not exceed 3 p.p.m.

B. Fusion Temperature of Silver as a Function of Oxygen Pressure

The method employed for the determination of the fusion points of silver was that used by Baker and Johnstone, in which fusion of a small strip of silver was detected electrically.[62]

Fig. (6) shows the assembly employed. The silver strip which was 6 to 7 mm long, about 1 mm wide and 0.051 (or 0.075) mm thick was roughened with emery paper prior to the run and was welded to two gold wires to complete the electrical circuit . After introducing the assembly into the pressure vessel, the vessel was flushed with oxygen, pressurized to the desired value and heated at a rate of 15-20° per minute; when the temperature reached 15-20° below the expected fusion point, the heating rate was adjusted to about 2° per minute. Melting of the strip was shown by the meter (A) giving

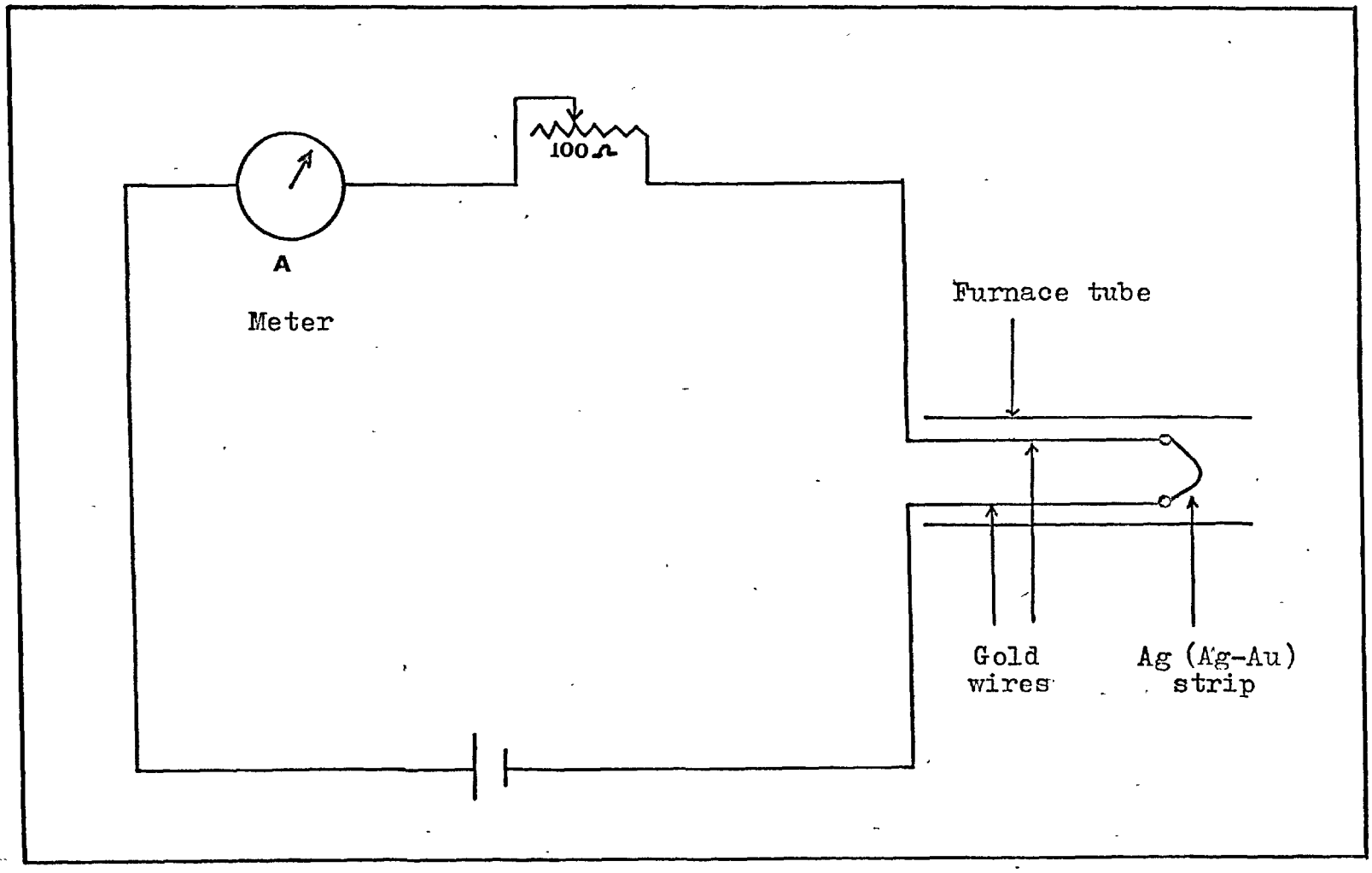

Fig. 6. Electrical circuit for detecting fusion points of silver-strip.

a zero reading. The current passing through the strip was about 5 milli amps.

The thermocouple, placed alongside the strip to measure the temperature, was oxidized at high oxygen pressures; the extent of oxidation being shown by the degree of blackening of the bead, which became significant at pres ures above 60 atm. For this reason, the thermocouples were properly checked at the gold point. The gold point method used was that in which a strip of "specpure" gold was incorporated in a differential thermocouple arrangement. When checked, the blackened thermocouples were found to yield temperatures $2\text{-}3^0$ lower than the exact melting point of gold . Throughout all the experiments at high pressures, therefore, new thermocouples were used after every two runs.

Fusion temperatures at oxygen pressures up to 500 atm. are given in Table 5 and are plotted in Fig. 7. The lowest value of pressure, namely, 0.2 atm, at which the melting point was determined, was obtained in the air.

At pressure up to about 250 atm., fusion temperatures are considered to be accurate within $\pm 1^0$; at higher pressures, the accuracy is probably within $\pm 3^0$.

C. Fusion Temperatures of Silver-Oxide as a Function of Oxygen Pressure

Fusion temperatures of silver oxide as a function of oxygen pressure were determined by heating the oxide under a constant pressure of oxygen and measuring the change in electrical resistance

Table 5

Fusion Temperatures of Silver under Oxygen Pressures

Oxygen Press. p(atm.)	Fusion Temp. $t^{\circ}C$	log p	$\frac{1000}{T^{\circ}K}$
0.21	950.0	$\bar{1}.3222$	0.8177
1.00	938.0	0.0000	0.8257
1.59	930.0	0.2014	0.8312
2.32	925.0	0.3655	0.8347
3.61	917.0	0.5575	0.8403
4.50	913.5	0.6532	0.8428
5.46	906.5	0.7372	0.8478
6.70	902.5	0.8261	0.8507
8.53	896.0	0.9309	0.8552
11.50	887.0	1.0607	0.8621
13.35	881.5	1.1258	0.8661
13.99	879.0	1.1459	0.8681
16.28	876.0	1.2116	0.8703
18.28	868.5	1.2620	0.8760
20.30	863.0	1.3075	0.8804
24.18	857.0	1.3834	0.8850
24.38	855.0	1.3870	0.8868
27.90	850.0	1.4456	0.8906
30.82	846.0	1.4889	0.8940
35.20	835.5	1.5465	0.9021
37.50	833.0	1.5740	0.9045
45.00	823.0	1.6532	0.9119
59.50	801.5	1.7745	0.9305
70.00	796.5	1.8451	0.9350
76.00	790.0	1.8808	0.9406
80.00	781.0	1.9031	0.9487

Table 5 contd.

Oxygen Press. p(atm.)	Fusion Temp. $t^{o}C$	log p	$\frac{1000}{T^{o}K}$
85.00	777.0	1.9294	0.9524
88.20	773.0	1.9455	0.9560
104.30	762.0	2.0182	0.9663
105.50	753.0	2.0233	0.9749
116.50	75100	2.0664	0.9767
123.50	741.0	2.0916	0.9864
142.5	732.5	2.1538	0.9945
143.0	733.5	2.1553	0.9940
148.0	728.0	2.1703	1.0000
154.5	722.0	2.1889	1.005
157.3	720.0	2.1967	1.007
166.8	717.0	2.2222	1.010
172.0	714.0	2.2355	1.013
180.0	710.0	2.2553	1.017
181.8	705.0	2.2596	1.022
189.0	702.0	2.2765	1.026
194.5	702.5	2.2889	1.025
200.0	701.0	2.3010	1.027
210.5	697.0	2.3232	1.031
214.0	691.0	2.3304	1.037
222.8	690.0	2.3479	1.038
232.0	686.0	2.3655	1.042
278.0	661.0	2.4440	1.071
298.0	639.5	2.4742	1.095
341.0	605.5	2.5328	1.138
346.0	628.0	2.5391	1.110
415.0	593.0	2.6180	1.155
500.0	568.0	2.6990	1.189

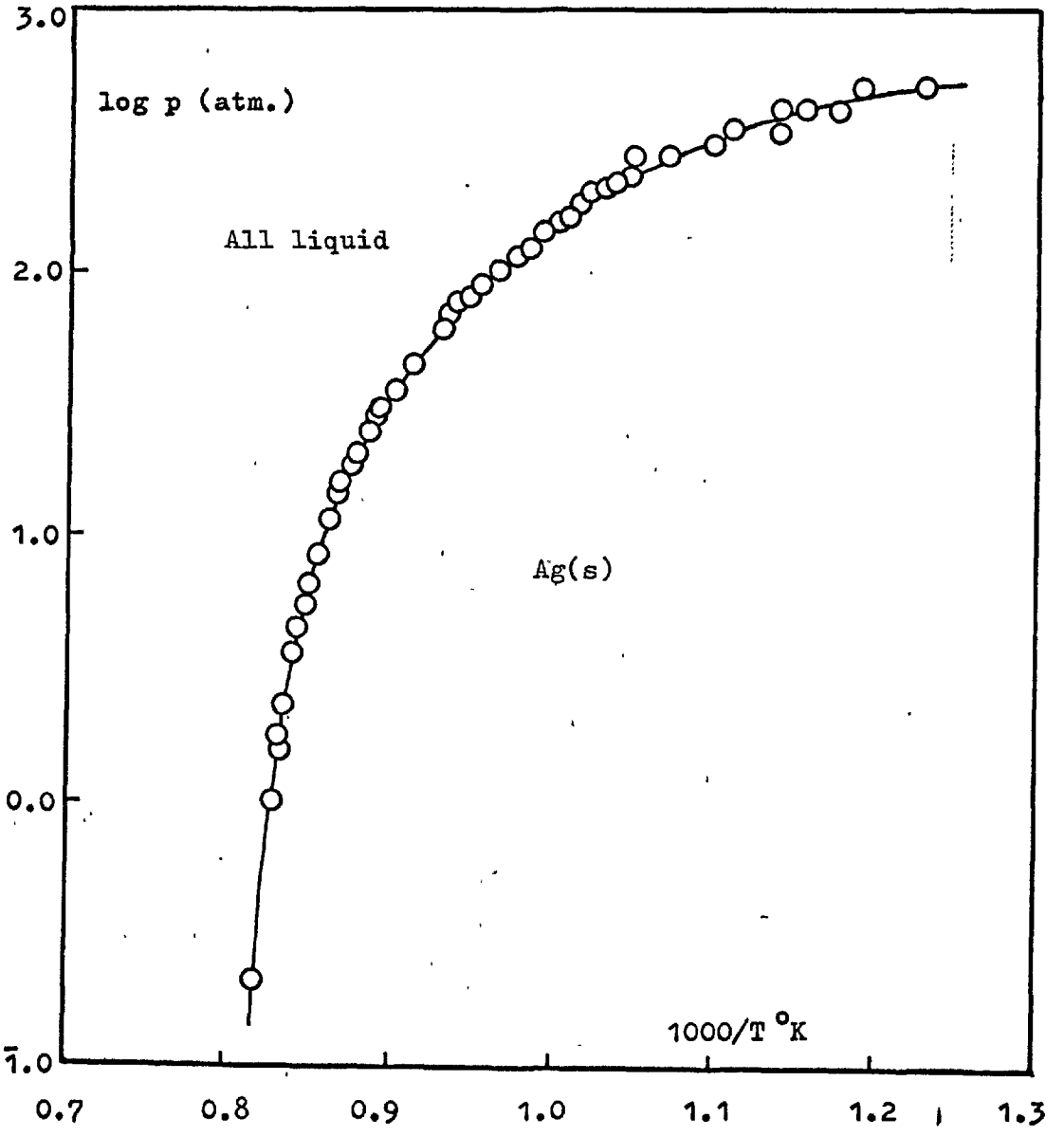

Fig. 7. Fusion temperature of silver as a function of oxygen pressure.

(Silver liquidus).

on melting. The assembly used is shown in Fig. 8 . The resistance was measured between two parallel gold wires 2 mm apart, which were buried in the oxide to a depth of about 5 mm; the oxide was contained in an alumina boat of length 2 cm; the sample weighed about 1 g.

The heating rate in the expected region of fusion was maintained at 2^0 per minute and the resistance of the sample was measured by means of a bridge (Norma type 185 RW1). To avoid electrolysis of the sample the bridge was connected only at the instant of each measurement.

The resistance values as a function of temperature are plotted in Fig. 9 for pressures up to 750 atm.

Owing to the non-uniform packing and the variation in geometry on melting, the curves differ markedly. Since the melting was not sharp, the melting point was taken just at the point where the resistance started dropping sharply.

Justification for this conclusion was obtained by examination of samples which were heated to temperatures just prior to this point and also just after.

The results are not of high accuracy; fusion temperatures are accurate within $\pm 8^0$. Fusion temperatures of the oxide up to a maximum pressure of 750 atm. are given in Table 6 .

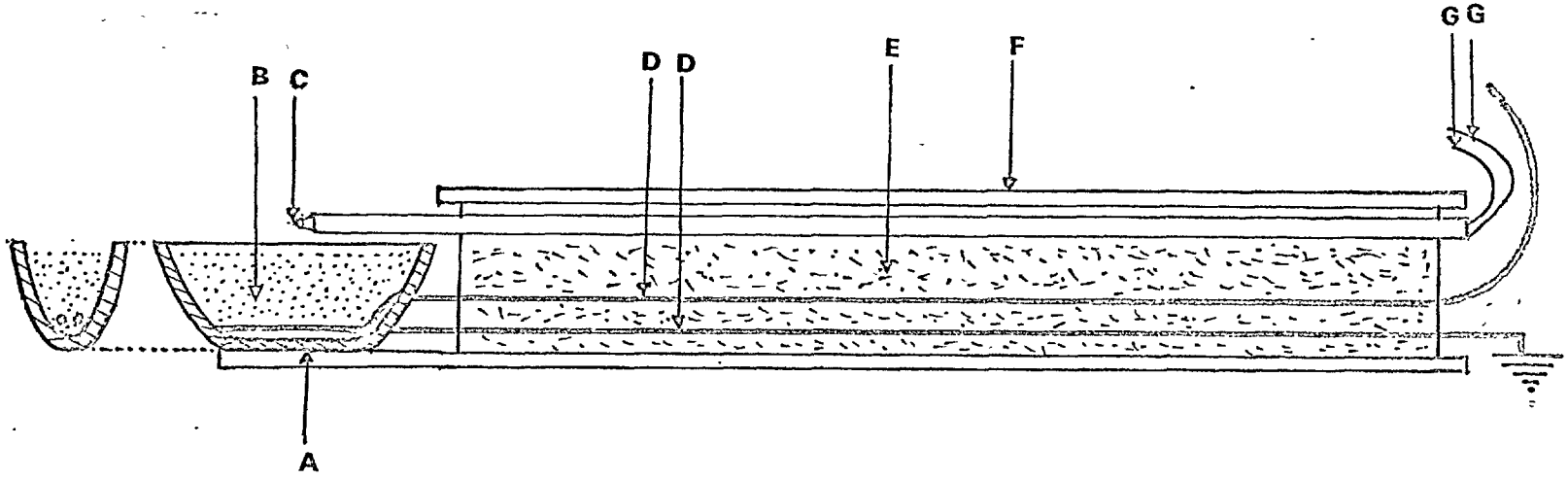

A. Alumina Boat
B. Silver oxide
C. 13% Rh-Pt/Pt thermocouple
D. Electrical conduction leads of gold
E. Asbestos wool
F. Quartz tube
G. Thermocouple wires

Fig. 8 . Boat assemly for the determination of fusion points of silver oxide.

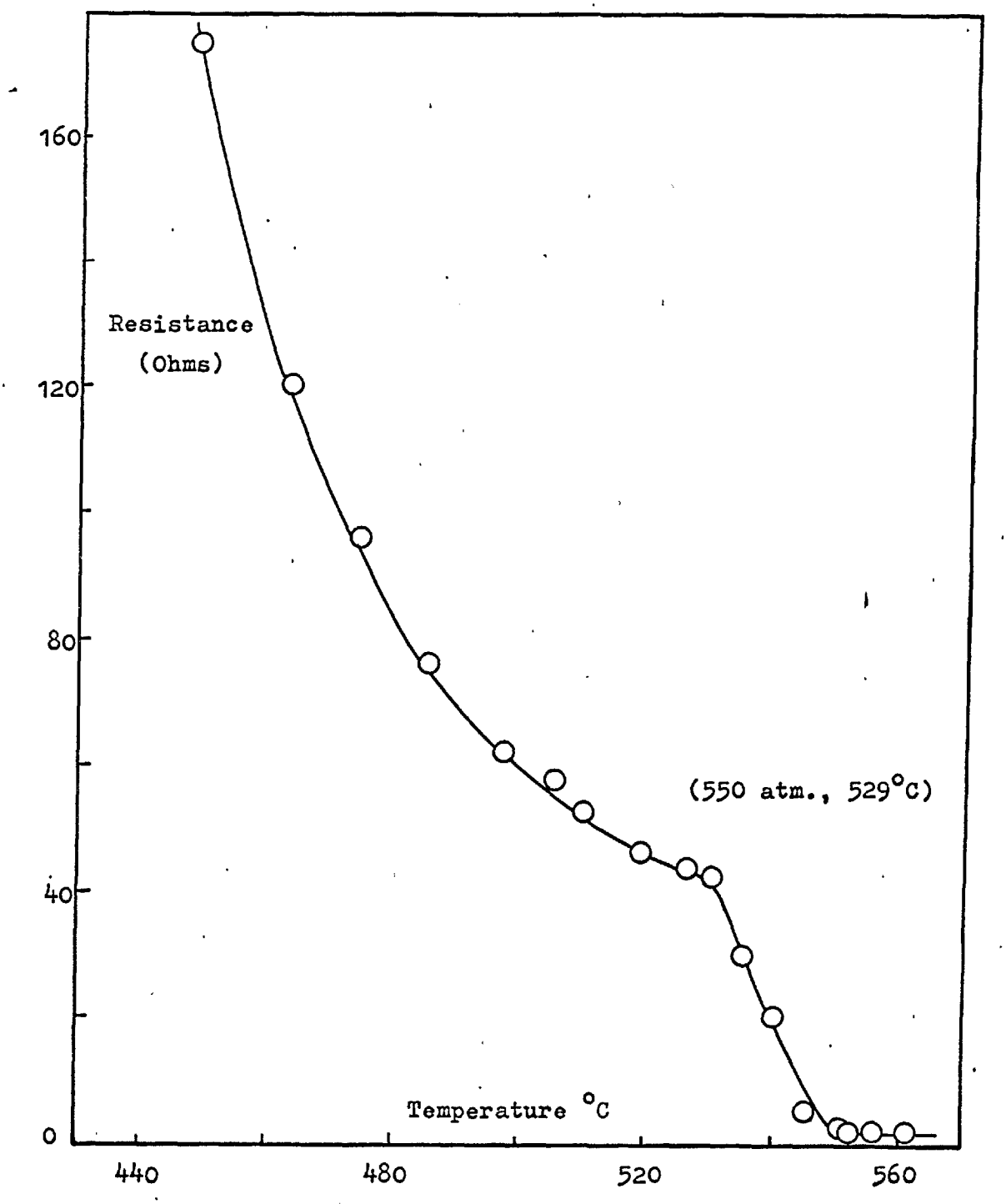

Fig. 9(a). Change in electrical resistance of silver oxide with temperature.

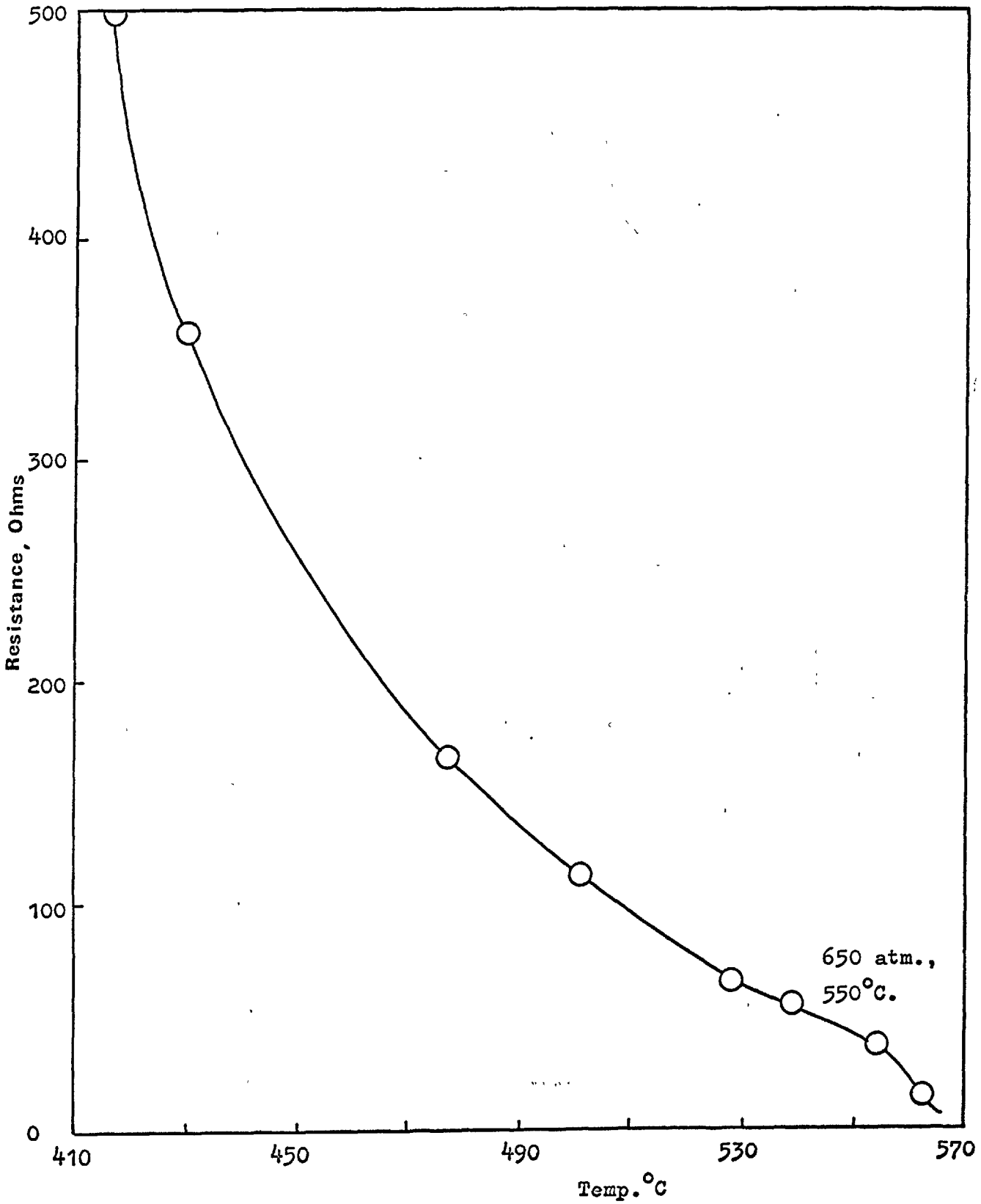

Fig.9(b). Change in electrical resistance of silver oxide with temperature.

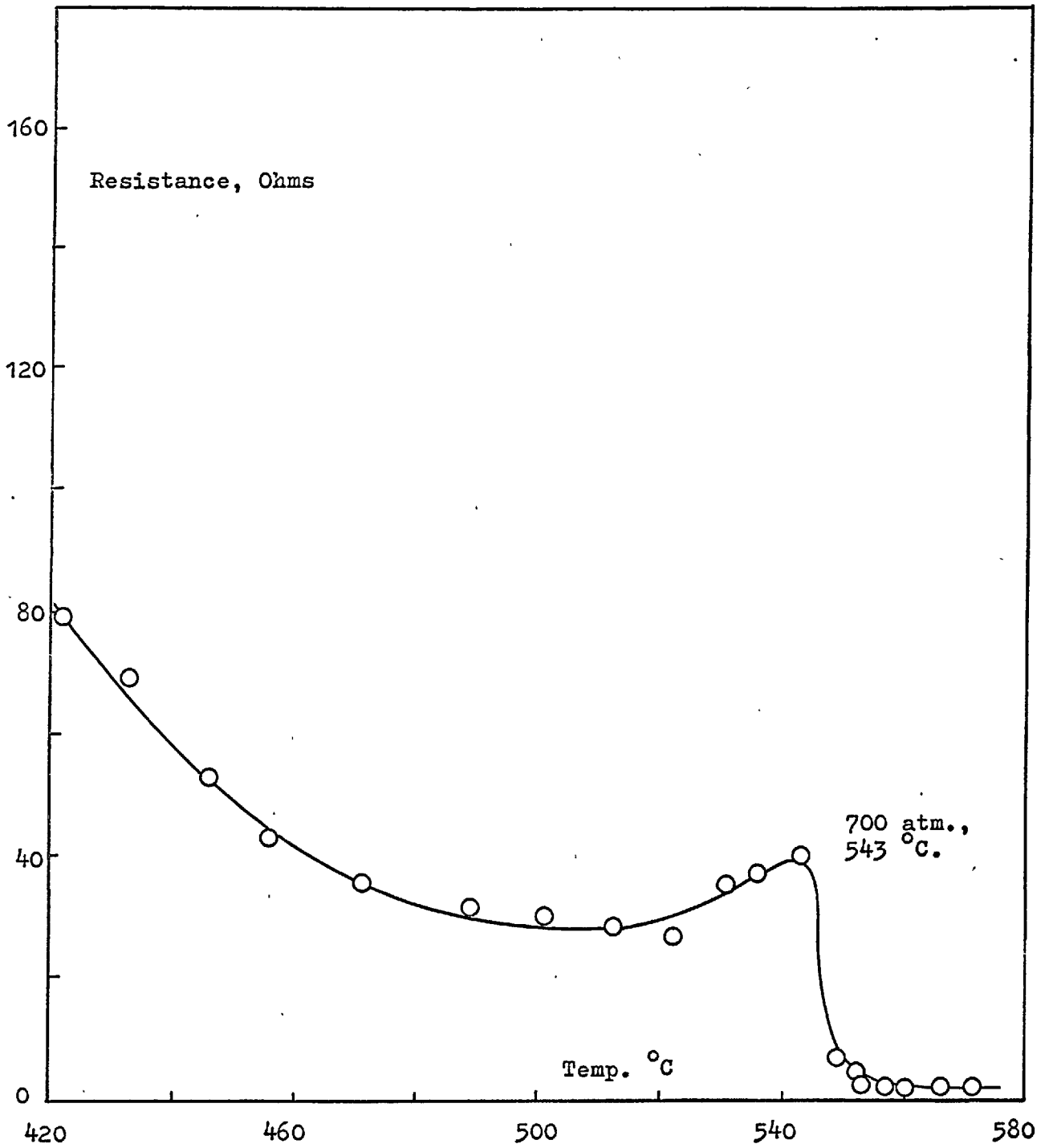

Fig.9(c). Change in electrical resistance of silver oxide with temperature.

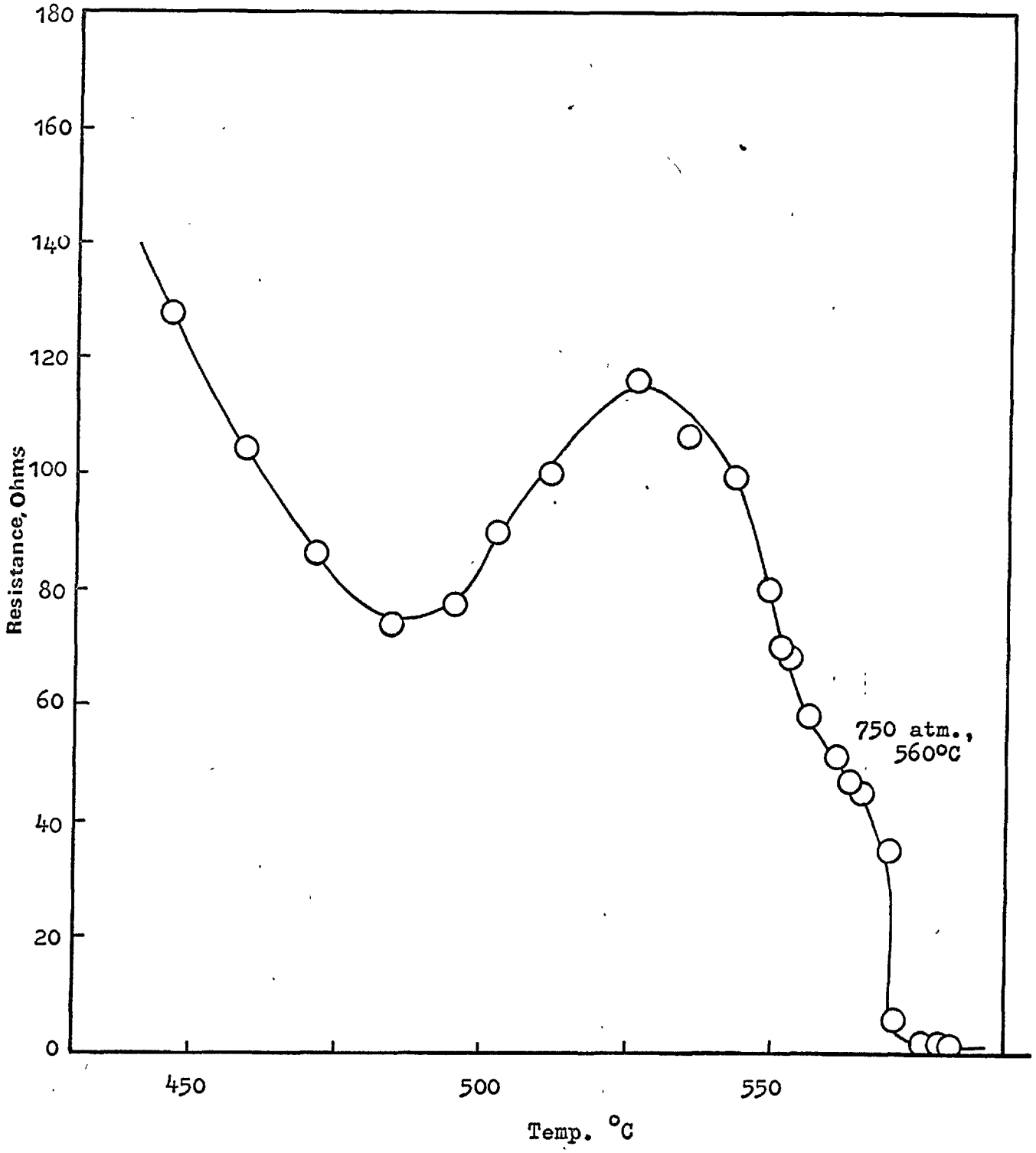

Fig.9(d). Change in electrical resistance of silver oxide with temperature.

Table 6

Fusion temperatures of silver oxide upto 750 atmosphere

Oxygen pressure p (atm.)	Fusion Temp. T °K	log p	$\frac{1000}{T}$
550	802	2.7404	1.247
650	823	2.8129	1.215
700	816	2.8451	1.225
750	833	2.8751	1.200

2. MEASUREMENTS OF THE CONDUCTIVITY OF SOLID SILVER OXIDE

During the determination of the fusion point of silver oxide by measuring the changes in electrical conductivity on melting, it was observed that the conductivity of the solid oxide increased greatly with temperature. Although silver oxide is classified as a p-type semi-conductor along with cuprous oxide, no conductivity measurements on the solid oxide have been reported. It was, therefore, decided to make a few measurements on the change in conductivity of the oxide as a function of pressure at a constant temperature and as a function of temperature at constant pressure.

The experimental technique was a modified version of that used in the oxide fusion experiments.

A pellet of silver oxide of 6 mm diameter and 5 mm thickness was prepared from "specpure" silver oxide by compressing at a pressure of 2000 p.s.i. in a hydraulic press. The packing density of the pellet was about 6.3 g/cc. The pellet was then placed between two thin, circular gold foils onto which were welded two gold wires to act as electrode-leads. To ensure good contact between the gold-foils and the surface of the pellet, a compressive spring was used to keep the pellet pressed against a flat alumina base. The thermocouple was placed in contact with one of the gold foils.

The arrangement is shown in Fig.10.

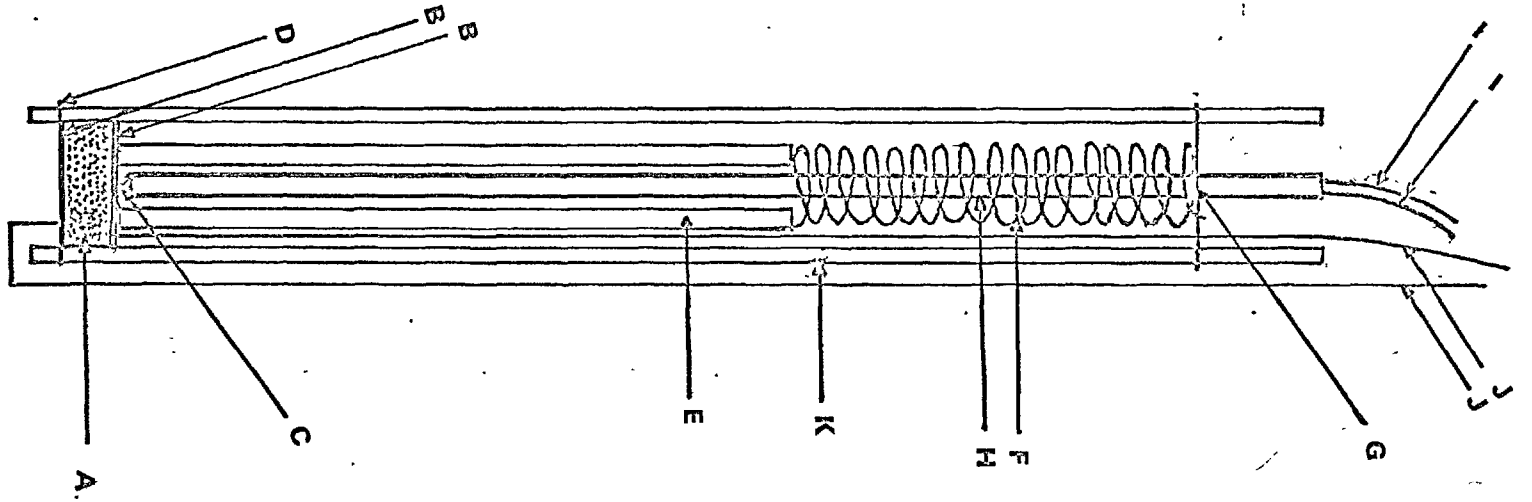

A. Silver oxide pellet
B. Thin circular gold foils
C. 13% Rh-Pt/Pt thermocouple
D. Flat alumina support
E. Narrow-bore alumina tube
F. Compressive spring
G. Pin to contain the spring
H. Alumina thermocouple sheath
I. Thermocouple wires
J. Gold conducting leads
K. Quartz tube

Fig.10 . Pellet assembly for measuring the conductivity of silver oxide.

A. Conductivity of Solid Silver Oxide at 300 and 450 atm. as a Function of Temperature.

Conductivity measurements were made by means of a Wayne Kerr Universal Bridge (B221) operating at 1592 cycles/sec. At thelow resistance range the adapter of type Q 221 was used in conjunction with the bridge which was set at range 3 so that the bridge read resistance directly.

At each temperature, conductivities were measured over a period of 60 to 90 min. at different intervals of time. While the temperature was being raised, the conductivity gradually increased; when the required temperature was reached, it still continued increasing slowly for another 30 min. or so until a constant value was reached. A further 30 to 60 min. were, therefore, allowed to ensure the attainment of complete equilibrium.

During this extended time period the temperature was controlled within $\pm$ 1°. Since the conductivity was sensitive to this small variation of temperature, readings were taken when the exact required temperature was attained during each cycle. The two readings obtained on heating and cooling differed slightly. A number of such pairs of values were therefore obtained at each temperature. The average of the readings obtained by reaching the temperature from below and of those obtained by reaching the temperature from above, was separately calculated. The mean of these two averages was then taken to be the best conductivity value at the given temperature.

The results are given in Table 7 .

Table 7(a)

Data on the electrical resistance of the silver oxide pellet at a constant pressure and different temperatures

A. At 300 atm. oxygen pressure

Temperature °C	Time (min.)	Resistance (Ohms)	Remarks
400	00*	5.93 +**	Pellet dimension:
	05	5.91 +	0.6 cm. dia.
	09	6.03 -	0.5 cm. thickness
	10	5.96 +	
	11	5.93 +	
	12	6.05 -	The Wayne Kerr Bridge in conjunction with the adapter was used.
	15	5.95 +	
	20	6.05 -	
300	00*	40.7 +	
	02	41.9 -	
	05	41.3 +	
	10	41.3 -	
	11	41.4 -	
	12	40.9 +	
	15	41.9 -	
	17	40.8 +	
	19	41.8 -	
	21	40.5 +	
	24	41.7 -	

contd.

* Time of starting measurements.

** +'s and -'s indicate the readings taken at exact temperatures reached from below and above respectively.

Table 7(a) contd.

A. At 300 atm. oxygen pressures

Temp. °C	Time, min.	Conductance (m Mho)	Remarks
250	00	8.26 +	The Wayne Kerr
	05	8.16 -	Bridge alone
	08	8.29 +	was used.
	11	8.26 -	
	13	8.34 +	
	16	8.30 -	
	21	8.28 -	
	28	8.50 +	
	32	8.40 -	
	40.	8.46 +	

Table 7(b)

Conductivities at 300 atm. calculated from the above data :

Temp. °K	Mean conductance (m Mho)	Conductivity $(Ohm\text{-}cm.)^{-1}$	$\log \sigma$	$\frac{1000}{T^{\circ}K}$
673	166.94	0.2950	$\bar{1}.4698$	1.486
573	24.25	0.0429	$\bar{2}.6325$	1.745
523	8.30	0.0147	$\bar{2}.1673$	1.912

Table 7(c)

B. At 450 atm. oxygen pressure

Temp., °C.	Time, min.	Conductance (m Mho)	Remarks
212	00	2.54 -	The Wayne
	30	2.54 -	Kerr Bridge
	40	2.56 +	alone was
	42	2.54 -	used.
	45	2.56 +	
	50	2.54 -	
275	00	14.62 -	
	48	14.82 +	
	53	14.72 -	
	58	14.80 +	
	63	14.64 -	
	66	14.86 +	
	68	14.71 -	
	75	14.76 +	
	80	14.90 +	
	83	14.58 -	
	86	14.72 -	
	88	14.62 -	
	92	14.94 +	
	94	14.63 -	
	96	14.86 +	
	98	14.61 -	
	103	14.96 +	
	107	14.83 +	
	112	14.72 -	
	118	14.94 +	

contd.

Table 7(c) contd.

B. At 450 atm. oxygen pressure

Temp., °C	Time, min.	Resistance, Ohms	Remarks
365	00*	8.532 +	The Wayne
	05	8.572 -	Kerr Bridge
	07	8.592 -	in conjunc-
	08	8.484 +	tion with
	10	8.538 -	the adapter
	15	8.460 +	was used.
	20	8.578 -	
	25	8.424 +	
	30	8.550 -	
	35	8.538 -	
	41	8.460 +	
	45	8.460 +	
	50	8.500 -	
405	00	4.925 -	
	05	4.882 +	
	10	4.930 -	
	15	4.880 +	
	20	4.912 -	
	35	4.904 +	

Table 7(d)

Conductivities at 450 atm. calculated from the above data:

Temp., °K	Mean conductance (m Mho)	Conductivity σ $(\text{Ohm-cm.})^{-1}$	log σ	$\frac{1000}{T^{\circ}K}$
485	2.55	0.0045	$\bar{3}.6532$	2.062
548	14.77	0.0261	$\bar{2}.4166$	1.825
638	117.51	0.2077	$\bar{1}.3175$	1.567
678	203.87	0.3603	$\bar{1}.5567$	1.475

B. Conductivity of Solid Silver Oxide at 400° C as a Function of Oxygen Pressure.

The temperature 400° C was chosen so that the equilibrium would be obtained in a reasonable length of time.

To measure the conductivity at 400° C, the sample was initially subjected to an oxygen pressure of 300 atm. at room temperature. The temperature of the sample was then carefully raised to 400° C. Some of the oxygen was then let out to adjust the pressure to 300 atm. A number of readings was taken at different intervals of time until a constant value was obtained. This required a period of 60 to 120 min. As before, the temperature was controlled within $\pm$ 1° and the bridge readings were taken when the exact temperature was reached.

While taking the pressure up, measurements were also made at 500 and 700 atm. The pressure was then lowered and the measurements were repeated at 500, 400, 300 and 200 atm. The results are given in Table 8 .

Table 8(a)

Data on the electrical resistance of the silver oxide pellet at a constant temperature and different pressures

At 400 °C

Pressure, p (atm.)	Time, min.	Resistance, Ohm	Remarks
300	00	7.00	Increasing pressure
	45	6.60	
	100	6.60	
500	00	5.10	
	15	4.90	
	35	5.00	
	45	4.90	
	60	5.00	
700	00	4.00	
	35	4.20	
	50	4.30	
	68	4.25	
	88	4.30	
	120	4.25	
500	00	4.90	Decreasing pressure
	15	4.80 -	
	17	4.85 +	
	25	5.00 +	
	30	4.95 -	
	45	5.00	

contd.

Table 8(a) contd.

Pressure, p (atm.)	Time, min.	Resistance, Ohm	Remarks
400	00	5.40	Decreasing pressure
	15	5.45	
	35	5.45	
300	00	5.90	
	03	6.00	
	18	6.00	
	45	6.00	
200	00	6.60	
	10	6.66	
	40	6.66	

Table 8(b)

Conductivities at 400 °C calculated from the above data :

Pressure (p atm.)	Mean conductance (m Mho)	Conductivity σ $(\text{Ohm-cm.})^{-1}$	log σ	log p
300	0.1515	0.2678	$\bar{1}.4278$	2.4771
500	0.2000	0.3535	$\bar{1}.5484$	2.6990
700	0.2353	0.4159	$\bar{1}.6189$	2.8451
500	0.2000	0.3535	$\bar{1}.5484$	2.6990
400	0.1835	0.3243	$\bar{1}.5109$	2.6021
300	0.1667	0.2946	$\bar{1}.4692$	2.4771
200	0.1502	0.2655	$\bar{1}.4240$	2.3010

CHAPTER IV

Experimental Section 3

HIGH PRESSURE THERMOGRAVIMETRY

1. GENERAL INTRODUCTION

Thermogravimetry may be defined as an experimental technique to measure the weight changes in a sample as it is exposed to heat. The change in weight of the sample may be recorded as a function of time at constant temperature or as a function of both temperature and time; the correspondin g methods are known as isothermal and dynamic thermogravimetry. After Honda[79] built his thermobalance in 1915, thermogravimetry has undergone immense development in its technique and applications. This has been illustrated by an extensive review, with 332 references, on thermogravimetric analysis by Coats and Redfern[80]. But although this technique has been developed to a high degree of sophistication for studying systems under atmospheric and vacuum conditions[81,82,83], thermogravimetric studies under high pressure have been rather scarce. The three main publications on high-pressure thermogravimetry are due to Rabatin and Card[84], Biermann and Heinrichs[85] and Baker[86].

Rabatin and Card employed a modified torsion balance as the mass sensitive element and an optical lever photoelectric cell transducer system to develop voltage proportional to mass for automatic recording.

In Biermann and Heinrichs' design, which was used with a pressure range from 0 to 60 atm., the mass sensitive element was a tool-steel cantilever rod rigidly fixed on one end, which undergoes varying displacement on the free end as the sample, supported on the free end,

changes mass. The amount of displacement was determined by a linear variable differential transformer (LVDT) whose output was demodulated and fed to a recording potentiometer.

Baker's mass sensitive element was a Pyrex glass spring whose extension was proportional to the total load; extension of the spring was read optically with a cathetometer.

Of these, the first two methods are quite involved so far as their design and construction are concerned; the spring balance, on the other hand, is simple and convenient.

The use of spring balances in high pressure thermogravimetry, e.g., in the study of high pressure oxidation of metals by McKewan and Martin Fassell[87] and in the study of carbonate systems by Baker is relatively new. It's use otherwise, however, dates back to 1915[88]. McBain[89,90] used spring balances for a variety of studies under vacuum. Glass and silica (quartz) springs have been in extensive use; but because of their fragility, springs of tungsten[91] or copper-beryllium[92] alloy have been developed.

The sensitivity of a spring balance is dependent on the diameter of the fibre and the coil, the number of coils per unit length of the spring and the temperature of the spring. The range, which is the maximum variation in mass that the balance can take for a given load and the capacity which is simply the maximum permissible load, dictate the sensitivity to be selected.

In order to obtain reliable results from a thermobalance, it should possess the features suggested below.

The balance should be capable of recording weight changes with adequate capacity and sensitivity. It may, however, be pointed out that the sensitivity of a balance usually decreases with increasing capacity and that spring balances are affected more than the beam balances in this respect.

Since a thermobalance is to be used at various temperatures, it should be designed so that the accuracy will not be affected by variations in ambient temperatures. Otherwise corrections must be applied for such effects.

To obtain reproducible thermogravimetric results, it is important that the sample-holding crucible should always be located in the same lateral and vertical position, preferably the centre of the furnace tube for each experiment. Likewise, the thermocouple or other temperature sensing device should be placed in the same position for all the experiments and should be positioned as close as possible to the sample.

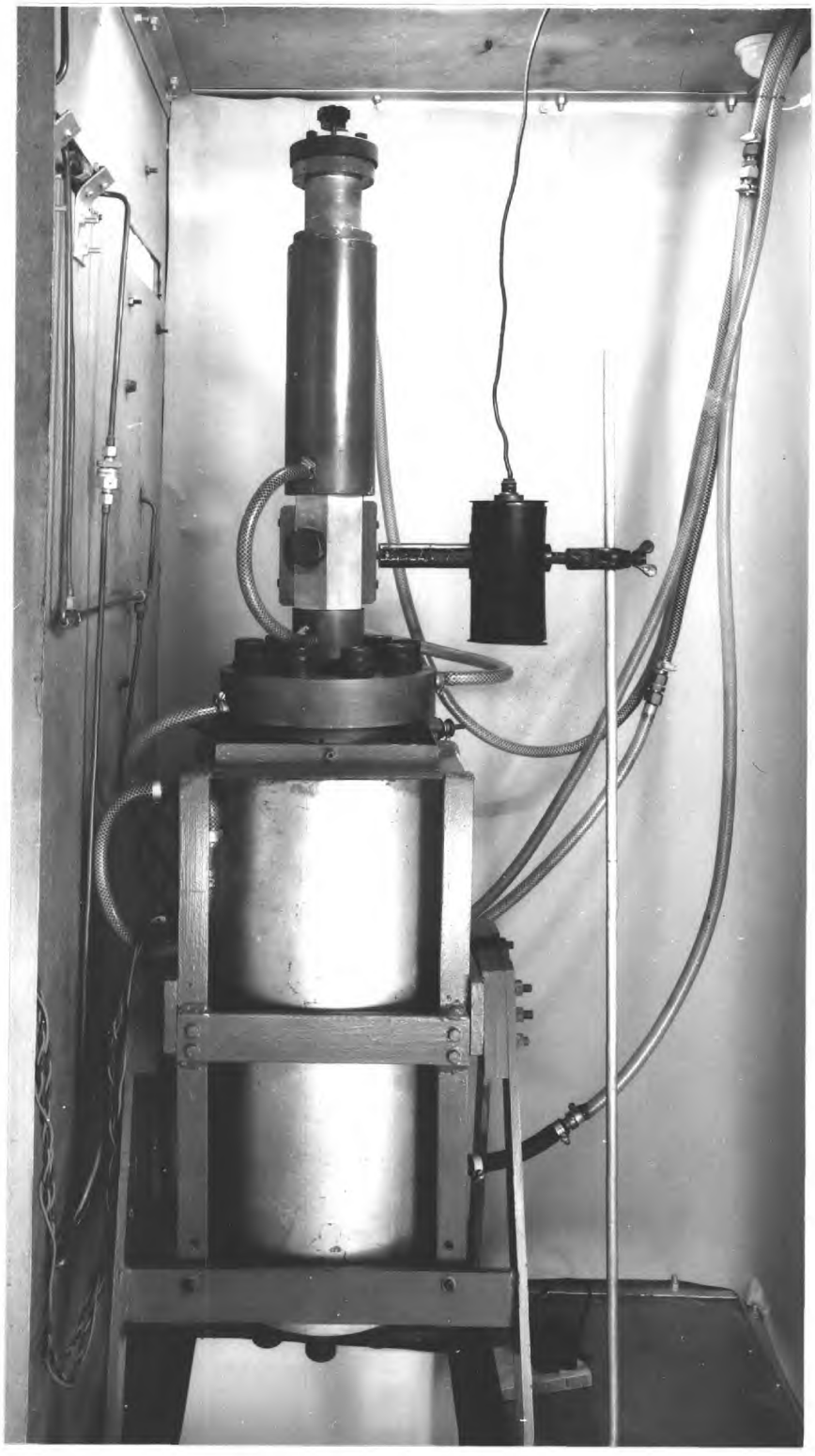

Plate No. 3a. A photograph of the thermogravimetric set up.

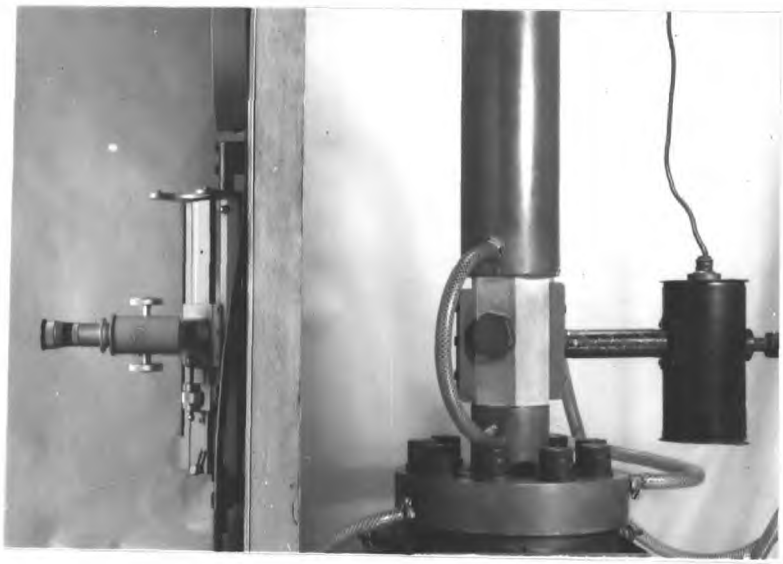

Plate No. 3 b. Part of the thermogravimetric set up showing the Cathetometer for measuring the spring extension.

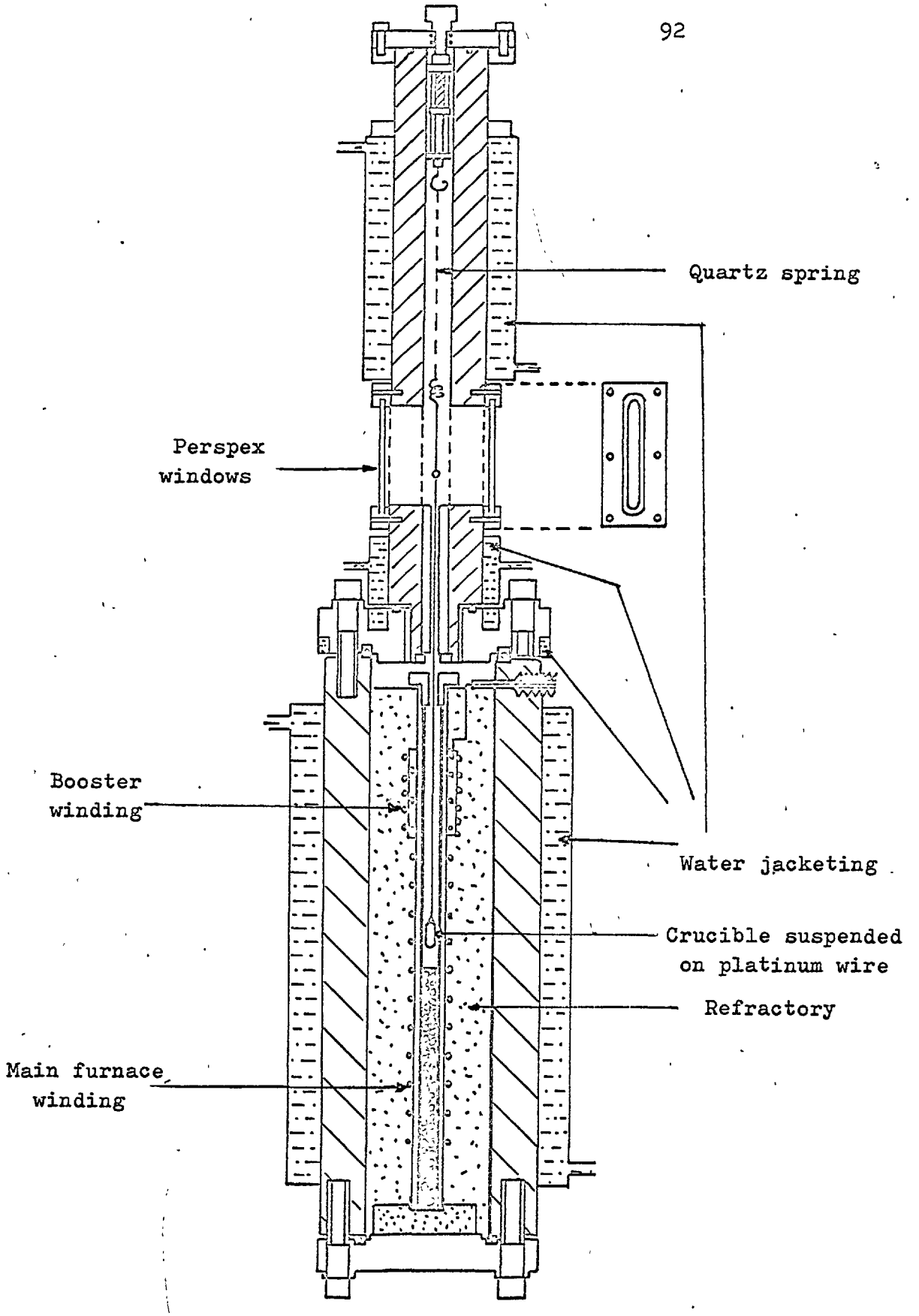

Fig. 11 . A sectional view of the thermogravimetric set-up ($\times \frac{1}{6}$).

2. THE THERMOGRAVIMETRIC SET-UP

The thermogravimetric apparatus used for measuring the solubility of oxygen in liquid silver was an improved version of that used by Baker[93] in his study of carbonate systems. The main improvements were: jacketing of the wide length of the housing,containing the quartz spring; the use of a larger pressure vessel incorporating a longer furnace winding; incorporation of power terminals isolated electrically from the vessel. The essential unit of the apparatus was a resistance furnace enclosed in a pressure vessel fitted with a spring-housing for the spring. The rest of the equipment was used for measuring and controlling temperature and gas pressure and was the same as that described earlier. A photograph of the thermogravimetric set-up is shown in Plate 3 and a sectional view of the apparatus is shown in Fig. 11.

A. Furnace

Two furnaces were used; one for temperatures up to 950° C and the other for the higher temperature range. Both furnaces had booster windings to compensate for thermal losses at the top of the furnace.

The lower-temperature furnace tube was of mullite, and was 55 cm in length with a bore diameter of 2.5 cm. The heating element was oxidized Nichrome wire of 16 S.W.G. The furnace was wound linearly on a lathe at 6 turns of wire per inch. The length of the main winding was 40 cm.

The element of the booster winding was also Nichrome, but of 22 S.W.G. The length of the booster winding was 12 cm and it was wound over the top third of the main furnace element. Six Mullite-strips acted as an insulator between the two elements. The winding density of the booster was 10 turns per inch.

The resistance of the main and booster windings were respectively 5 and 18 ohms at room temperature.

The higher-temperature furnace tube was of alumina, and was 52.5 cm in length with a bore diameter of 2.6 cm. But to minimize gas turbulance, the bore diameter was reduced to 1.8 cm by sliding another alumina tube inside it. The heating element was 10% Rhodium-Platinum wire of 20 S.W.G. The same wire was used also for the booster winding. The winding densities for the main and booster windings were respectively 8 and 10 turns per inch and the resistances were respectively 3.5 and 0.5 ohms at room temperature.

For both furnaces, pure alumina cement was used to keep the furnace windings in position.

For the lower-temperature furnace, the refractory between the furnace and walls of the vessel was Fiberfrax. This was an alumina-silica fibre supplied by the Carborundum Co. Long staple medium fibre was used at a recommended packing density of about 6 lbs per cubic feet.

Owing to the fact that Fiberfrax is unsatisfactory for temperatures above 1150° C, the central part of the higher-temperature furnace was insulated with alumina powder; only the top and bottom portions were

insulated with Fiberfrax. The fiberfrax at the top part of the furnace served to prevent transfer of alumina powder into the furnace tube when flushing with oxygen.

The temperature distribution for the Nichrome-wound furnace at a pressure of 30 atm. of oxygen is shown in Fig. 12. The temperature distribution for the platinum furnace was also checked and found to be similar.

B. Springs

Fused quartz springs were used to measure the weight changes. The springs used in the present work were of type T/A9S/72 No.40 for use with a maximum load of 10 g. and were supplied by Thermal Syndicate Ltd. The sensitivity (about 2 cm/g) for each spring was determined accurately by Thermal Syndicate Ltd.; careful checks, however, were made in the laboratory and sensitivities were always found to agree with those determined by the supplier.

The spring was maintained at a constant temperature of 18 ± 1^0 by continuous water circulation around the spring-housing. Baffles were fitted below the spring to protect it, as far as possible, from convection currents from the furnace.

To facilitate setting-up, the spring assembly and the baffles were fixed in a thin-walled tube which slid into the main housing.

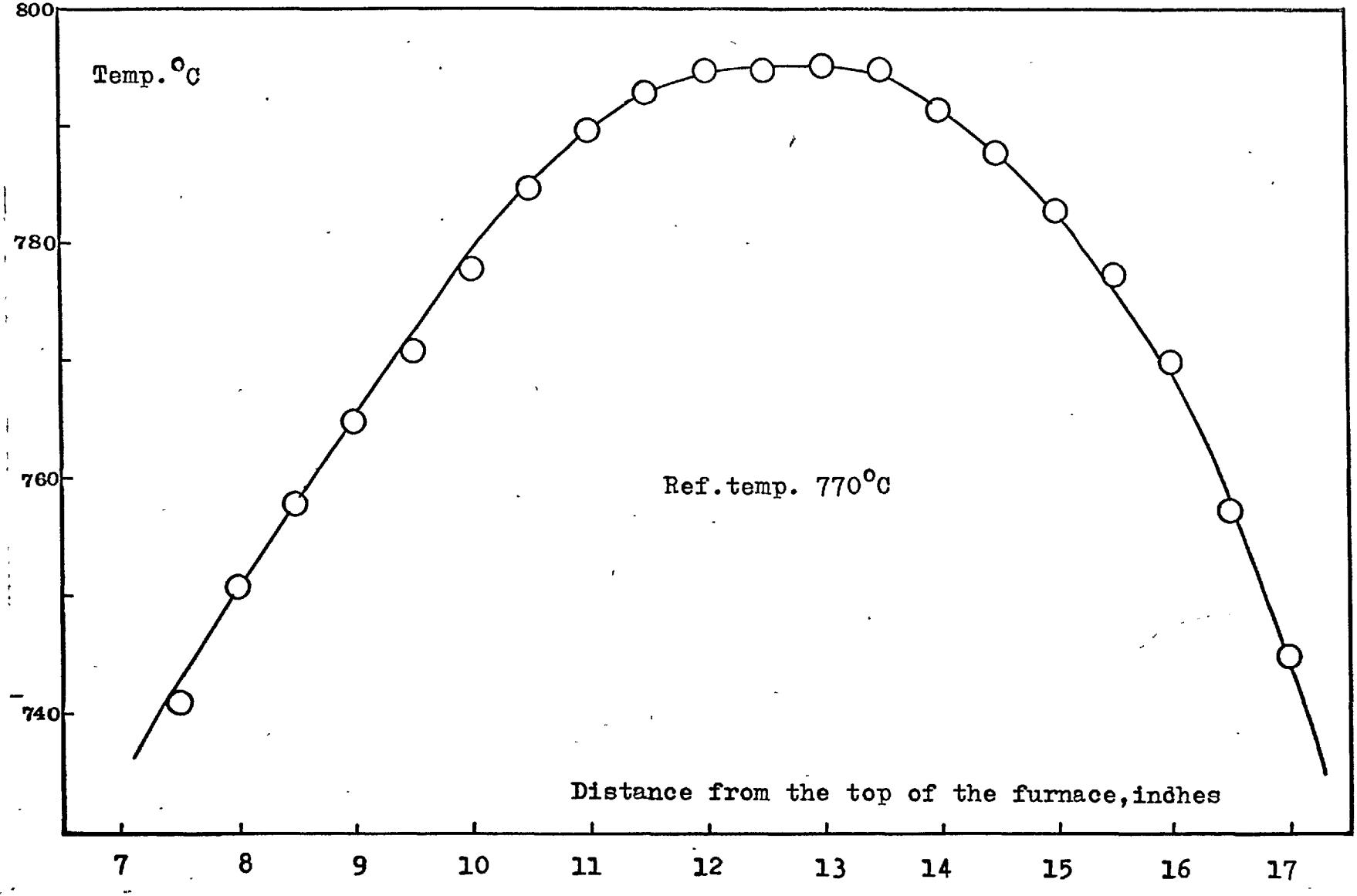

Fig.12(a). Temperature gradient along the length of the Nichrome-wound furnace in air:(only main winding used).

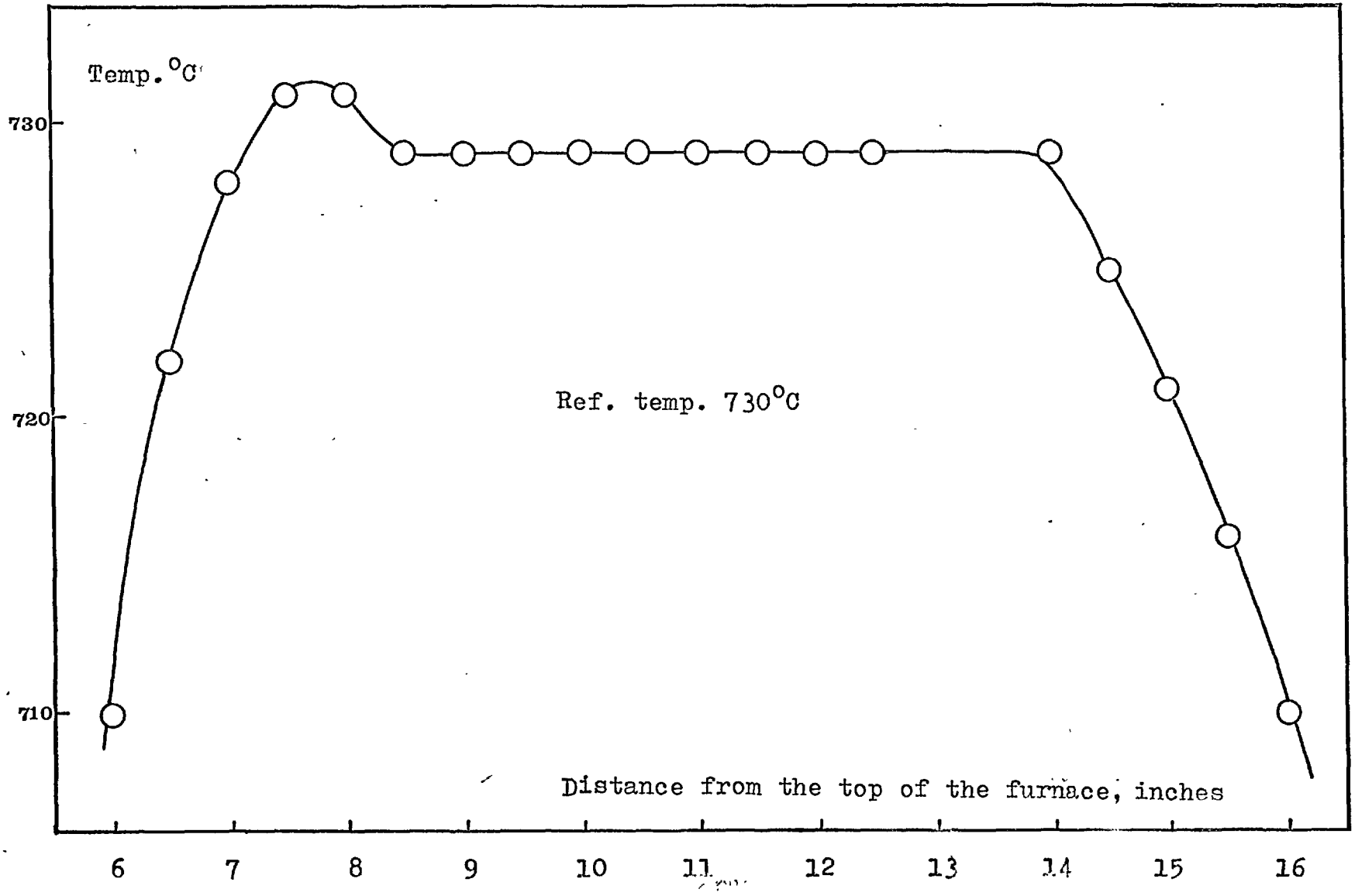

Fig. 12(b). Temperature gradient along the length of the Nichrome-wound furnace in air:(booster winding used).

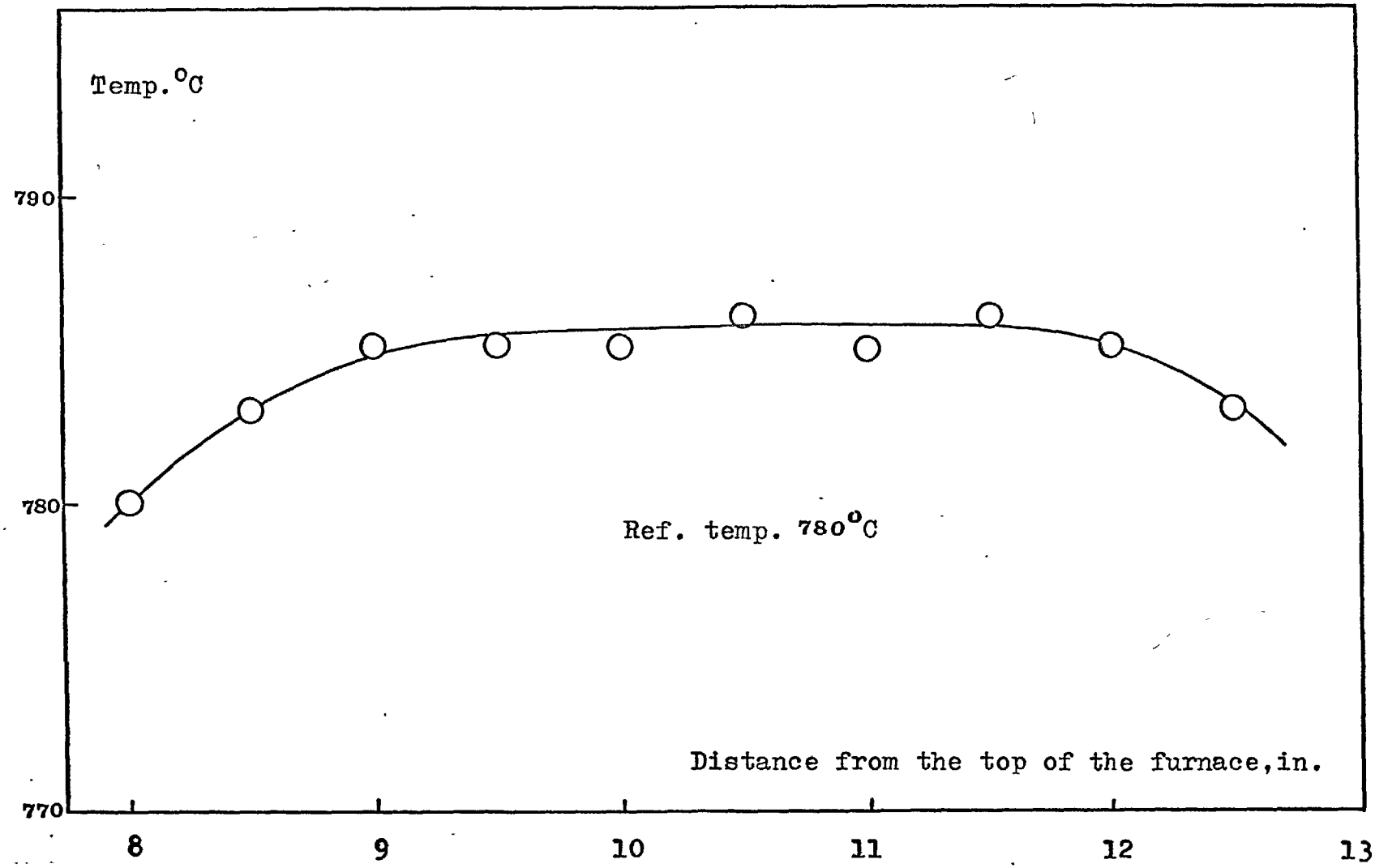

Fig.12(c). Temperature gradient along the length of the Nichrome-wound furnace at 30 atm.(booster winding used).

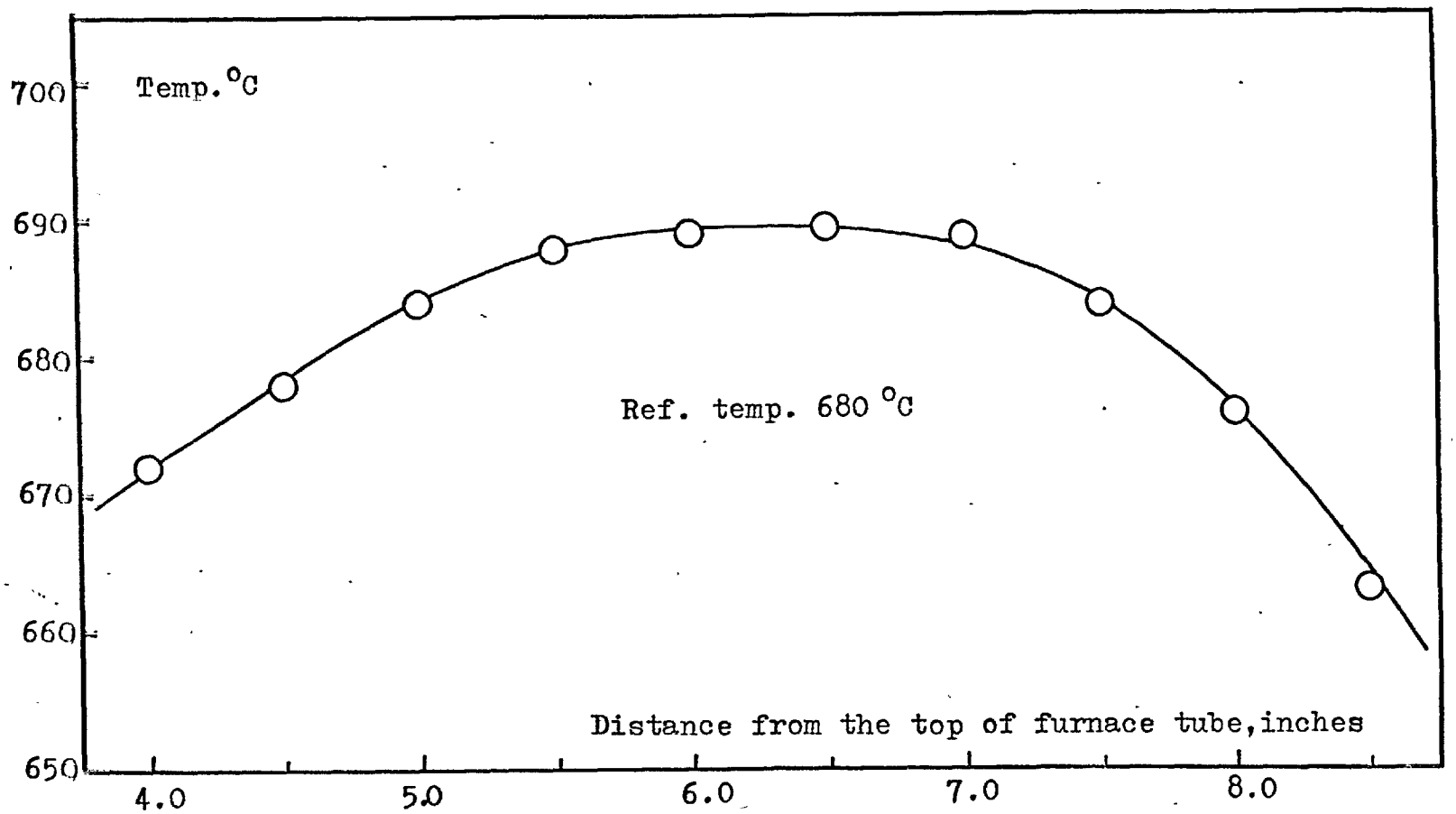

Fig. 12(d). Temperature gradient along the length of the singly wound Nichrome furnace in air (used at pressure s up to 750 atm. in horizontal high pressure furnace, cf. p. 52). Constant temp. zone is virtually independent of pressures.

C. Windows

The spring housing was provided with two Perspex windows of 1 cm thickness for observing the spring. Both windows were 1 cm wide and were clamped against gaskets fitted to slots, 5 mm wide, in the spring-housing.

D. Sample-Holding Crucibles

Recrystallized alumina crucibles of 1 cm bore and 2.5 cm length were used to contain samples. The crucibles, each with the platinum-suspension hook weighed usually between 3 to 3.5 g. and were hung from the spring by means of a platinum wire of 0.3 mm diameter. The length of the platinum wire was so adjusted as to place the crucible in the constant temperature zone of the furnace. Together with 5 g. of sample, the total weight did not exceed 9 g.

CHAPTER V

Experimental Section 4

MEASUREMENTS AND PROCEDURE

1. DETERMINATION OF THE MELT COMPOSITION ALONG THE SILVER LIQUIDUS *

By careful adjustment of the suspension wire, the crucible containing the sample was placed between the two thermocouples spaced 2.5 cm apart in the hot-zone of the furnace. The vessel was flushed with oxygen several times, it was then pressurized and the furnace temperature raised. During heating, the pressure of the gas increased and it was necessary to let out some of the gas from time to time to keep the pressure constant. The sample was heated to about 10-15° below the expected melting point and then the temperature was kept constant for about half an hour. This helped stabilize the gaseous environment and the temperature distribution of the furnace. After this, the initial reading of the spring was recorded. The temperature was then raised to about 15° C above the fusion point, kept there for about 30 minutes, then carefully lowered to the fusion point. This ensured that the fusion temperature was as accurately obtained as was possible. By means of the two thermocouples, near the bottom and top of the crucible, accurate control of the sample-temperature was maintained. The sample was kept at the fusion point until a constant weight was obtained; this required 3-4 hours.

It may be noted that more than 70 per cent of the oxygen dissolved in the silver in the first 15-20 min. However, this rather protracted length of time required to attain saturation was attributed to the slow dissolution of the last traces of solid. Typical solubility vs. time plots are shown in Fig.13. Compositions of the melt along the liquidus are given in Table 9.

* page 68

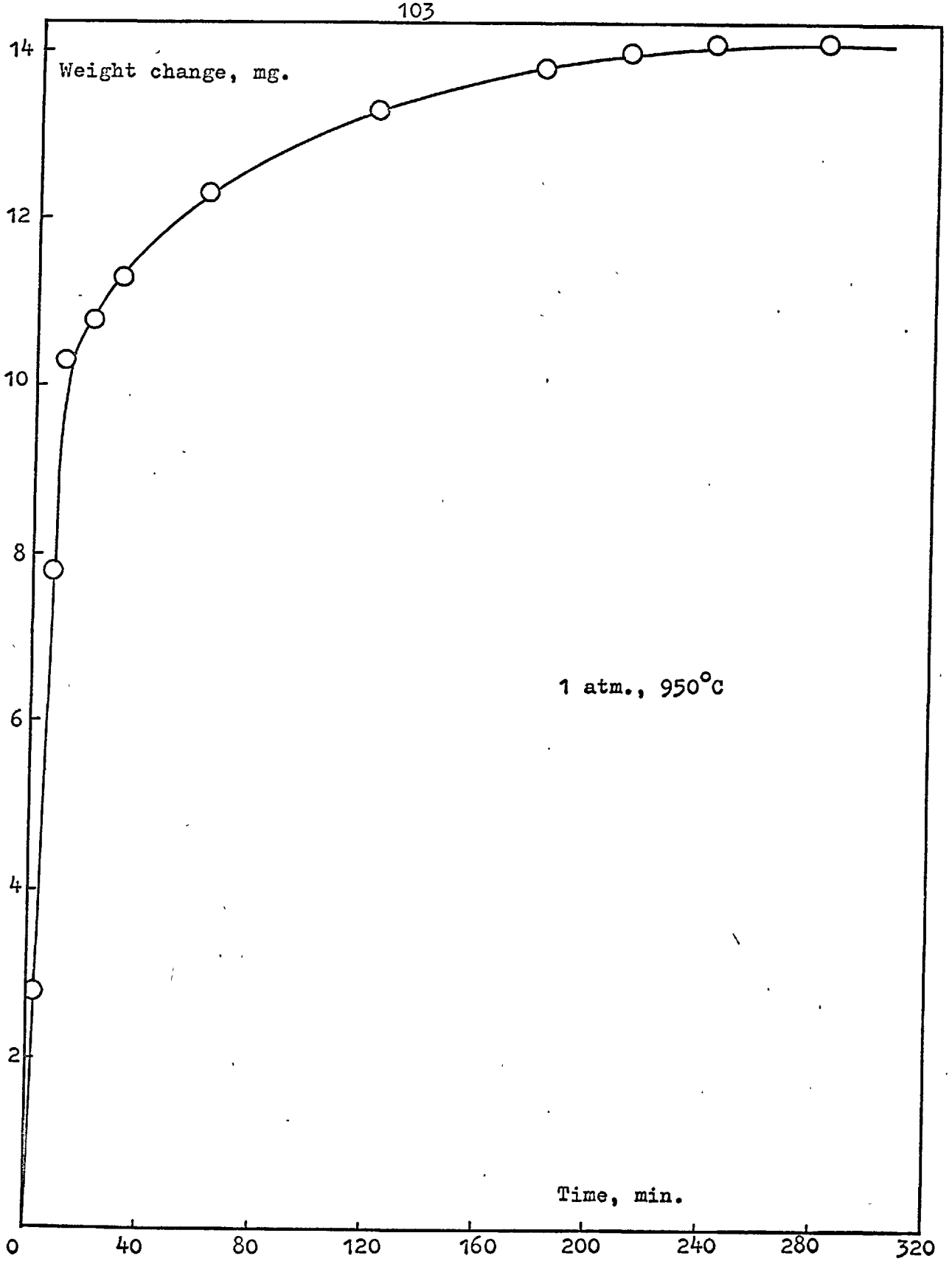

Fig.13(a). Solubility versus time curve.

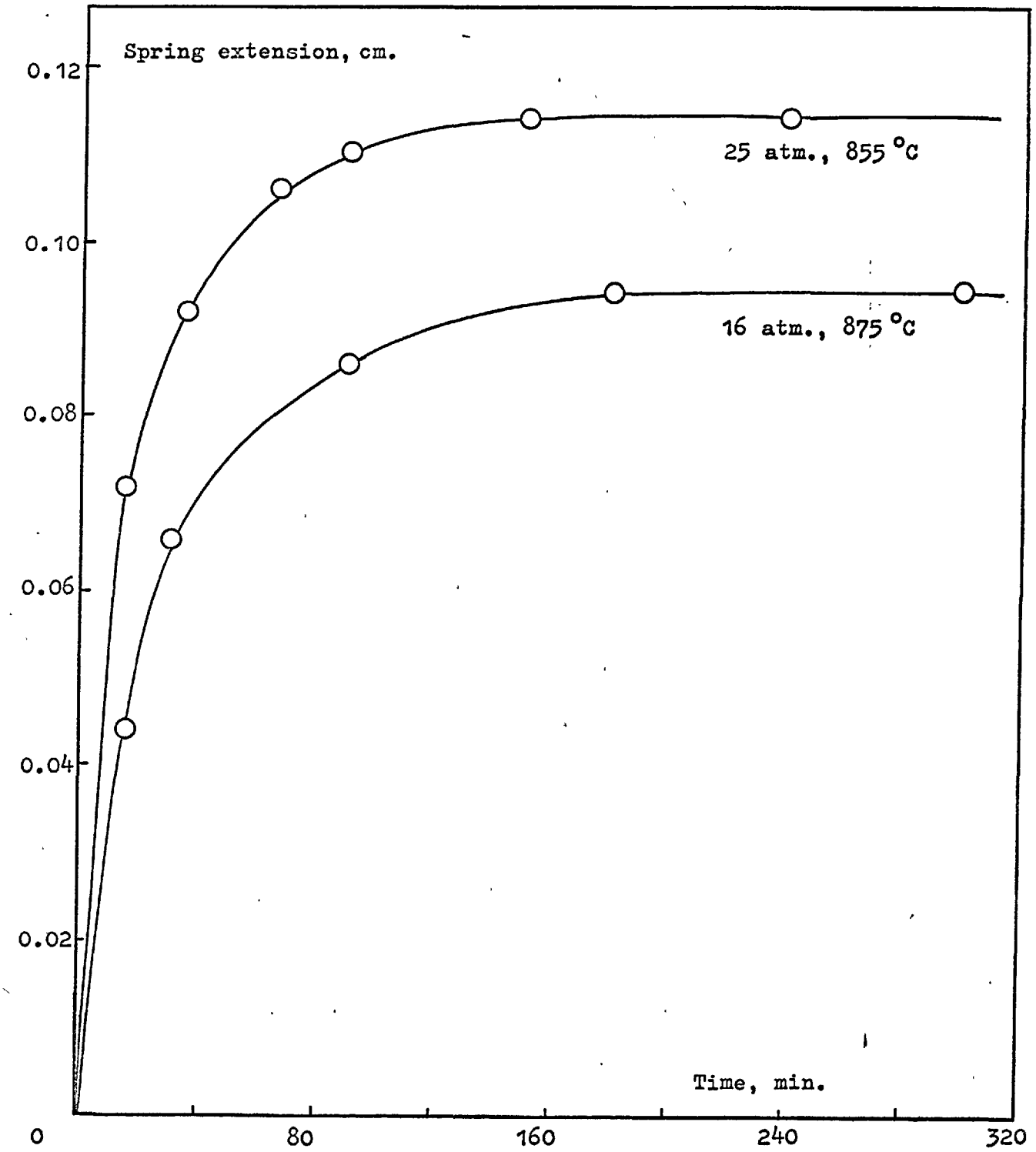

Fig.13(b). Solubility versus time curve.

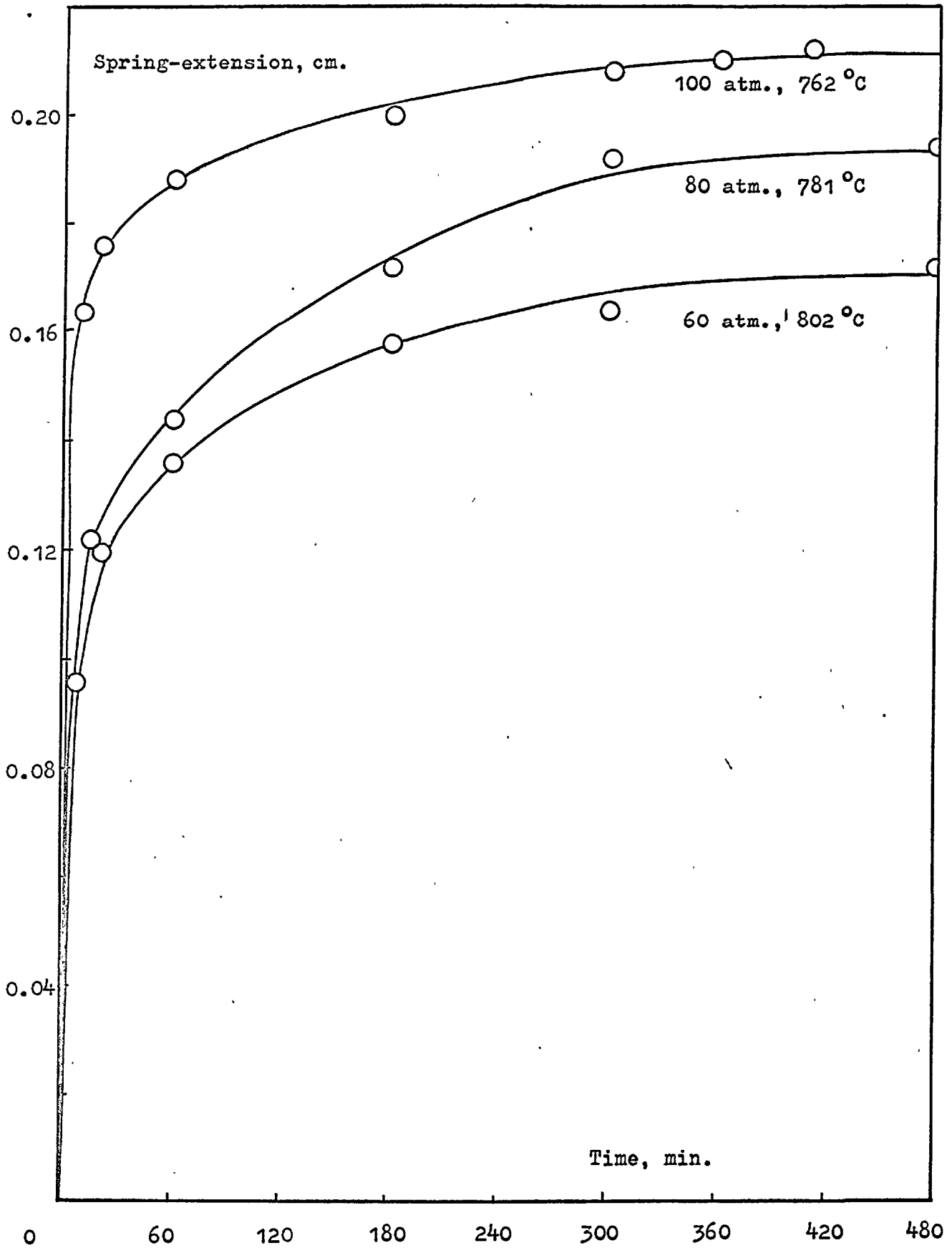

Fig. 13(c). Solubility versus time curve.

Table 9

Results of thermogravimetric measurements along the silver liquidus

p (atm.)	T °K	$N_O \cdot 10^2$	$N_{Ag_2O} \cdot 10^2$
2.5	1196	3.145	3.356
4.0	1188	4.027	4.380
9.0	1168	5.295	5.921
16.0	1148	6.857	7.949
20.0	1139	7.138	8.325
25.0	1128	7.961	9.470
30.0	1119	8.161	9.803
36.0	1109	8.947	10.900
45.0	1095	9.720	12.067
60.0	1075	10.727	13.650
80.0	1054	11.904	15.620
100.0	1035	12.900	17.380

2. DETERMINATION OF ISOTHERMAL COMPOSITIONS

The isothermal compositions of the melt in the liquid region at 950° C and 1050° C were determined. The procedure was similar to that above except that after recording the initial setting of the spring at 10-15° below the fusion point, the sample was taken directly to the required temperature. Since diffusion of oxygen into the liquid was the rate determining factor, at these higher temperatures, constant weight was readily obtained within the two hours. But because the initial reading of the spring was taken at a lower temperature and the final reading was taken at a considerably higher temperature, the change in buoyancy due to the variation in gas density had to be taken into account. At 60 atm., for example, the initial setting of the spring was made at about 780° C where the gas density was higher than that at the temperature of the solubility measurement. Buoyancy corrections have consequently been applied to the results at the highest pressures. Changes of buoyancy resulting from the change in volume of the silver on fusion was insignificant, whilst the spring itself was protected from any buoyancy variation owing to its housing being maintained at constant temperature and pressure.

Compositions determined thermogravimetrically are considered to be accurate, on an average, with $\pm$ 2%.

Because of the limitation of the sensitivity of the spring (2 cm/g), accuracy of the measurements involving low weight changes were also limited. Consequently, a Stanton Automatic balance

(type MF-H5) was used for measuring solubility at 1 atm. pressure of oxygen.

Both uncorrected and corrected compositions of the melt at 950° and 1050° C are given in Table 10. Details of buoyancy correction are given in Appendix 3.

Another factor which could become significant at these elevated temperatures and therefore affect the solubility measurements adversely, is the volatility of silver. It is known that the vapour pressure of a substance is dependent on an applied inert-gas pressure, the dependence being expressed by the relation

$$\frac{dp}{dP} = \frac{V_{cond.}}{V_{gas}}$$

where P is the pressure of the inert gas; but in view of the small value of $\frac{V_{cond.}}{V_{gas}}$ (of the order of 10^{-4}) the pressure effect on the vapour pressure at low applied pressure is negligible. However, very large external pressures could, of course, result in noticable changes in the vapour pressure. Formation of volatile oxides is more likely to increase the loss of silver in an oxygen atmosphere; Alcock's[94] study of the volatility of platinum metals in oxygen atmospheres typically illustrate this point.

That the vapour pressure of silver increases with oxygen pressure has been reported[95,96]. As a result, experiments were carried out to see if the volatility could cause detectable errors in the solubility measurements. The experiments were as follows:

Table 10 a

Results of thermogravimetric measurements on silver-oxygen system at 950°C (1223°K)

p (atm.)	$No^{*}.10^{2}$	$No.10^{2}$	$N_{Ag_2O}.10^{2}$
1	1.870	1.870	1.943
2	2.789	2.789	2.954
4	3.549	3.549	3.820
9	5.092	5.092	5.669
16	6.453	6.376	7.308
25	7.480	7.364	8.636
40	9.175	8.929	10.870
60	10.186	9.716	12.059
100	11.815	10.844	13.848

No^{*} = uncorrected atom fraction of oxygen.

No = atom fraction of oxygen corrected for buoyancy.

N_{Ag_2O} = Mole fraction of silver oxide.

Table 10 b

Results of thermogravimetric measurements on silver-oxygen system at 1050°C(1323°K)

p (atm.)	$No.^{*}10^2$	$No.10^2$	$N_{Ag_2O}.10^2$
1	1.790	1.790	1.856
2	2.249	2.249	2.355
4	3.156	3.156	3.369
9	4.496	4.496	4.940
16	5.868	5.727	6.468
25	6.706	6.494	7.464
40	8.224	7.796	9.237
60	9.456	8.822	10.712

No^{*} = uncorrected atom fraction of oxygen.

No = atom fraction of oxygen corrected for buoyancy.

N_{Ag_2O} = Mole fraction of silver oxide.

In some of the high pressure measurements, the sample was heated for a further two hours after it had attained a constant weight to see if the weight ultimately decreased. Since no apparent diminution in weight was observed, the volatilization of silver was considered to be insignificant. Confirmation of this was also obtained by heating a weighed sample of silver at 950° C and 14.5 atm. of oxygen pressure for 5 hours in a crucible sufficiently long to eliminate loss by spitting and weighing after cooling; less than 0.003% of the silver was lost by volatilization. On the other hand, in measurements with the Stanton Automatic balance where a flow of oxygen was maintained, significant volatilization was observed. For example, when a sample at 1050° C and under atmospheric pressure of oxygen, was kept at this temperature for a further period of 4 hours after the attainment of the constant weight, it lost 0.1% by evaporation. The diminution in the volatility under a static oxygen pressure is probably due to a blanketing effect which inhibits diffusion of silver (or a volatile oxide) away from the sample.

CHAPTER VI

Experimental Section 5

GOLD-SILVER ALLOYS

1. MEASUREMENTS ON THE GOLD-SILVER-OXYGEN SYSTEM

A. Effect of Oxygen Pressure on the Melting Point of Gold-Silver Alloys

In order to study the effect of alloyed gold on the solubility of oxygen in liquid silver, alloys of three different compositions, namely, 10%, 20% and 40% gold were selected.

To determine the fusion points of the alloys, the procedure followed was the same as that for the determination of the pressure-temperature relation for silver, except that the alloy in wire-form was welded to the ends of two platinum wires instead of gold wires. The alloy wires, 0.5 mm in diameter, were supplied by Johnson and Matthey and were of purity better than 99.99%. The results are given in Table 11. The melting points of these alloys determined under an argon pressure of 1 atmosphere are given at the end of the Table11.

B. Measurements of the Oxygen Solubility in Alloys

From the smaller depressions of the melting points of the alloys compared to those of silver it follows that the solubility of oxygen in the alloys must be lower than that in silver.

Isothermal solubility measurements at 1050° C were made thermogravimetrically. The alloys, however, were prepared "in situ" from weighed amount of pure gold and silver. .Operational procedure was as follows:

The vessel was first flushed with nitrogen several times to ensure removal of the last traces of air. It was then pressurized with

Table 11(a)

Fusion Temperatures of 10% Au-Ag alloy* under Oxygen pressures

Oxygen Press. p(atm.)	Fusion Temp. T °K	log p	1000/T °K
0.21	1239.5	$\bar{1}.3222$	0.8068
1.00	1233.5	0.0002	0.8107
2.24	1225.0	0.3502	0.8163
3.57	1223.0	0.5527	0.8177
3.62	1222.0	0.5587	0.8183
5.30	1213.0	0.7242	0.8244
11.0	1204.0	1.0414	0.8306
13.5	1201.0	1.1303	0.8326
22.5	1185.0	1.3622	0.8439
62.0	1159.0	1.7924	0.8628
80.0	1155.0	1.9031	0.8658
82.8	1154.5	1.9180	0.8662
101.8	1141.5	2.0076	0.8760
111.0	1138.0	2.0453	0.8787
121.5	1136.5	2.0845	0.8799
128.5	1129.0	2.1089	0.8857
170.0	1119.0	2.2304	0.8937
200.0	1112.5	2.3010	0.8989
220.5	1111.0	2.3433	0.9001

* Melting Temperature under 1 atm. of Argon is 1247 °K.

Table 11(b)

Fusion Temperatures of 20% Au-Ag alloy* under Oxygen pressures

Oxygen Press. p(atm.)	Fusion Temp. T °K	log p	1000/T °K
0.21	1254	$\bar{1}$.3222	0.7974
1.00	1249	0.0000	0.8006
2.58	1248	0.4116	0.8013
5.30	1238	0.7243	0.8078
8.70	1236	0.9395	0.8090
23.5	1228	1.3711	0.8143
50.0	1219	1.6990	0.8203
67.0	1209	1.8261	0.8270
76.0	1209	1.8808	0.8271
98.5	1189	1.9934	0.8410
101.0	1190	2.0043	0.8400
131.0	1199	2.1173	0.8340
150.0	1190	2.1761	0.8403
170.0	1187	2.2304	0.8425
191.0	1178	2.2810	0.8489

* Melting Temperature under 1 atm. of Argon is 1259 °K.

Table 11(c)

Fusion Temperature of 40% Au-Ag alloy* under Oxygen pressures

Oxygen Press. p(atm.)	Fusion Temp. T °K	log p	1000 / T °K
0.21	1278	$\bar{1}$.3222	0.7825
1.00	1277	0.0000	0.7830
3.56	1277	0.5514	0.7834
9.50	1272	0.9777	0.7862
21.3	1269	1.3284	0.7880
40.5	1266	1.6075	0.7899
61.0	1264	1.7853	0.7911
101.0	1258	2.0043	0.7949
139.0	1251	2.1430	0.7994
188.5	1253	2.2754	0.7981
207.0	1251	2.3160	0.7994
212.0	1250	2.3263	0.8000

* Melting Temperature under 1 atm. of Argon is 1280 °K.

nitrogen to a pressure 1 atm. higher than the oxygen pressure intended to be used. The sample was then heated to 1050° C. During heating, some of the nitrogen had to be let out to keep the pressure constant. After allowing for the stabilizing period, the initial reading of the spring was taken. Nitrogen was then let out slowly until the pressure fell to 1 atm. Oxygen was then introduced to the desired pressure. When, for example, the desired pressure of oxygen was 25 atm., the oxygen was run in until the pressure gauge read 26 atm. Since the initial reading of the spring was taken at a nitrogen pressure 1 atm. above the required pressure (in this case at 26 atm.), no buoyancy correction was necessary. The success of this method depended on the fact that the densities of oxygen and nitrogen were nearly the same. That the replacement of nitrogen by oxygen did not have any detectable buoyancy effect on the spring reading was confirmed by carrying out a blank experiment in which the alumina crucible alone was suspended, and the nitrogen was replaced by oxygen at the same pressure. No variation in spring reading was observed. This tedious pressurizing procedure was necessary because normal flushing would have caused dissolution and explosive evolution of oxygen.

The result of solubility measurements are given in Table 12.

Table 12

Results of thermogravimetric measurements on Au - Ag - O alloys at 1050°C (1323°K)

Alloys	Press. (p atm.)	$10^3 . n_O/n_{Ag}$	$10^2 . N_O$	$10^2 . N_{Ag_2O}$
10 % Au-Ag,	1	13.86	1.290	1.324
n_{Au}/n_{Ag} =	2	15.77	1.465	1.509
0.06084,	4	23.66	2.182	2.282
	9	33.80	3.088	3.291
N_{Au}=	16	45.33	4.098	4.463
0.0574	25	51.12	4.598	5.064
	40	68.16	6.037	6.866
	60	73.61	6.520	7.498
20 % Au-Ag,	1	8.91	0.776	0.788
n_{Au}/n_{Ag} =	2	13.92	1.209	1.239
0.1369	4	20.11	1.734	1.796
	9	28.39	2.436	2.561
N_{Au} =	16	38.15	3.247	3.472
0.1205	25	44.35	3.755	4.060
	40	53.35	4.482	4.923
	60	65.73	5.100	5.679
40 % Au-Ag,	1	3.09	0.226	0.227
n_{Au}/n_{Ag} =	9	13.16	0.955	0.973
0.3651	16	17.54	1.267	1.300
N_{Au} =	25	22.37	1.612	1.666
0.2674	40	28.76	2.063	2.152
	60.	35.15	2.510	2.643

N_i = Atom fraction i. n_i = number of moles i.

CHAPTER VII

Results and Discussion

1. THE EUTECTIC POINT

The melting temperatures of silver and silver oxide as functions of oxygen pressure have been combined with the pressure-temperature relation of Keyes and Hara for the dissociation of solid silver oxide[50] to obtain the eutectic point for the system (Fig.14).

Before making further comment on this eutectic point (530° C and 530 atm.), it is worth discussing the effect of the purely mechanical pressure exerted by the gas phase on the system. In principle, the effect of external pressure on the melting temperature of a solid can be calculated by using the Clapeyron equation, i.e.,

$$\frac{dP}{dT} = \frac{\Delta H_f}{T(V_L - V_S)} \qquad (10)$$

where, V_S and V_L are, respectively, the molar volumes of the component in the solid and liquid state, in equilibrium at the temperature, T, and ΔH_f the heat of fusion. The significance of the estimation of this effect will, therefore, depend on how accurately the molar volumes are known as functions of applied pressure and temperature, and the heat of fusion as a function of temperature.

For silver, the molar volumes as a function of pressure are not known. The densities of the solid[97] and liquid[98] silver, as functions of temperature, are available.

However, using the equation (10) and by taking the molar volumes and the heat of fusion at the melting point as temperature-independent

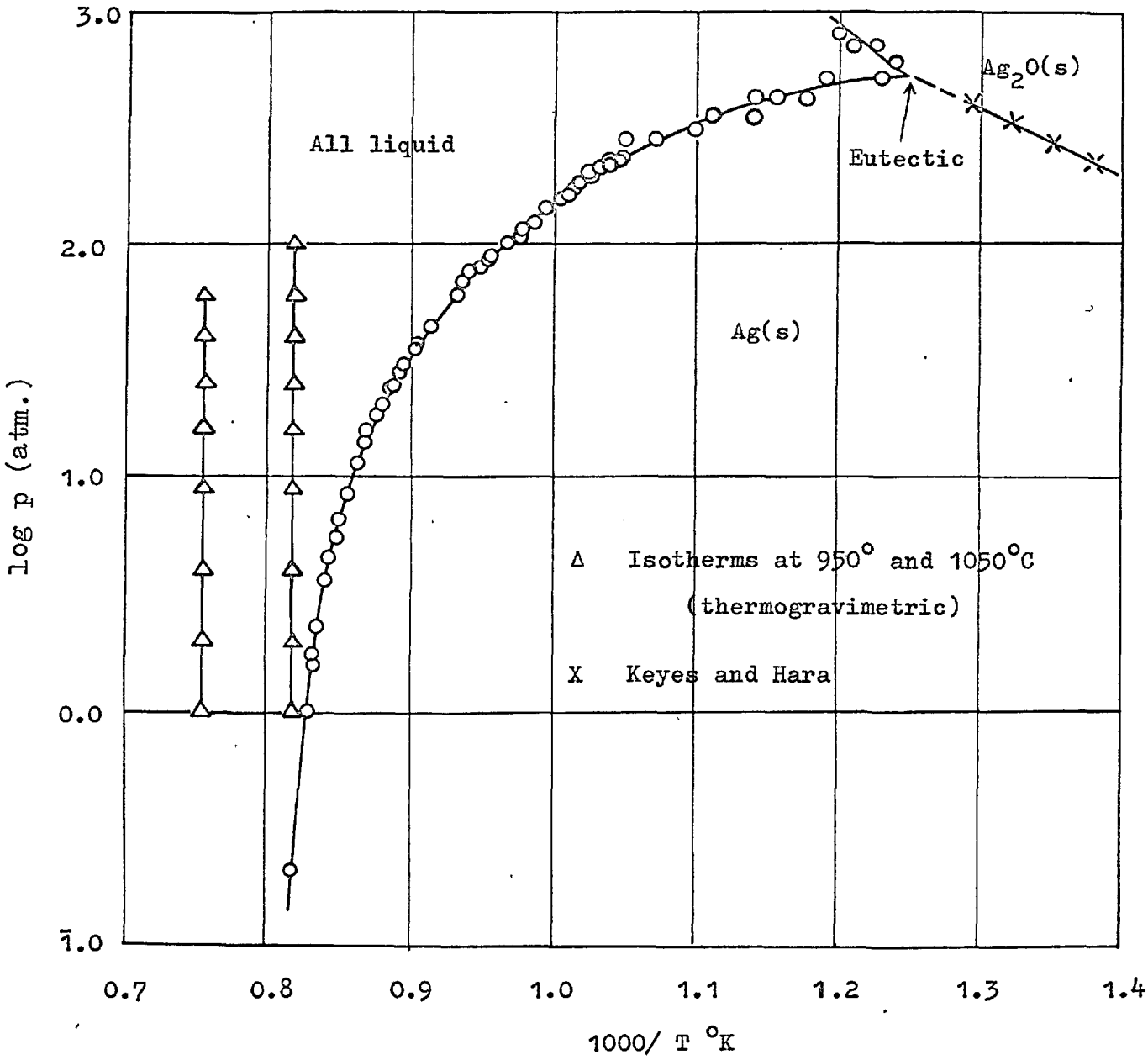

Fig. 14 . Pressure-temperature relation for silver-oxygen system.

constants, an approximate calculation of the effect of applied pressure on the silver liquidus at the eutectic point is made. This shows that the eutectic temperature is raised by about 7° C, e.g.,

$$\Delta T = \frac{529 \times 1234 \left(\frac{107.88}{9.346} - \frac{107.88}{10.5}\right) \times 1.01325 \times 10^6}{2855 \times 4.1845 \times 10^7} \text{ degree}$$

$$= 529 \times 1.3281 \times 10^{-2} = 7.026 \text{ degree.}$$

This calculation is bound to be more approximate because of the fact that the molar volume of the silver containing dissolved oxygen will not necessarily be the same as that of pure silver.

It is also worthwhile to consider the effect of mechanical pressure on the dissociation line, (Fig.14), which represents the equilibrium,

$$2Ag_2O = 4Ag + O_2 \qquad (11)$$

whence,

$$K = \frac{a_1^4 f}{a_2^2} \qquad (12)$$

Here, a_1 and a_2 are, respectively, the activities of silver and silver oxide, f is the fugacity of oxygen and K is the equilibrium constant. At low pressures, the fugacity is replaced by pressure and the effect of pressure on the activities of solids is considered negligible. Therefore,

$$K = p \qquad (13)$$

However, at high temperatures, the dissociation pressure is high

enough to affect both the activities of solids as well as the activities of gaseous oxygen and the equilibrium constant is required to be corrected for pressure. This entails calculating the effect of pressure on the activities of solids and on the behaviour of the gas as well. For the gas, therefore, the pressure is replaced by the fugacity; fugacity can be obtained from the Tables of the Thermal Properties of Gases[99]. The effects of pressure on the activities of solid silver and silver oxide can be calculated by applying the relation,

$$RT \ln a = \int_1^P v \, dp \qquad (14)$$

and assuming that the molar volumes of silver and silver oxide are independent of temperature and pressure.

It is expected that the activities of the oxide will be more affected by the pressure than those of silver and the overall effect on the equilibrium constant will be dependent on how the ratio of the solid and gaseous activities vary with pressure. In the present instance, since the fugacity coefficient of oxygen is greater than unity and the ratio (a_1^4/a_2^2) in equation (12) is less than unity, these two effects tend to cancel each other. Benton and Drake[51] have illustrated this in their calculation of two values of the equilibrium constant at two temperatures. Taking their calculations at 500^0 C, it is seen that the corrections amount to 29% for a_1^4, 14% for p and 48% for a_2^2 and the corrected equilibrium constant becomes 386.9 which

is almost equal to the uncorrected value of K = p = 386.5 of Keyes and Hara at 500° C. However, due to the various approximations applied, Benton and Drake's corrected value of K may be subjected to an error of 5 to 10%.

It is seen, therefore, that the pressure correction does not appreciably alter the position of the solid dissociation line. Hence the silver liquidus, corrected to the isobaric condition of 1 atm. will meet the Keyes and Hara's line at a slightly lower temperature and pressure (523° C , 495 atm.) than the experimental eutectic parameters. Owing to the lack of relevant data, no assessment can be made of the effect of mechanical pressure on the fusion of silver oxide.

Comparison of the Derived Eutectic Parameters with Previous Values:

The eutectic point obtained in the present study is different from that suggested by Allen and later quoted by Vacher and Hansen. As far as the temperature is concerned, Allen's value is not far away from the present value; however, the pressure of 414 atm. is considerably lower than the present value of 530 atm. It may be mentioned that the value of 414 atm. was obtained by extrapolating Allen's linear relation of the melting point of silver with the square root of oxygen pressure. But as was pointed out by Baker and Johnstone and as has been observed in the present study, the ideal behaviour of oxygen in silver is limited and consequently, the linear relationship is not valid even up to the small range of pressure that

Allen worked with. In view of this and also because of the fact that the extrapolation was carried over a large range of pressure and temperature, Allen's result is consequently approximate.

The present eutectic point is based on experimental data over a wide range of pressures and temperatures up to the eutectic point and beyond. The eutectic parameters of 530° C and 530 atm. which have been derived here, are, therefore, considered to be the best so far.

2. THE EUTECTIC COMPOSITION

The temperature-composition relation for the silver-oxygen system is shown in Fig.15 in terms of both Ag-O and Ag-Ag_2O. Extrapolation of the liquidus up to the eutectic temperature, 530° C, shows that the amount of oxygen (N_O) to be about 0.22 at the eutectic point; this corresponds to $N_{Ag_2O} = 0.39$.

Three other values of the eutectic composition, namely, 58, 51 and 56 mole per cent of silver oxide have been suggested. Of these, the first one has been obtained from the extrapolated phase diagram drawn from the combined data of Sieverts and Hagenaeker, Steacie and Johnson and Allen. The second value is due to Hennig[100]. From his estimated values of the melting point (815° C) and the heat of fusion (3650 cal/mole) of silver oxide, and taking 500° C as the eutectic temperature, Hennig calculated the eutectic composition of the oxide by using the relation,

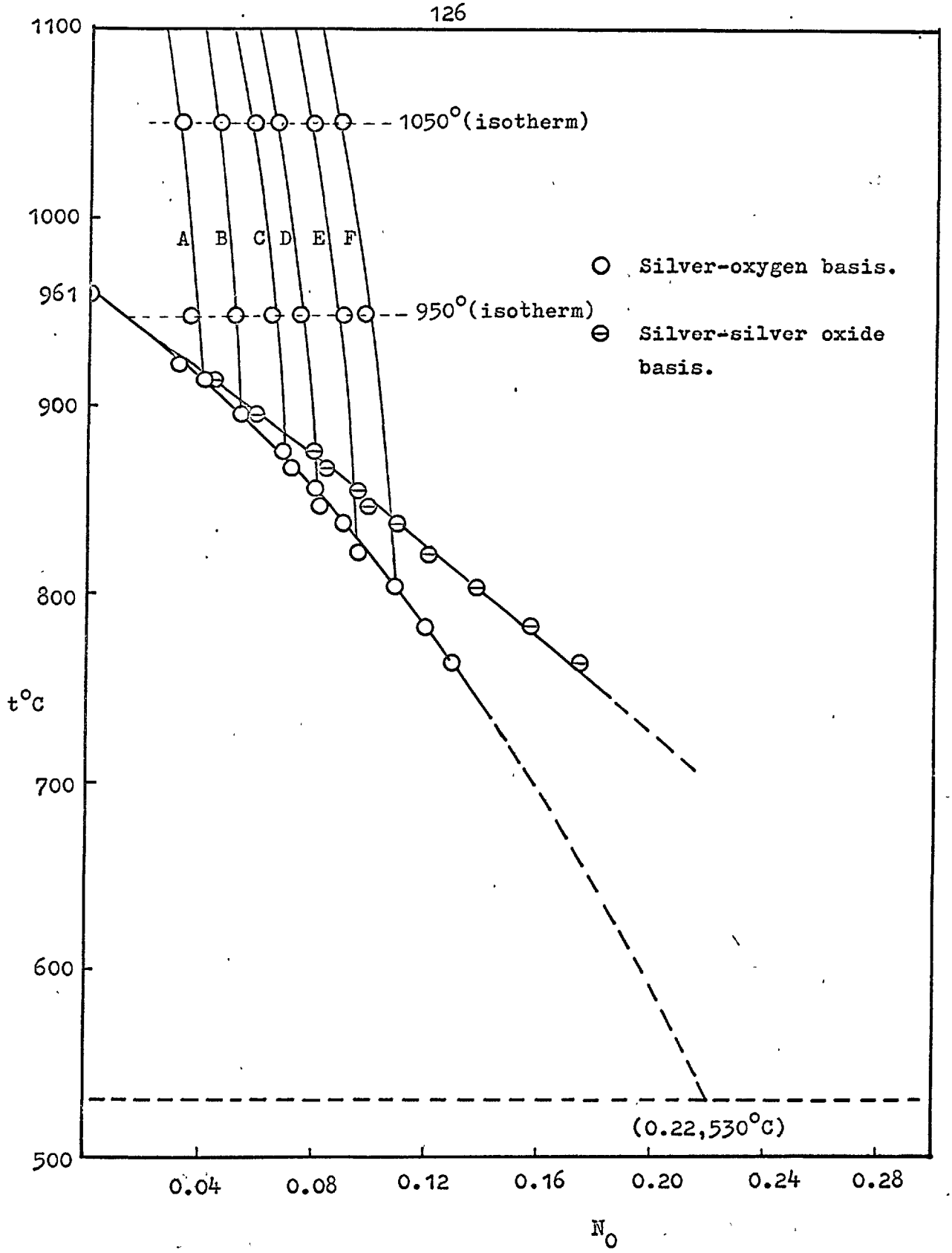

Fig. 15. Temperature-composition diagram of silver-oxygen system; A,B,C,D,E and F are isobars at 4,9,16,25,40 and 60 atm. respectively.

$$-\log N^{e}_{Ag_2O} = \frac{\Delta H_f}{4.576}\left(\frac{1}{T_e} - \frac{1}{T^{'}_{o}}\right) \qquad (15)$$

where N_{Ag_2O} is the mole fraction of Ag_2O and T_e and T^{o} are the eutectic point and the melting point of silver oxide. But the accuracy of the value, thus estimated, will be restricted both by the limitations of the data used and by the non-applicability of an ideal equation like (15) up to the eutectic point.

The third value was calculated by Kordes[101], again on the assumption of the ideal behaviour, by means of the relation,

$$\frac{T_{Ag} - T_e}{T_{Ag}} : \frac{T_{Ag_2O} - T_e}{T_{Ag_2O}} = N_{Ag} : N_{Ag_2O} \qquad (15a)$$

In deriving the relation (15 a), heat of fusion of silver and silver oxide was considered close enough to be cancelled out.

It is seen, therefore, that the above three values are bound to be approximate. During the present research, the experimental liquidus compositions have been established over a wide concentration range, up to about 13 atom per cent of oxygen. The present value of the extrapolated eutectic composition is, therefore, suggested to be more acceptable.

Some of the melts obtained by fusion of silver oxide were quenched and examined metallographically to see the distribution of the two components. Two typical metallographs are shown in Plates 4 and 5. It is seen that fine silver particles are dispersed amongst silver oxide in irregular patterns. Some of the silver will have undoubtedly

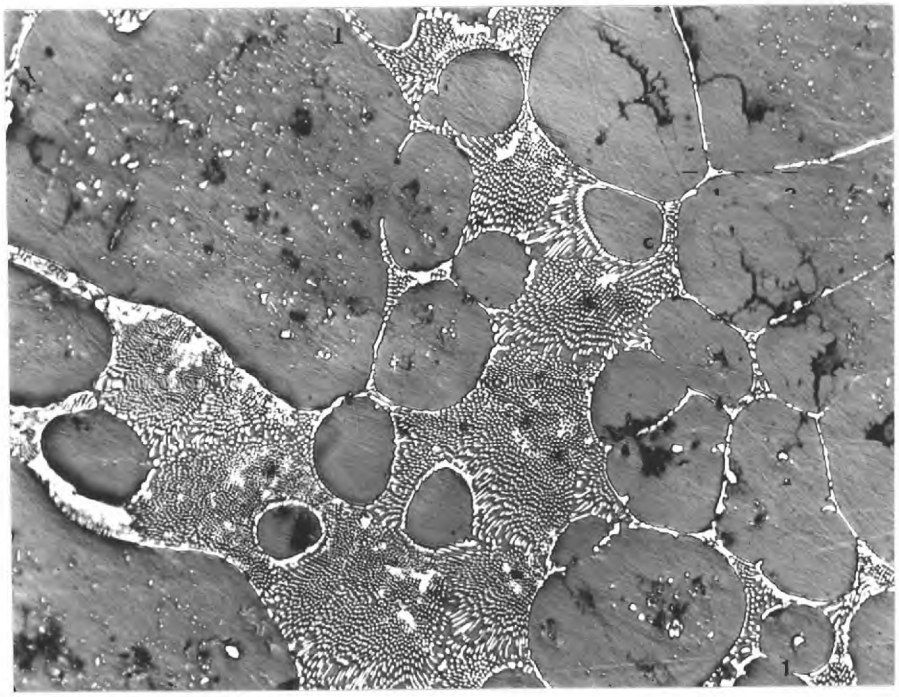

Plate no. 4. Metallograph of the quenched silver oxide melt x 200
(Pressure, 700 atm.; Temp., 816°K)

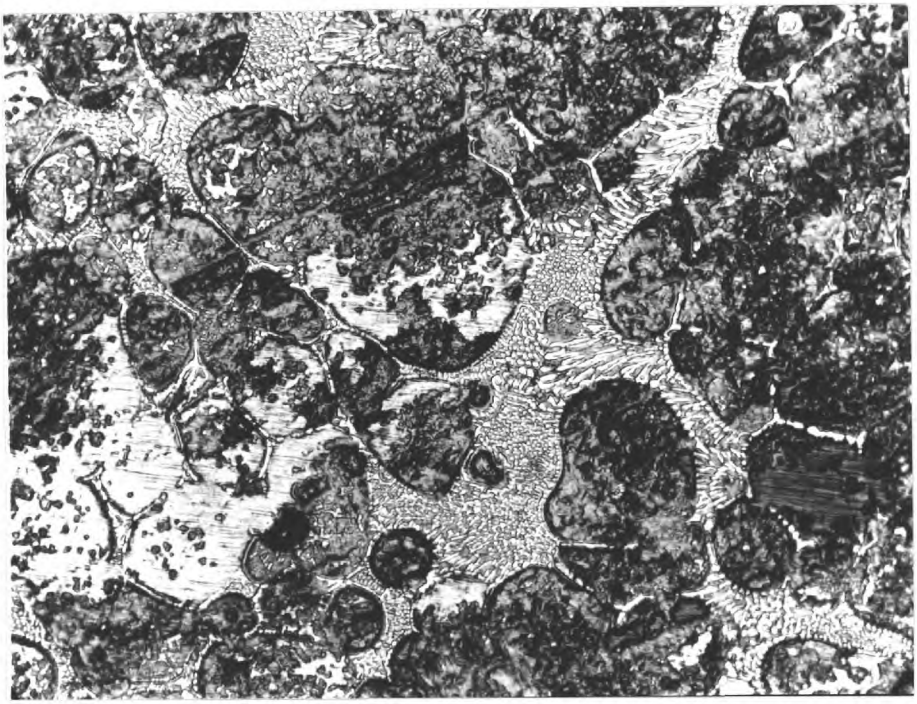

Plate no. 5. Metallograph of the quenched silver oxide melt x 200
(Pressure, 750 atm.; Temp., 833°K)

reverted to oxide during quenching.

Allen heated a mixture of silver and silver oxide, packed closely in a steel bomb, up to 600° C, quenched the melt and took a metallograph of it. His metallograph is similar to those shown in the present plates and shows the same pattern of distribution of fine silver particles amongst the silver oxide.

3. THE THREE-DIMENSIONAL PHASE DIAGRAM

From the pressure-temperature relations and the compositions of the melts, a three dimensional phase diagram for the silver-oxygen system has been constructed. This is shown in Fig.16. Surface ABCD represents the equilibrium between the solid silver and silver oxide below the eutectic point E. The space behind the surfaces ABCD and BFGC can be regarded as the pressure-temperature region where the solid silver oxide is stable, while the space in front of the surfaces ABCD and BHLC can be regarded as the pressure-temperature region where the solid silver is stable; the small solubility of oxygen in solid silver is considered negligible. The lines EH and EK give the composition of the liquid in equilibrium with solid silver and solid oxide respectively. The all liquid region is represented by the surface EKJIH. The three isobars, MN, PQ and RS have been constructed from the data in Tables 9 and 10 and show the character of the all liquid surface in the region studied.

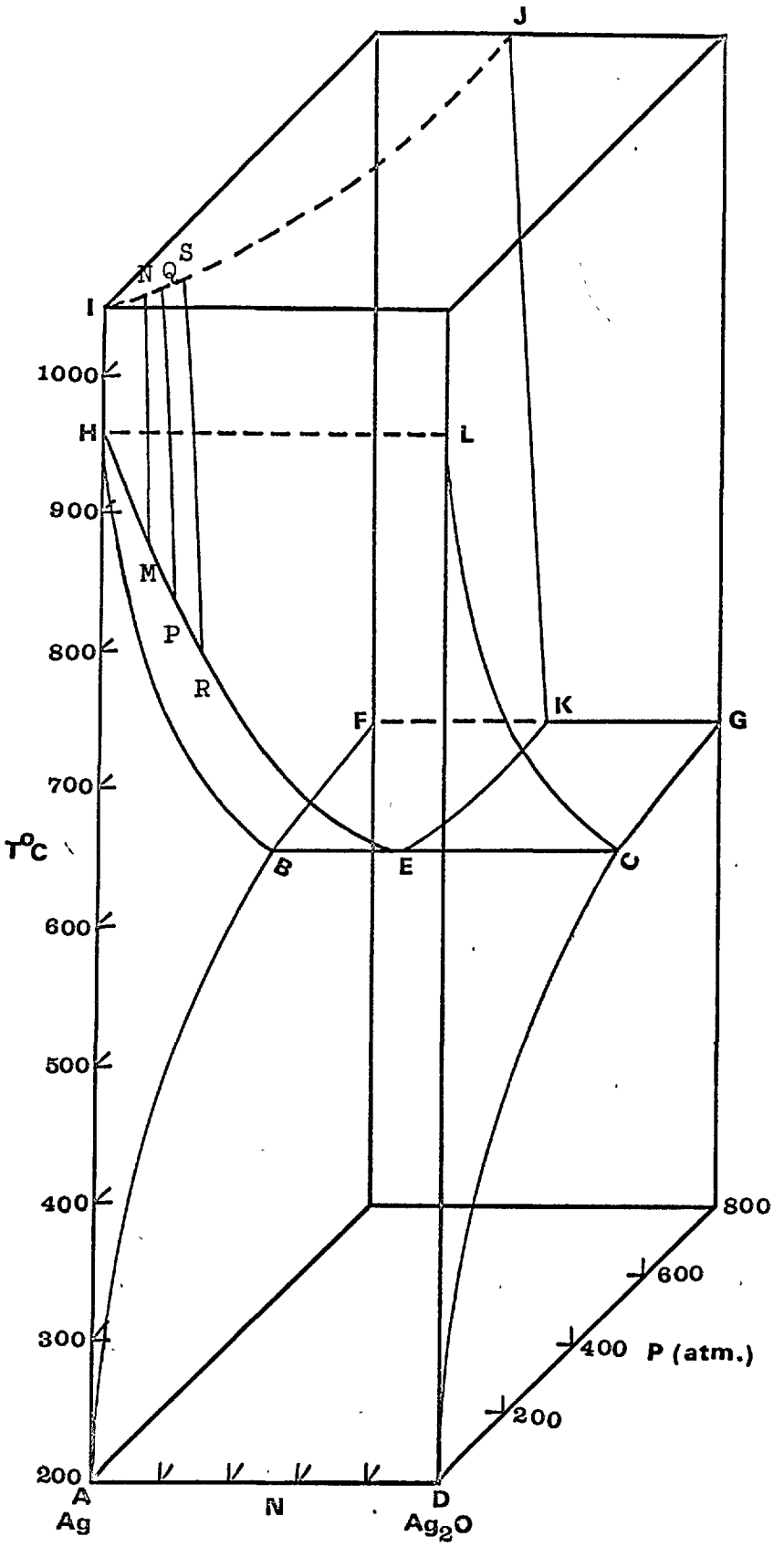

Fig.16. Phase diagram for the silver-silver oxide system.

It may be noted that the composition of the melt along the liquidus EH has been determined up to 100 atm. corresponding to 762° C. Because of the limitations of the thermogravimetric method above 100 atm., measurements could not be made beyond this pressure; the remaining part of the line EH has been extrapolated. For the same reason, no thermogravimetric measurements could be made along EK. The fixing of the eutectic point E has been discussed earlier (cf. page 125). The extrapolated composition at E is: silver 61 atom per cent and silver oxide, 39 mole per cent.

From the trend of EK (cf. Fig.16), the melting point of silver oxide is suggested to be ca. 1000° C at about 10^4 atm.

4. SOLUTION OF OXYGEN IN LIQUID SILVER

In a dilute solution, oxygen is considered to dissolve in liquid silver in atomic form. The process is represented as follows:

$$\tfrac{1}{2}O_2\,(g) \;=\; \underline{O}\;; \tag{16}$$

therefore,

$$K \;=\; \frac{a_O}{p^{\frac{1}{2}}} \tag{17}$$

where, a_O is the activity of the dissolved oxygen, $\underline{O}$, p is the pressure of oxygen in the gas phase and K is the equilibrium constant. If the solution obeys Henry's law in the dilute range, then,

$$a_O = f_O\, N_O \tag{18}$$

where, N_O is the atom fraction of dissolved oxygen and f_O is the Henrian activity coefficient. Combination of (17) and (18), yields,

$$f_O\, N_O = K p^{\frac{1}{2}}$$

or

$$N_O = \frac{K}{f_O}\, p^{\frac{1}{2}} = k_1\, p^{\frac{1}{2}} \tag{19}$$

Equation (19), which states that for a diatomic gas, the concentration of the dissolved gas is proportional to the square root of the pressure of the gas, represents the original Sieverts' Law.

From equation (17), we have,

$$p^{\frac{1}{2}} = \frac{a_O}{K} \;=\; k a_O \;=\; k f_O\, N_O \tag{20}$$

where $$k = \frac{1}{K} .$$

Now taking the dilute solution as the reference state such that

$$\frac{a_O}{N_O} = f_O = 1 \quad \text{as } N_O \longrightarrow 0,$$

equation (20) becomes,

$$p^{\frac{1}{2}} = k N_O \qquad (21)$$

for a reference solution. Any deviation from the linearity represented by the equation (21), will be attributed to the deviation of the Henrian activity coefficient, f_O, from unity. The Henrian activity coefficient will be given by

$$f_O = \frac{a_O}{N_O} = \frac{p_1^{\frac{1}{2}}}{p^{\frac{1}{2}}} \qquad (22)$$

where $p_1^{\frac{1}{2}}$ and $p_2^{\frac{1}{2}}$ represent, respectively, the values of the square root of pressure at a given concentration, on the reference line represented by equation (21) and the experimental curve (cf. Fig.17).

In the region where Sieverts' Law applies, i.e., for values of N_O up to 0.02, the solubility constant, K, as a function of temperature can be represented by the relation of Diaz et al[58], namely,

$$\log K = \log \frac{N_O}{p^{\frac{1}{2}}} = \frac{737.6}{T} - 2.281 \qquad (23)$$

The heat of solution and entropy of solution of oxygen in silver are respectively -3380 cal per $\frac{1}{2}$ mole of O_2 and -1.3 cal deg^{-1} at 1 atom % (cf. page26).

Results of isothermal solubility measurements given in Table 10 are plotted in Fig.17 as $p^{\frac{1}{2}}$ vs N_O. The dotted portion of the curve, the 950° isotherm is meant to indicate that at this temperature, the liquid region does not exist at an oxygen pressure less than 0.21 atm. Both the isotherms show that Sieverts' law is obeyed by dissolved oxygen up to at least $N_O = 0.02$.

Taking dilute solution as the reference state, the activities and activity coefficient at round compositions are calculated by means of equations (18) and (22) respectively. These values are given in Table 13.

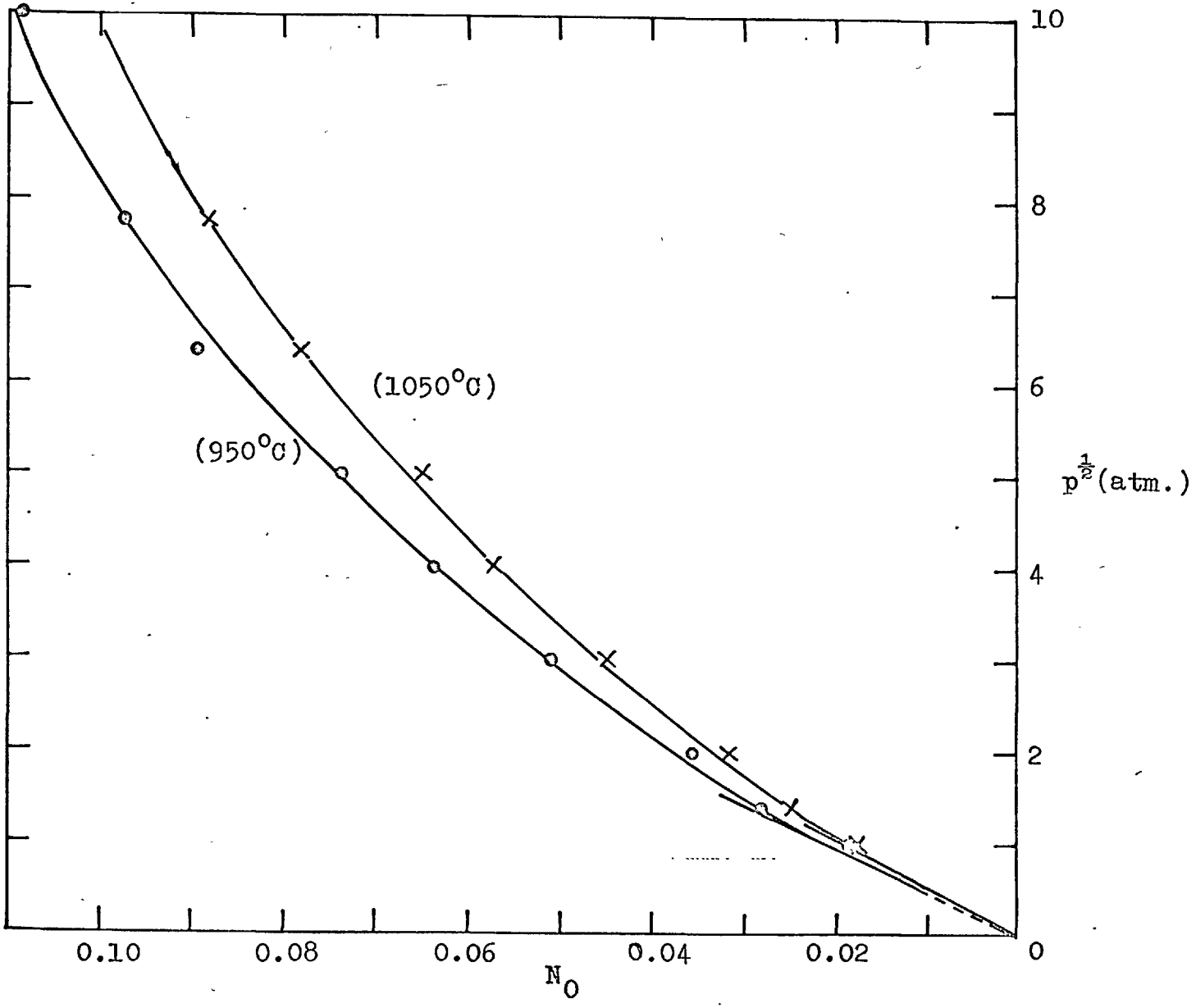

Fig. 17. Effect of pressure on the solubility of oxygen in liquid silver.

Table 13

Activities and activity coefficients of oxygen at round compositions

Temp. °C	Atom fraction of oxygen(N_O)	$p^{\frac{1}{2}}$	Activity, $a_O = K^* p^{\frac{1}{2}}$	Activity coef., $f_O = a_O/N_O$
950	0.02	0.952	0.020	1.000
	0.04	2.20	0.046	1.155
	0.06	3.75	0.079	1.313
	0.08	5.65	0.119 (0.119)**	1.483
	0.10	8.20	0.172 (0.174)	1.722
1050	0.02	1.053	0.020	1.000
	0.04	2.50	0.048	1.188
	0.06	4.30	0.082	1.362
	0.08	6.60	0.125 (0.126)	1.568
	0.10	9.33	0.177 (0.180)	1.773

* K is Sieverts' constant and is equal to 0.021 and 0.019 at 950° and 1050°C respectively.[58]

** Bracketted values were corrected for pressure-effects by replacing pressure with fugacity.

5. ACTIVITIES OF SILVER ALONG THE SILVER LIQUIDUS

Taking pure (supercooled) liquid at the specified temperature of the freezing point of a solution as the standard state, the activity of a pure solid, a(s), crystallizing out of a solution is given by

$$RT \ln a(s) = G(s) - G^0(l) \tag{24}$$

or,

$$\ln a(s) = \int \frac{\Delta H}{RT^2} dT \tag{25}$$

where ΔH is the heat of transition from the solid to the liquid phase. Assuming the liquid silver, acting as the solvent, to be in equilibrium with pure solid silver (since solid solubility of oxygen in silver is very small), and referring to the same supercooled liquid standard state, the activity of the liquid silver at the liquidus, $a_{Ag}(l)$, is also given by (25), that is,

$$\ln a_{Ag}(l) = \int \frac{\Delta H}{RT^2} dT \tag{26}$$

Therefore, if ΔH is known as a function of temperature, equation (26) can be solved to obtain the activity of liquid silver at the liquidus. If ΔH as a function of temperature is not available experimentally, it can be estimated from the heat capacities of the solid and liquid, given as functions of temperature, by using Kirchoff's equation,

$$\left(\frac{\partial \Delta H}{\partial T} \right)_p = \Delta C_p \tag{27}$$

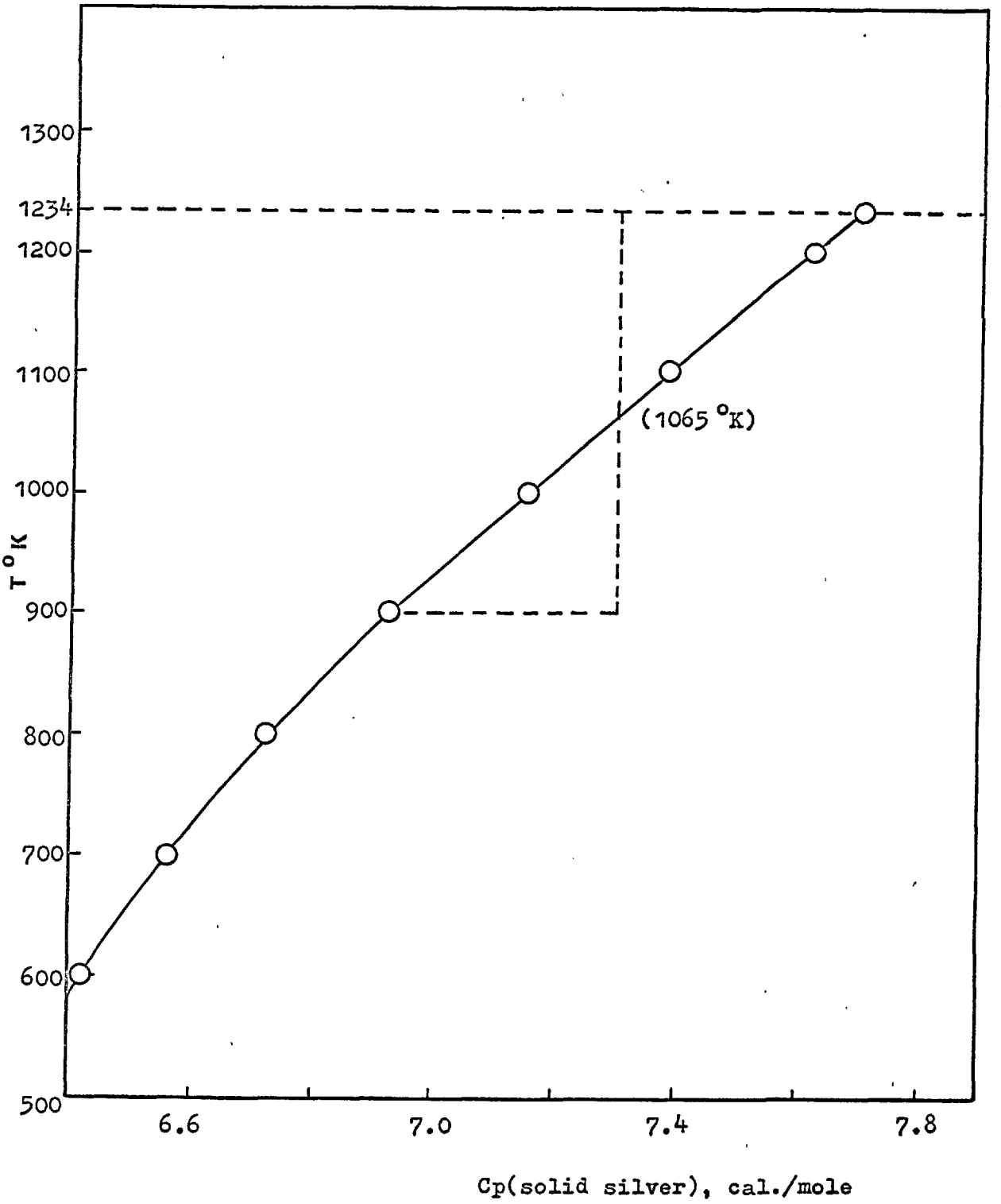

Fig. 17a. Variation of heat capacity of solid silver with temperature.

where ΔC_p is equal to $(C_p(l) - C_p(s))$ and is expressed as a function of temperature. Often ΔC_p itself is taken as a temperature-independent constant by taking the difference between the mean heat capacities of the solid and liquid, within the temperature range of interest. Integration of (27), taking ΔC_p as constant, yields,

$$-\ln a_{Ag}(l) = \frac{\Delta H_f}{R}\left(\frac{1}{T} - \frac{1}{T_o}\right) + \frac{\Delta C_p}{R}\left(\ln \frac{T_o}{T} + 1 - \frac{T^0}{T}\right) \quad (28)$$

where ΔH_f is the heat of fusion of silver at the melting point T_o.

The heat capacity of solid silver is available as a function of temperature up to the melting point, but that of the liquid silver is given as a temperature-independent constant. They are:

$$C_p(s) = 5.09 + 2.04 \cdot 10^{-3} T + 0.36 \cdot 10^5 \; T^{-2}$$

$$C_p(l) = 7.3$$

These are represented graphically in Fig. 17a for the temperature range of present interest. It is seen from the figure that ΔC_p disappears at about 1065^0 K and changes sign at this point while it varies from -0.4 cal/mole at 1234^0 K (m.p.) to +0.4 cal/mole at about 900^0 K. The mean value of ΔC_p within this temperature range is zero, which, in turn, reduces ΔC_p-term in equation (28) to zero. Therefore, in the absence of more accurate data on the heat capacity of liquid silver, above and below the melting point, the remaining part of the equation (28), namely,

$$-\ln a_{Ag}(l) = \frac{\Delta H_f}{R}\left(\frac{1}{T} - \frac{1}{T_o}\right) \quad (29)$$

which is much more simple and convenient, is used to calculate the activity of liquid silver at the liquidus. Substituting the numerical values of the melting point (1234° K) and heat of fusion (2855 cal/mole)[110] and converting to common logarithmic form, the following operating equation is obtained:

$$\log a_{Ag}(l) = -\frac{623.907}{T} + 0.5056 \qquad (30)$$

This equation has been used to calculate the activities of silver along the silver liquidus from the depression of the melting point resulting from the solubility of oxygen in liquid silver. The results are given in Table 14.

The bracketed values of activities, 0.8397 and 0.7975, at 60 and 100 atm. of oxygen pressure respectively, are the values corrected for the small solid solubility of oxygen in silver at these pressures. The approximate solid solubilities of oxygen at 60 and 100 atm. pressure, 0.002478 and 0.002568, respectively, have been calculated by using the equation of Steacie and Johnson.[41] Assuming ideal behaviour, the corresponding mole fractions of silver are 0.9975 and 0.9974 respectively. These values are so close to unity that hardly any error is incurred (less than 0.4%) as is evident from the pairs of values at 60 and 100 atm., by assuming that pure solid silver is in equilibrium with liquid silver at the liquidus. At lower oxygen pressures, the error is even less.

Table 14

Activities and Activity coefficients of silver at different compositions along the silver liquidus (considering silver-oxygen system)

T °K	N_{Ag} (= 1-N_O)	a_{Ag}	γ_{Ag}
1196	0.9686	0.9636	0.9948
1188	0.9597	0.9559	0.9960
1168	0.9471	0.9363	0.9886
1148	0.9314	0.9164	0.9839
1139	0.9286	0.9074	0.9772
1128	0.9204	0.8964	0.9739
1119	0.9184	0.8872	0.9660
1109	0.9105	0.8770	0.9632
1095	0.9028	0.8626	0.9555
1075	0.8927	0.8418 (0.8397)	0.9430
1054	0.8810	0.8198 (0.8177)	0.9305
1035	0.8710	0.7995 (0.7975)	0.9179

The bracketted values are the activities corrected for the solubility of oxygen in solid silver.

6. ISOTHERMAL ACTIVITIES OF SILVER AT 950 and 1050° C

Isothermal activities of silver were determined from the known activities of oxygen and melt compositions by means of the Gibbs-Duhem relation. The following procedure was employed.

Since, $$a_O = kp^{\frac{1}{2}} \tag{31}$$

then, $$d \log a_O = \tfrac{1}{2} d \log p \tag{32}$$

because k is a constant at a given temperature. Now the Gibbs-Duhem relation is,

$$N_{Ag} \, d \log a_{Ag} + N_O \, d \log a_O = 0 \tag{33}$$

substitution of (32) in (33) leads to

$$N_{Ag} \, d \log a_{Ag} + \tfrac{1}{2} N_O \, d \log p = 0$$

or

$$\int d \log a_{Ag} = -\tfrac{1}{2} \int_{N_O}^{N_O} \frac{N_O}{N_{Ag}} \, d \log p \tag{34}$$

Integrating the equation (34) between the limits $N_O = 0.02$ and $N_O = N_O$ corresponding to $a_{Ag} = N_{Ag} = 0.98$ and $a_{Ag} = a_{Ag}$, yields

$$\int_{0.98}^{a_{Ag}} d \log a_{Ag} = -\tfrac{1}{2} \int_{N_O = 0.02}^{N_O = N_O} \frac{N_O}{N_{Ag}} \, d \log p \, , \tag{35}$$

or

$$\log (0.98) - \log a_{Ag} = \frac{1}{2} \int_{N_O = 0.02}^{N_O = N_O} \frac{N_O}{N_{Ag}} \, d \log p$$

The replacement of the activity of silver by its mole fraction at $N_O = 0.02$ is justified by the fact that the Sieverts' Law is obeyed by the dissolved oxygen, at least, up to this concentration and correspondingly Raoult's Law is obeyed by silver.

Isothermal activities of silver at 950 and 1050° C, thus determined, the activity coefficients and the respective pressure and composition are given in Table 15. The activity-composition relation at 950° C and 1050° C and the relationabng the silver liquidus are shown graphically in Fig. 18.

Baker[102] reported carbonate systems as being approximately regular. In view of the apparent similarity of the present system to the carbonate systems, a test of regularity was made by plotting the α function as a function of compositions (Fig.19). It is apparent that the system is not regular. It may be mentioned that because of the very nature of assumptions underlying the definition of a regular solution, namely, the finite heat of mixing of solution and an entropy of solution due entirely to perfectly random mixing, the model is inherently self-contradictory. However, because of the negligible magnitude of the excess entropy, many metallic solutions conform to this model[103].

Table 15

Activities and activity coefficients of silver at 950°and 1050°C

On Ag-O basis				On $Ag-Ag_2O$ basis	
N_{Ag}	a_{Ag}	γ_{Ag}	Temp.°C	N_{Ag}	γ_{Ag}
0.9725	0.9713	0.9988	950	0.9705	1.0008
0.9633	0.9608	0.9974		0.9618	0.9990
0.9491	0.9432	0.9938		0.9433	1.0000
0.9368	0.9263	0.9888		0.9269	0.9994
0.9258	0.9116	0.9853		0.9136	0.9978
0.9140	0.8933	0.9774		0.8913	1.0022
0.9029	0.8750	0.9691		0.8794	0.9960
0.8906	0.8485	0.9527		0.8615	0.9849
0.9762	0.9752	0.9990	1050	0.9765	0.9987
0.9675	0.9665	0.9990		0.9663	1.0002
0.9550	0.9497	0.9945		0.9506	0.9991
0.9435	0.9379	0.9941		0.9353	1.0028
0.9338	0.9221	0.9875		0.9254	0.9964
0.9220	0.9084	0.9852		0.9076	1.0009
0.9118	0.8927	0.9791		0.8929	0.9998

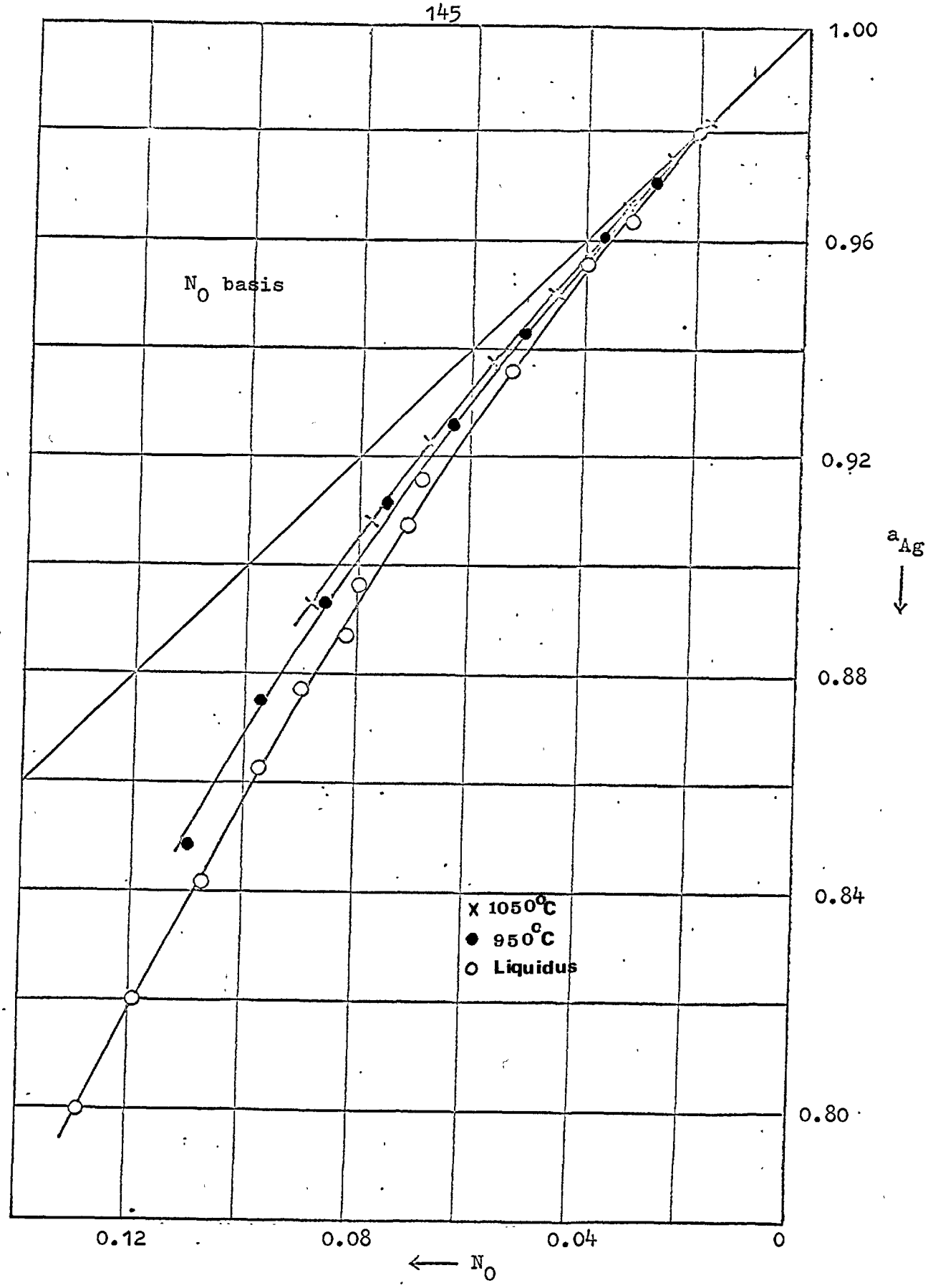

Fig. 18 . Activity of silver on the silver-oxygen basis along the silver liquidus and at 950° and 1050°C.

Table 16

Data for the plot of α^* function against composition

N_O	$\gamma_{Ag}(950^\circ)$	$\gamma_{Ag}(1050^\circ)$	$\alpha_{Ag}(950^\circ)$	$\alpha_{Ag}(1050^\circ)$
0.04	0.9959	0.9968	- 1.05	- 0.875
0.06	0.9877	0.9919	- 1.50	- 0.972
0.08	0.9786	0.9835	- 1.47	- 1.125
0.10	0.9647	0.9715	- 1.52	- 1.270
0.12	0.9454	0.9535	- 1.69	- 1.437

* $\alpha_{Ag} = \ln \gamma_{Ag} / (1-N_{Ag})^2 = 2.303 \log \gamma_{Ag} / N_O^2$.

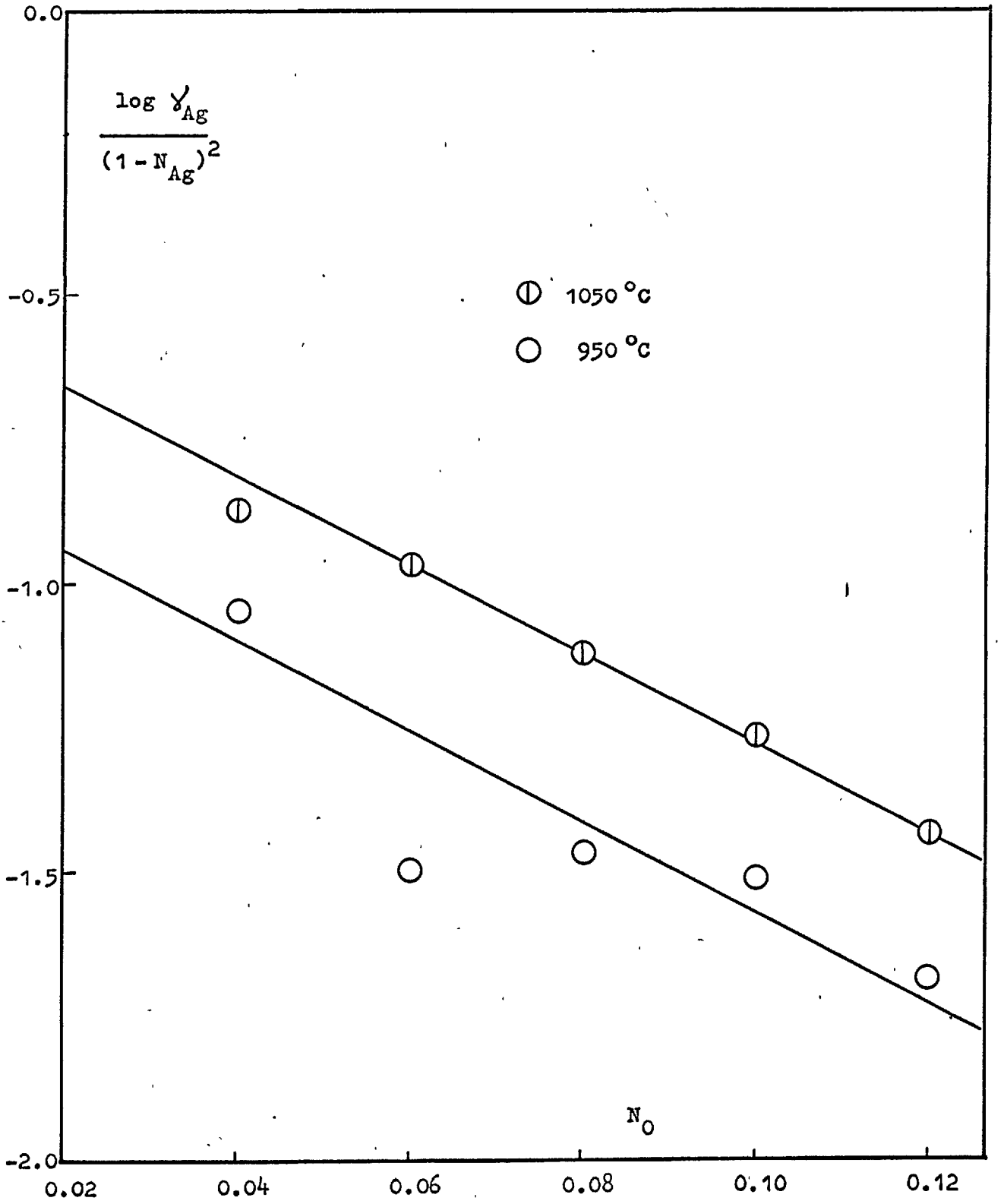

Fig. 19 . Plot of α_{Ag} for the Ag - O system at 950° and 1050°C.

Other assumptions such as the constancy of the co-ordination number and the energy of interaction between pairs of the same component at all temperatures and compositions, further restricts the scope of the model. In a gas metal system, where, the gaseous species in the liquid encounters an environment entirely different from that of the gaseous phase and where there is large differences in the electronegativities of the metallic and the non-metallic species, the regular solution model is hardly expected to apply.

7. DERIVATION OF FURTHER THERMODYNAMIC QUANTITIES

A. The Partial Molal Enthalpy and Entropy of Solution of Oxygen in Liquid Silver

The enthalpy and entropy of solution of oxygen are determined respectively from the slope and intercept of the plot of $\frac{1}{2}$ log p against $\frac{1}{T}$. These plots are shown in Fig.20. Because of the limited accuracy of data in the dilute range no pattern of the enthalpy of solution with composition is established. The average value of the $\Delta\overline{H}_O$ in the concentration range 0.02 to 0.10 atom-fraction of oxygen is found to be -3500 ± 200 cal/atom. The enthalpy and entropy values are given in Table 18.

B. The Partial Molal Enthalpy and Entropy of Solution of Silver

These quantities are determined from the slopes and intercepts of the plot of log a_{Ag} against $\frac{1}{T}$. The plots are shown in Fig. 21. The enthalpy and entropy data are given in Table 18.

The quantities are also plotted as a function of compositon in Fig. 22.

Also included in the plot are the ideal partial molal entropies of silver as a function of composition. The excess partial molal entropy of silver are in keeping with the tendency of compound formation, but the results, owing to the limited accuracy, are really qualitative.

Table 17

Data for the estimation of $\Delta\bar{H}_0$ and $\Delta\bar{S}_0$ at round compositions

N_0	Temp. ^oK	$\frac{10^3}{T^oK}$	$p^{\frac{1}{2}}$	$\frac{1}{2}\log p$
0.02	1211	0.8260	0.930	$\bar{1}.9488$
	1223	0.8177	0.952	$\bar{1}.9786$
	1323	0.7559	1.053	0.0224
0.04	1188	0.8420	2.15	0.3324
	1223	0.8177	2.20	0.3424
	1323	0.7559	2.50	0.3979
0.06	1157	0.8643	3.55	0.5502
	1223	0.8177	3.75	0.5740
	1323	0.7559	4.30	0.6335
0.08	1125	0.8889	5.18	0.7143
	1223	0.8177	5.65	0.7520
	1323	0.7559	6.60	0.8195
0.10	1090	0.9174	7.00	0.8451
	1223	0.8177	8.20	0.9138
	1323	0.7559	9.33	0.9700

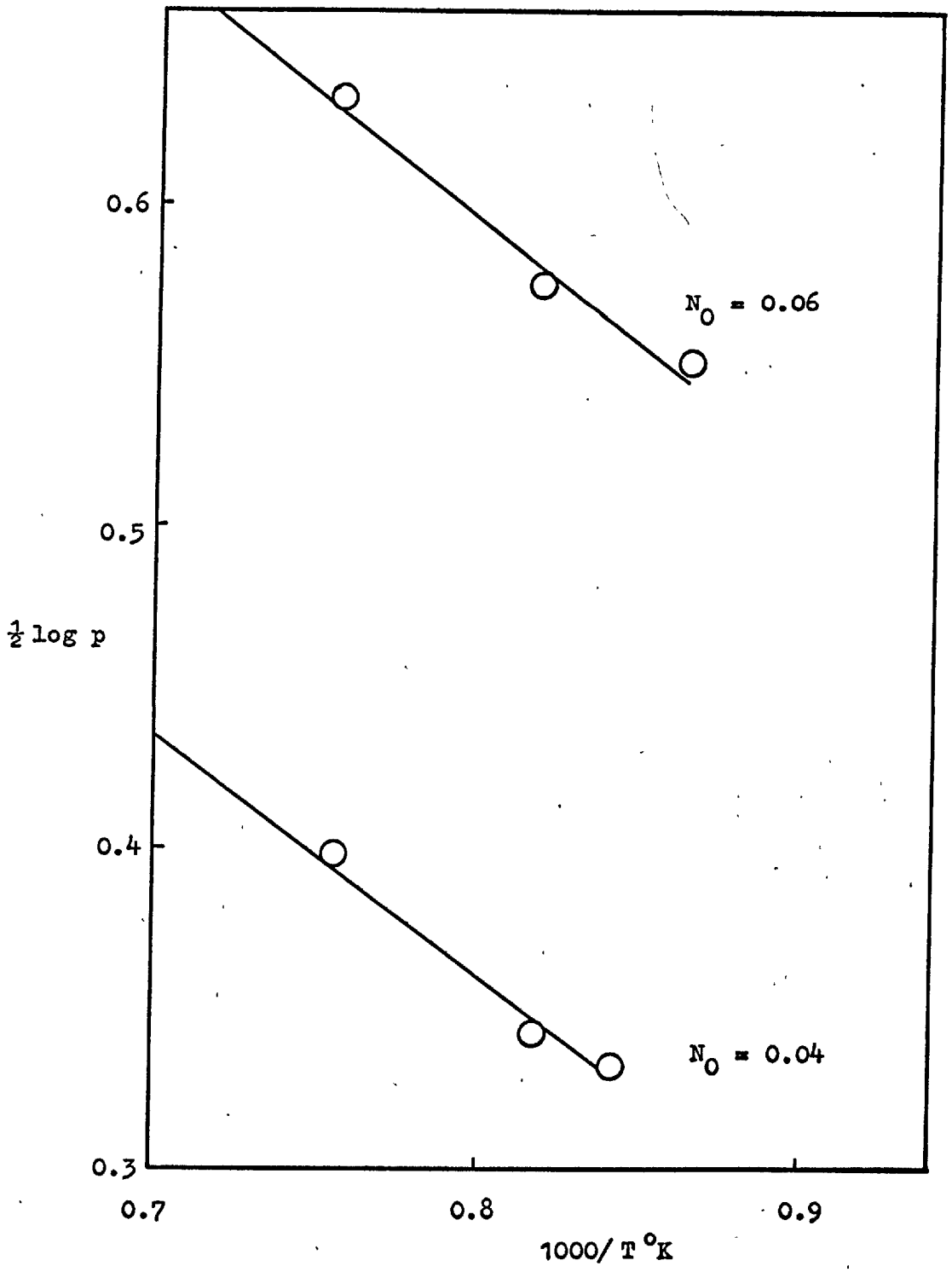

Fig.20a . Plot for the estimation of enthalpy and entropy of solution of oxygen in silver.

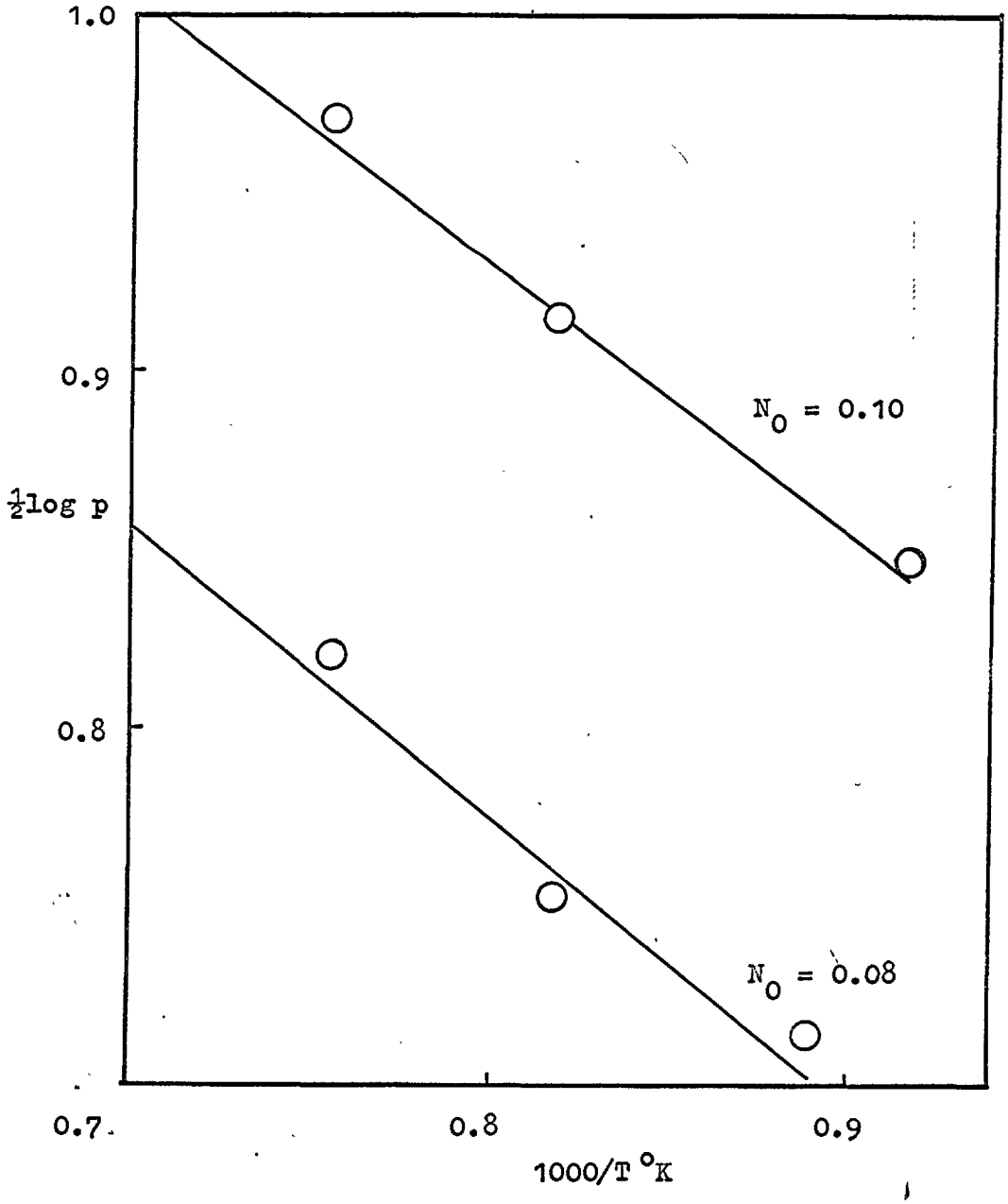

Fig.20b. Plot for the estimation of enthalpy and entropy of solution of oxygen in silver.

Table 18

Partial molal quantities of silver and oxygen at round compositions

N_O	$-\Delta\bar{S}_O$ cal./g.atom /deg.	$-\Delta\bar{H}_{Ag}$ cal./g.atom	$\Delta\bar{S}_{Ag}$ cal./g.atom /deg.	$\Delta\bar{S}^{id}_{Ag}$ cal./g.at. /deg.
0.02	2.67	0	0.040	0.0403
0.04	4.35	46	0.052	0.0810
0.06	5.57	137	0.037	0.1231
0.08	6.47	197	0.049	0.1657
0.10	7.07	252	0.075	0.2096

Table 19

Data for the estimation of $\Delta\bar{H}_{Ag}$ and $\Delta\bar{S}_{Ag}$

Temp. ^{o}K	$\frac{10^3}{T^{o}K}$	N_{Ag}	a_{Ag}	log a_{Ag}
1188	0.8420	0.96	0.9555	$\bar{1}.9802$
1223	0.8177	0.96	0.9560	$\bar{1}.9805$
1323	0.7559	0.96	0.9570	$\bar{1}.9809$
1157	0.8643	0.94	0.9255	$\bar{1}.9663$
1223	0.8177	0.94	0.9285	$\bar{1}.9677$
1323	0.7559	0.94	0.9325	$\bar{1}.9696$
1125	0.8889	0.92	0.8930	$\bar{1}.9509$
1223	0.8177	0.92	0.9005	$\bar{1}.9544$
1323	0.7559	0.92	0.9050	$\bar{1}.9566$
1090	0.9174	0.90	0.8570	$\bar{1}.9330$
1223	0.8177	0.90	0.8690	$\bar{1}.9390$
1323	0.7559	0.90	0.8740	$\bar{1}.9415$

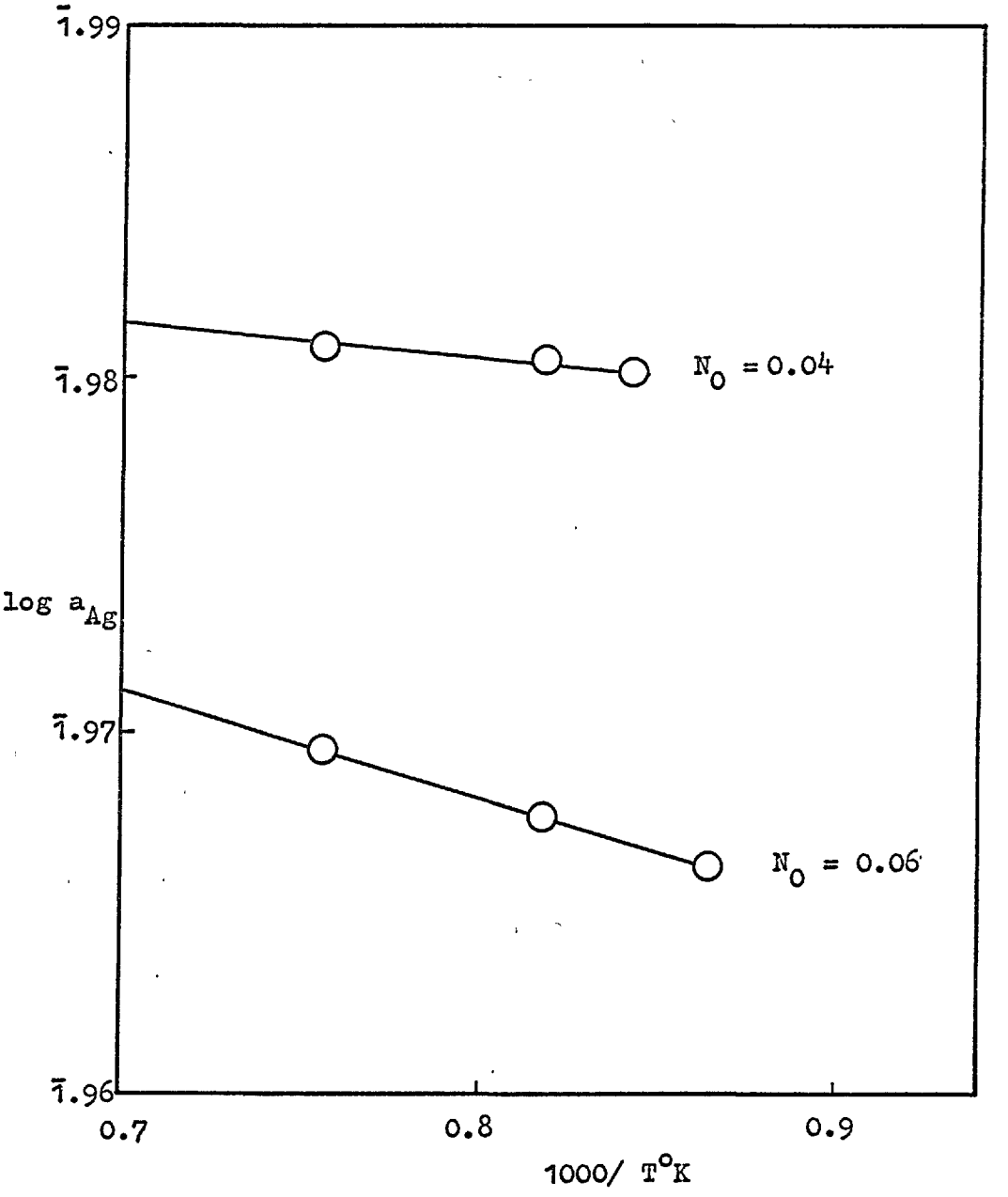

Fig.21a Variation of activity of silver with temperature.

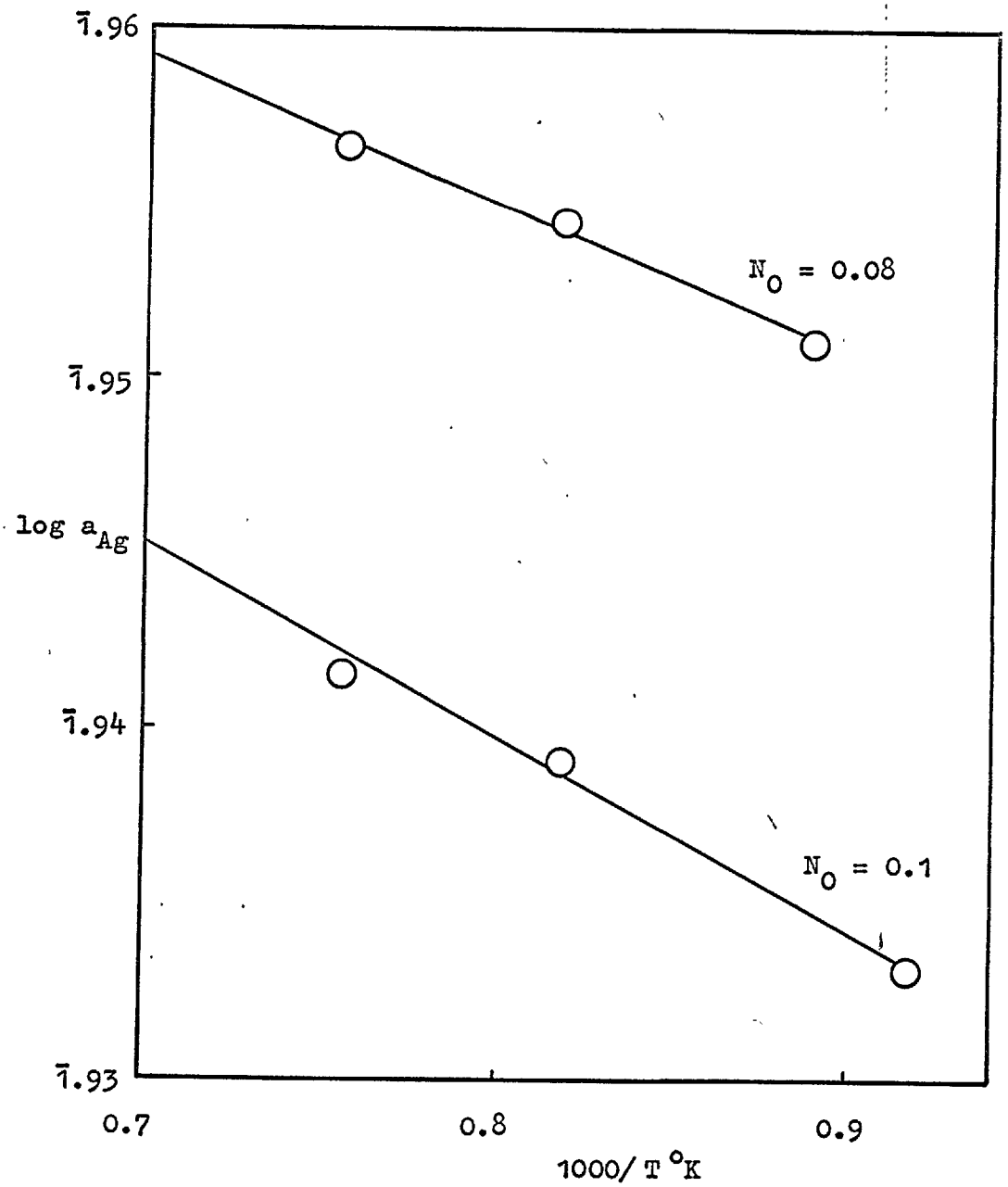

Fig.21b. Variation of activity of silver with temperature.

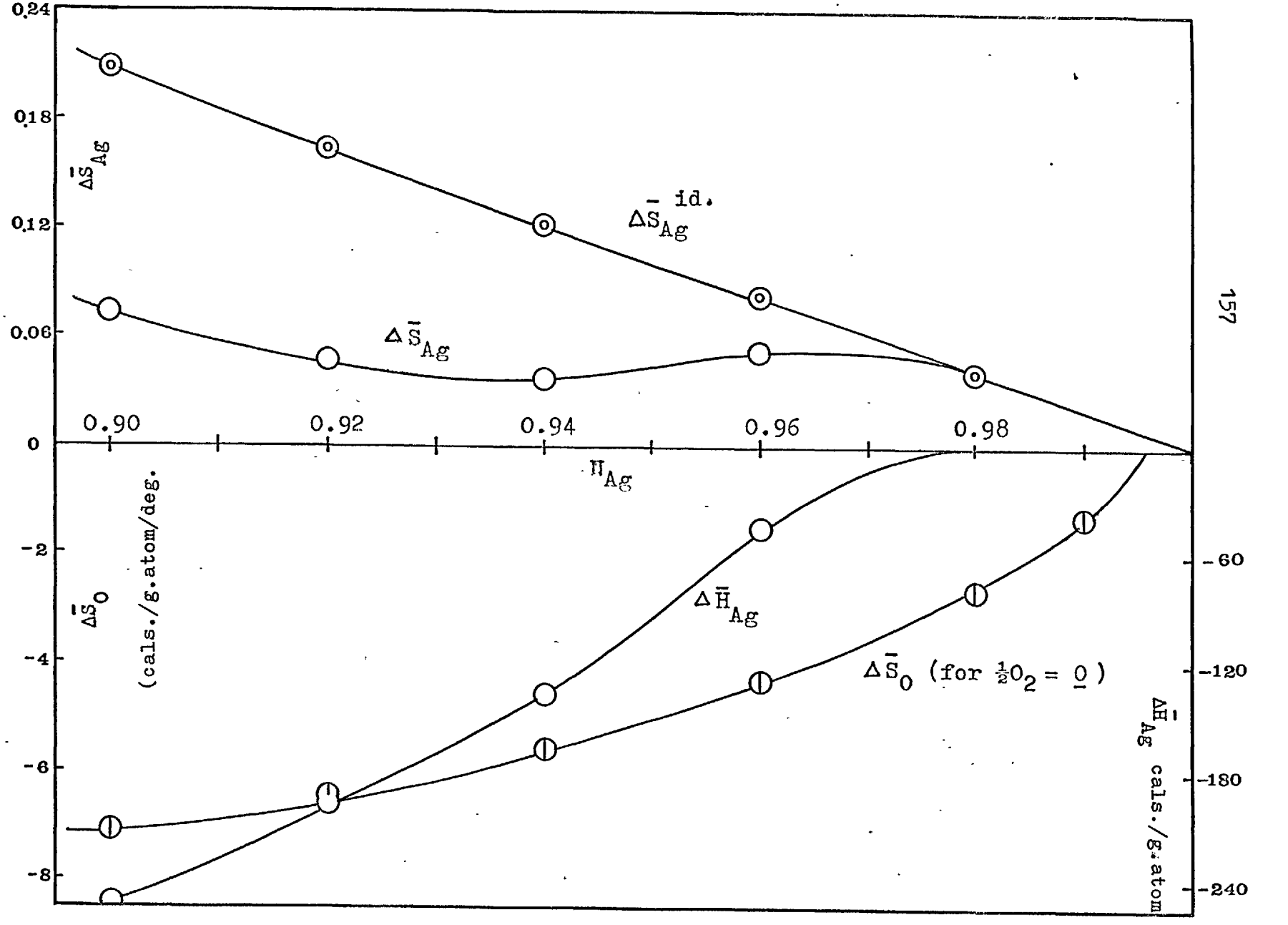

Fig. 22. Partial molal enthalpies and entropies as a function of composition.

8. TREATMENT OF THE SYSTEM AS SILVER-SILVER OXIDE

If the system is considered as a silver-silver oxide rather than a silver-oxygen system, then, at a given activity of silver, its atom fraction, N_{Ag}, alters from $(1-N_O)$ to $(1-N_{Ag_2O})$, assuming that the entire amount of the dissolved oxygen combines with silver to form silver oxide. As a result, a different activity-composition relation yielding different activity coefficients is obtained. (cf. Table 15)

The activity-composition plots for silver on this basis are shown in Fig. 23.

Identical results are also obtained by integrating a special form of Gibbs-Duhem relation which can be derived as follows:

The equilibrium constant for the reaction,

$$Ag_2O = 2Ag + \tfrac{1}{2}O_2 \qquad (36)$$

is given by

$$K = \frac{a_{Ag}^2 \; p^{\frac{1}{2}}}{a_{Ag_2O}} \qquad (37)$$

Taking logs,

$$\log a_{Ag_2O} = 2 \log a_{Ag} + \tfrac{1}{2} \log p - \log K$$

Differentiating,

$$d \log a_{Ag_2O} = 2 \, d \log a_{Ag} + \tfrac{1}{2} \, d \log p \qquad (38)$$

Now writing the usual Gibbs-Duhem relation,

$$N_{Ag} \, d \log a_{Ag} + N_{Ag_2O} \, d \log a_{Ag_2O} = 0 \qquad (39)$$

and eliminating d log a_{Ag_2O}, the following expression is obtained

$$N_{Ag} \quad d \log a_{Ag} + N_{Ag_2O}(2 \, d \log a_{Ag} + \tfrac{1}{2} \, d \log p) = 0 \qquad (40)$$

or

$$d \log a_{Ag} = - \frac{\frac{1}{2} N_{Ag_2O} \, d \log p}{N_{Ag} + 2 N_{Ag_2O}}$$

Since $N_{Ag} + N_{Ag_2O} = 1$,

therefore,

$$\int d \log a_{Ag} = -\tfrac{1}{2} \int \frac{N_{Ag_2O}}{1 + N_{Ag_2O}} \, d \log p \qquad (41)$$

Integration of (41) between the limits $N_{Ag_2O} = 0.02$ to $N_{Ag_2O} = N_{Ag_2O}$, yields,

$$\log a_{Ag} = \log (0.98) - \tfrac{1}{2} \int_{N_{Ag_2O} = 0.02}^{N_{Ag_2O} = N_{Ag_2O}} \frac{N_{Ag_2O}}{1 + N_{Ag_2O}} \, d \log p \qquad (42)$$

The plots on the basis of silver-silver oxide show silver to behave more ideally than on the basis of silver oxygen. For example at an oxygen concentration of 10 atom percent (corresponding to 12.5 mole per cent of silver oxide), the activity coefficients of silver on the liquidus (817° C) and on the isotherm at 950° C are, respectively 0.952 and 0.966*; the corresponding values on the basis of silver-silver oxide, are respectively, 0.979 and 0.993. Values of

* p. 145

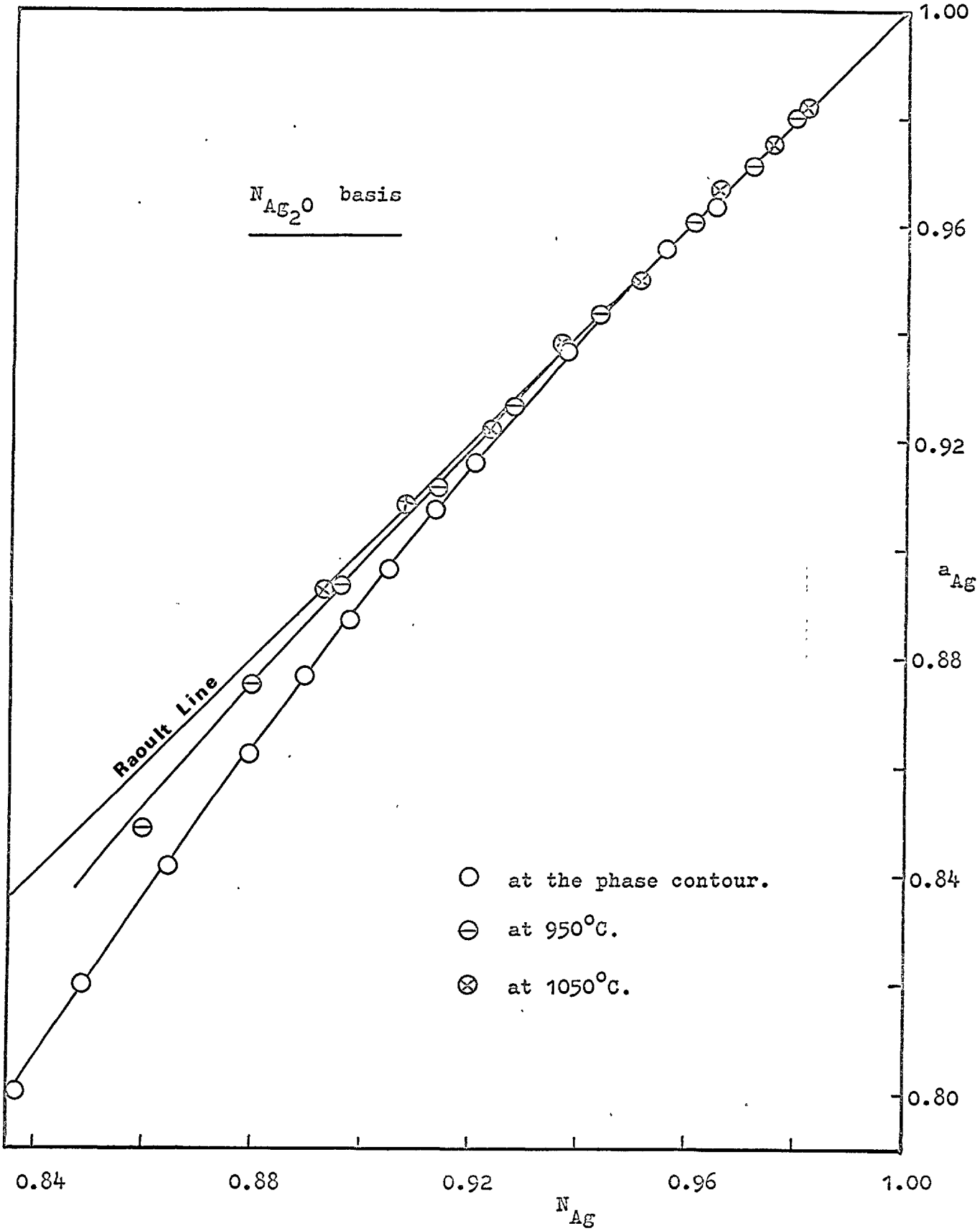

Fig. 23 Activity of silver on the silver-silver oxide basis.

activity coefficients of silver on the isotherm at 1050° C all become unity. It is therefore, expected that the dissolved Ag_2O will show a fair observance of Henry's Law.

From this more "ideal" tendency of the silver-silver oxide system, it appears likely that in the temperature and composition range studied here, much of the oxygen will be combined as Ag_2O. An isotherm above 1050° C would, on this basis, be shifted into the region of positive deviation; this would be quite in conformity with the expectation that formation of Ag_2O would be less at higher temperatures.

The idea of considering the system as silver-silver oxide is in line with the original suggestion of Donnan and Shaw and also with the recent trend of picturing dissolved oxygen in liquid metals in the form of molecular species of the type MxOy.[104,105] However, it is open to discussion whether Ag_2O is accommodated as a covalent angular molecule or as some form of ionic molecule, i.e., $(Ag\text{-}O)^{-}Ag^{+}$ in which interchange of silver atom could occur. In a melt of the present type, the presence of an ionic molecule appears to be more likely.

The behaviour of Ag_2O in solution can not be interpreted thermodynamically owing to the lack of activity data for the oxygen rich end of the phase diagram; this region is inaccessible because it means carrying out measurements at pressures around 10^4 atm.

9. CONDUCTIVITIES OF SILVER OXIDE

The log of conductivity, σ, is plotted against $\frac{1}{T}$ in Fig. 24. From the slope, the apparent activation energy obtained is 0.64 eV. This activation energy of silver oxide is within the range of usual activation energies of transition metal oxides, i.e., 0.1 to 0.7 eV and close to that of cuprous oxide[106] to which it is structurally similar. Substitution of this numerical value leads to the expression,

$$\sigma = 2.48 \times 10^{4} \exp(-0.64/kT) \qquad (43)$$

for the conductivity of silver oxide.

The log σ vs. log p plot is shown in Fig.25. The slope of the curve at higher and lower pressure regions are respectively $\frac{1}{2}$ and $\frac{1}{4}$. These show that the conductivity varies as $p^{\frac{1}{2}}$ to $p^{\frac{1}{4}}$.

Now the conductivity is given

$$\sigma = n e \mu$$

where n is the number of charge carriers per unit volume, e is the absolute electronic charge and μ is the mobility of charge carriers ($cm^2/Vsec$). Obviously, the conductivity will be determined by the contributions due to charge carrier concentrations as well as the mobility.

In the case of transition metal oxides the information about the contribution due to the charge carriers and the mobility is rather confused. The hopping model (Heikes et al[107]) suggests that the mobility varies exponentially with temperatures and only a minor

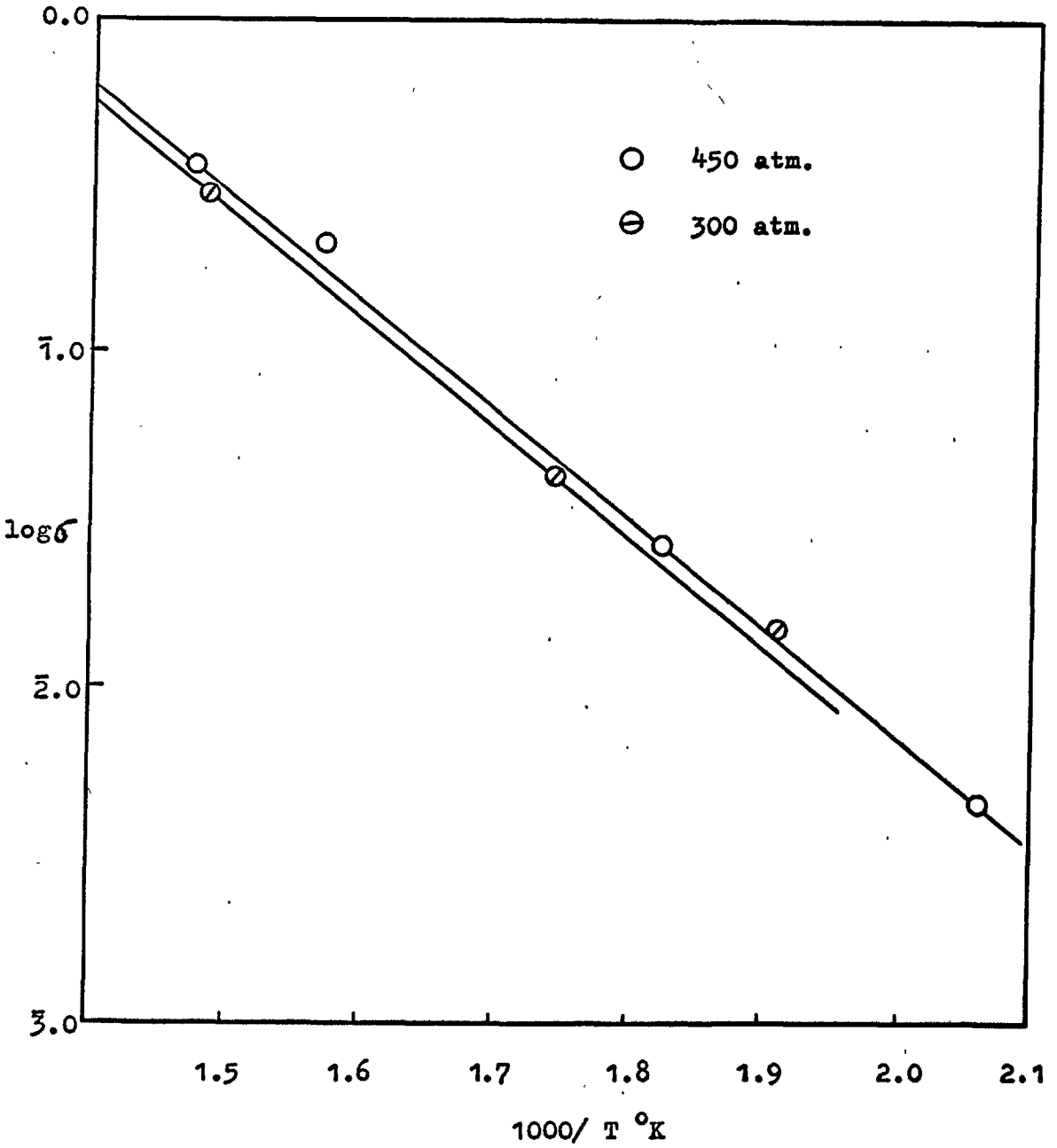

Fig. 24 . Variation of the conductivity of silver oxide, at constant pressure, with temperature.

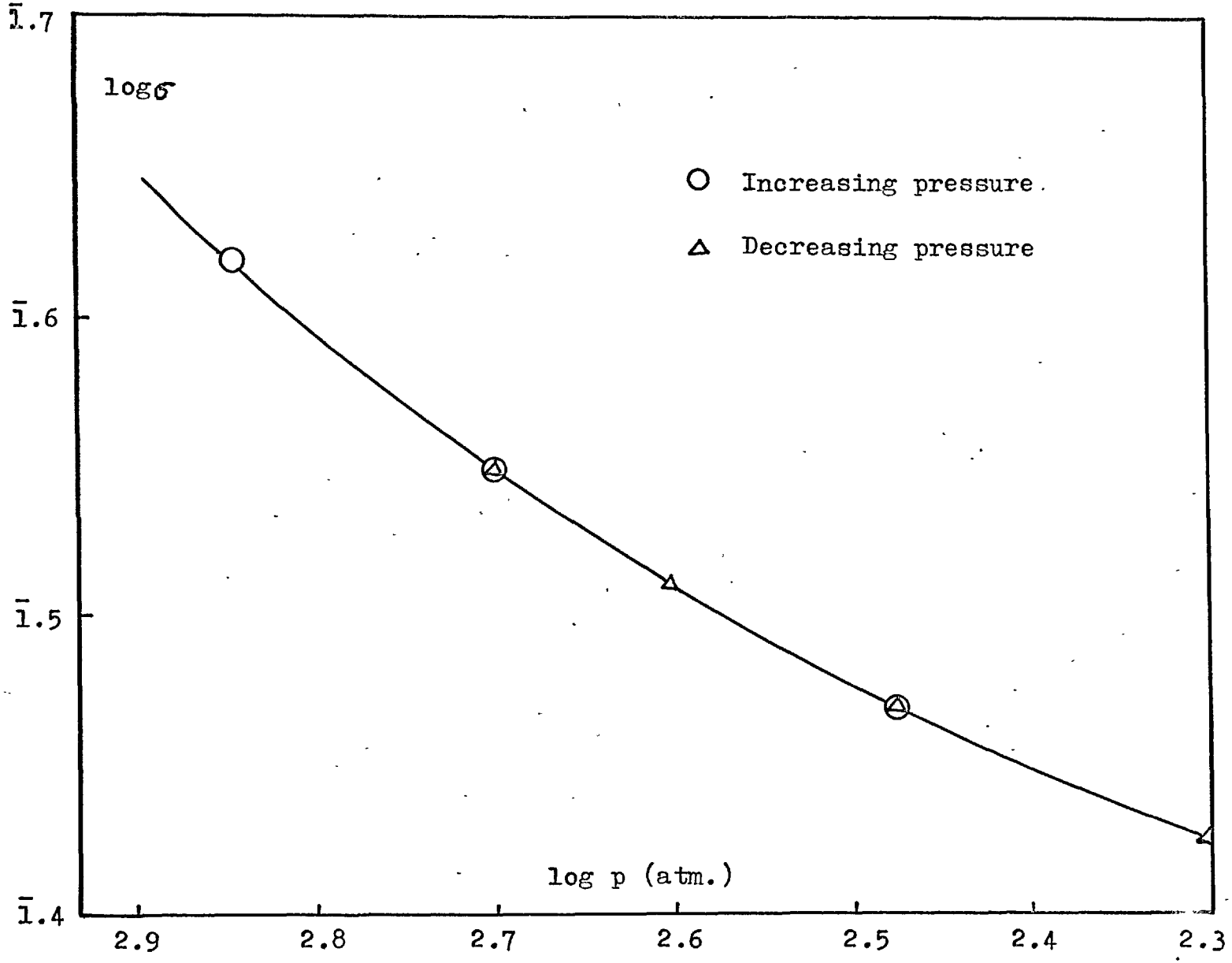

Fig. 25. Conductivity of silver oxide as a function of pressure at 400°C.

contribution is made by charge-carriers concentration. However, the data of other workers, e.g., Van Daal and Bosman[108], indicate that the mobility is virtually constant and that the variation of the conductivity is due to the variation of charge-carrier concentrations exponentially with temperatures.

The charge-carrier concentration may be related to pressure by the following equilibrium processes.

(i) $$\tfrac{1}{2}O_2(g) = O^{2-} + 2V_{Ag}^{+} \; ;$$

$$K_1 = \frac{[O^{2-}]\,[V_{Ag}^{+}]^2}{p^{\frac{1}{2}}} \; ;$$

therefore, $$[V_{Ag}^{+}] \propto p^{1/4} \; ;$$

(ii) $$\tfrac{1}{2}O_2 = O^{2-} + 2V_{Ag} + 2e^{+}$$

$$K_2 = \frac{[O^{2-}]\,[V_{Ag}]^2\,[e^{+}]^2}{p^{\frac{1}{2}}}$$

since, $$[V_{Ag}] = [e^{+}]$$

therefore, $$[e^{+}] \propto p^{1/8} \; .$$

Here, O^{2-} and V_{Ag} represent respectively lattice oxygen and silver vacancy in the oxide; e^{+} and V_{Ag}^{+} are respectively the free positive hole and the silver vacancy associated with the positive hole; K_1 and K_2 are equilibria constants.

Now, if the positive hole is associated with the cation vacancy, the conductivity will be dependent on the concentration of cation

vacancies and therefore, will vary as $p^{1/4}$. On the other hand, if the positive hole is dissociated from the cation vacancy, as is represented by (ii), the charge-carrier concentration and hence the conductivity vary as $p^{1/8}$.

In case of cuprous oxide, experimental results suggested a $p^{1/8}$ dependence of the conductivity. However, taking into account the pressure dependence of the conductivity, O'Keefe and Moore[109] obtained a pressure dependence of $p^{1/5}$.

It may be noted that the equilibrium considerations of the above processes are approximate because of the assumption that the vacancy concentration is small. In addition, the following limitations are also to be taken into account.

At low temperatures, the defect may be frozen in a non-equilibrium state. If the non-stoichiometry is small, the impurity may be the determining factor in the conductivity measurements.

Since the present measurements were carried out not with a single crystal, but with a compacted powder pellet, the result will suffer from certain weaknesses inherent in a powder sample. For example, the specimen produced by pressing a microcrystalline powder is not necessarily homogeneous. When such a sample is not in equilibrium with its atmosphere, a slow diffusion of impurities or imperfection, inward or outward, gives rise to a surface layer over individual crystallites; the electrical properties of these surface layers differ from those of the bulk.

Despite these limitations, it is significant that the activation energy obtained is reasonable for this type of material. Obviously, more information such as the Hall coefficient, the extent of non-stoichiometry, the dependence of hole mobility under pressure etc., are required before a coherent fundamental explanation of the conductivity behaviour of silver oxide could be offered. Measurements on these parameters under pressure would be very useful.

10. THE LIQUID GOLD-SILVER ALLOYS AND OXYGEN

Gold has a negligible affinity for oxygen*. The solubility of oxygen in silver, therefore, is expected to be lowered by the addition of gold. Consequently, the depression of freezing points of the alloys as a function of oxygen pressure should also be smaller.

The log p vs. $\frac{1}{T}$ plots for the three alloys together with that of silver (Fig.26) show the relative effects of oxygen pressure on the fusion points. Fig.27 shows the solubilities of oxygen in the alloys as well as in the pure silver, at 1050° C, as a function of the square root of oxygen pressure and Fig. 28 shows the solubilities as a function of gold concentration. All these plots bear out the above expectations.

From the limiting slopes of the curves of Fig. 27, the Sieverts' constants for each of the alloys at 1 atm. oxygen pressure and 1050° C are derived; since the Sieverts' constant, k equals $N_O/p^{\frac{1}{2}}$, these constants are the same as the corresponding atom fractions of dissolved oxygen at 1 atm. These are given in Table 20.

A. Heats of Fusion of the Alloys

In view of the closeness of the solidus and the liquidus lines of the silver-gold system (Fig.29)[110,111] a solid alloy of a given composition will melt to a liquid of approximately the same composition. Then treating the alloy in the same way as a pure component (solvent) and considering it to obey Raoult's Law in the range where the oxygen

* See Appendix 1

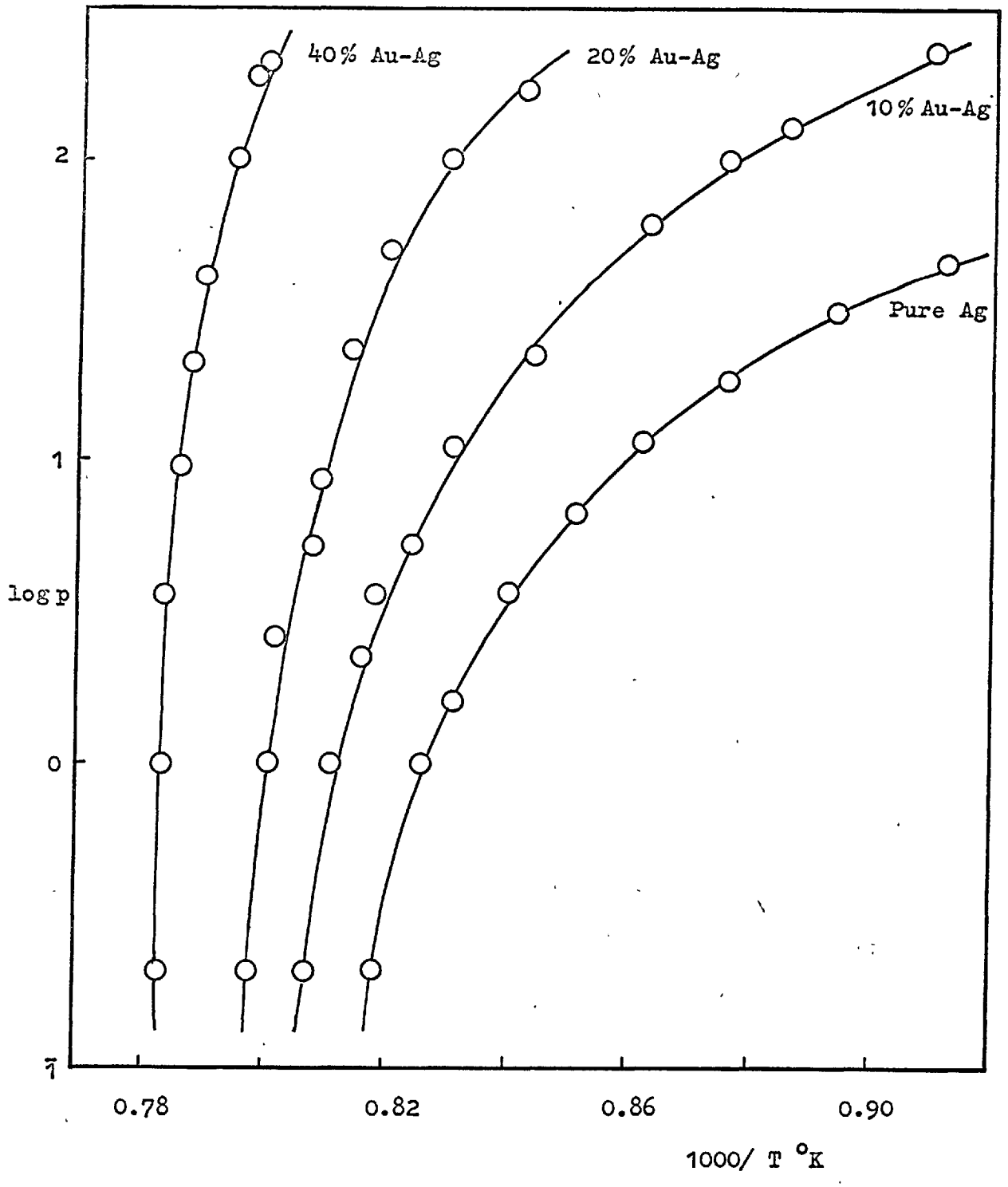

Fig. 26. Pressure-temperature relation for gold-silver alloys and oxygen system.

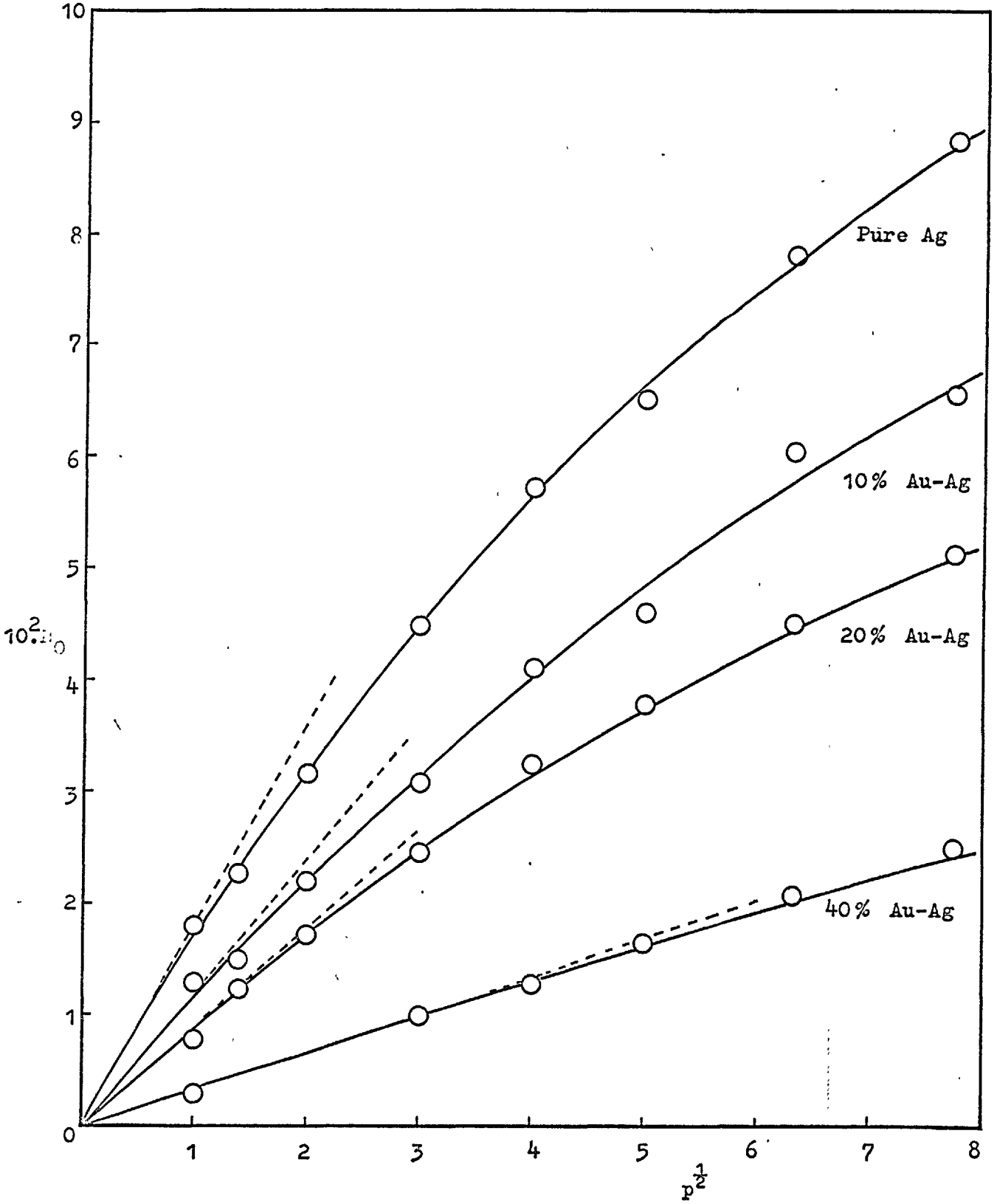

Fig.27 . The effect of pressure on the solubility of oxygen in liquid silver and liquid gold-silver alloys at 1050°C.

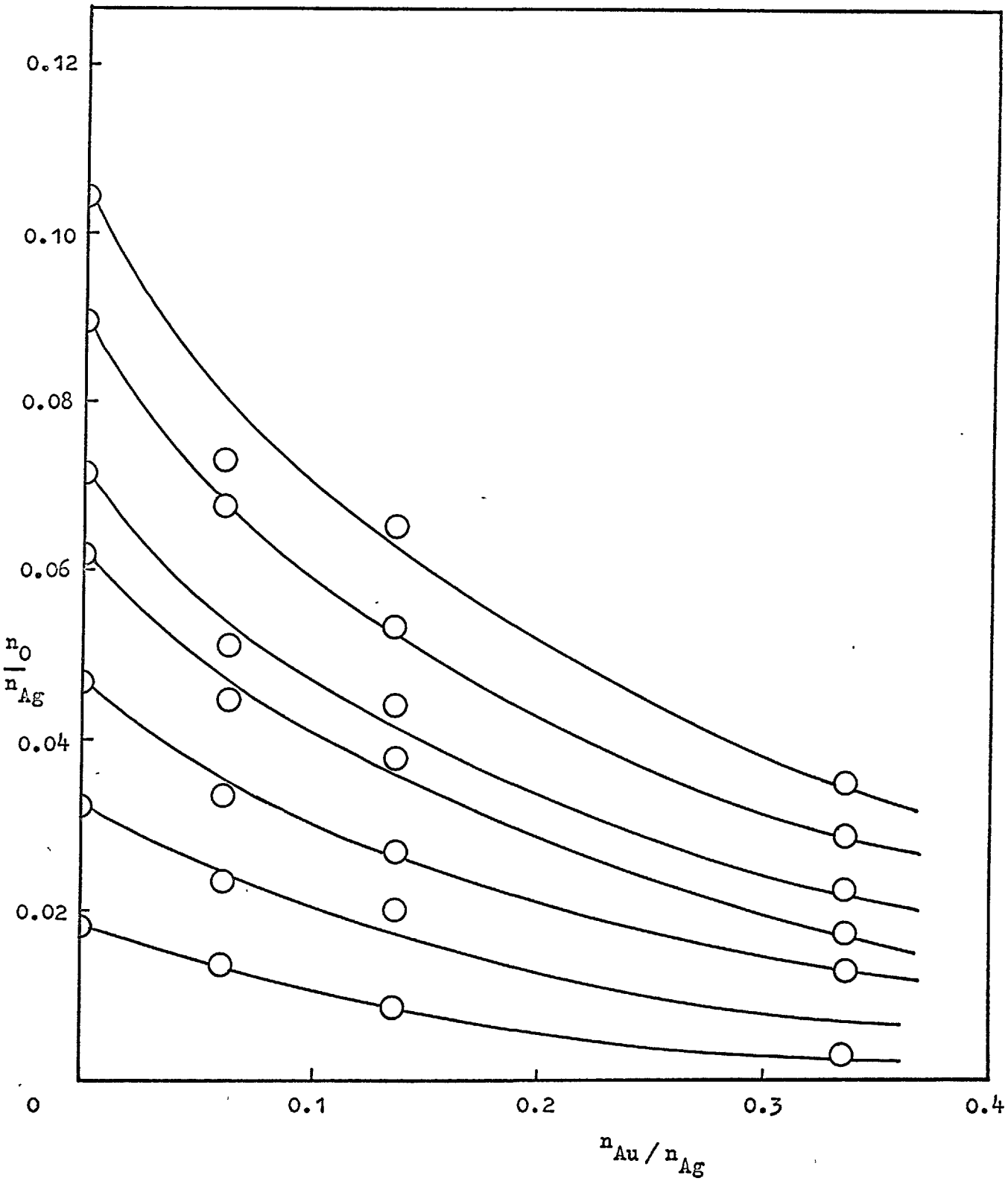

Fig. 28. Effect of gold concentration on the solubility of oxygen in gold-silver alloys.

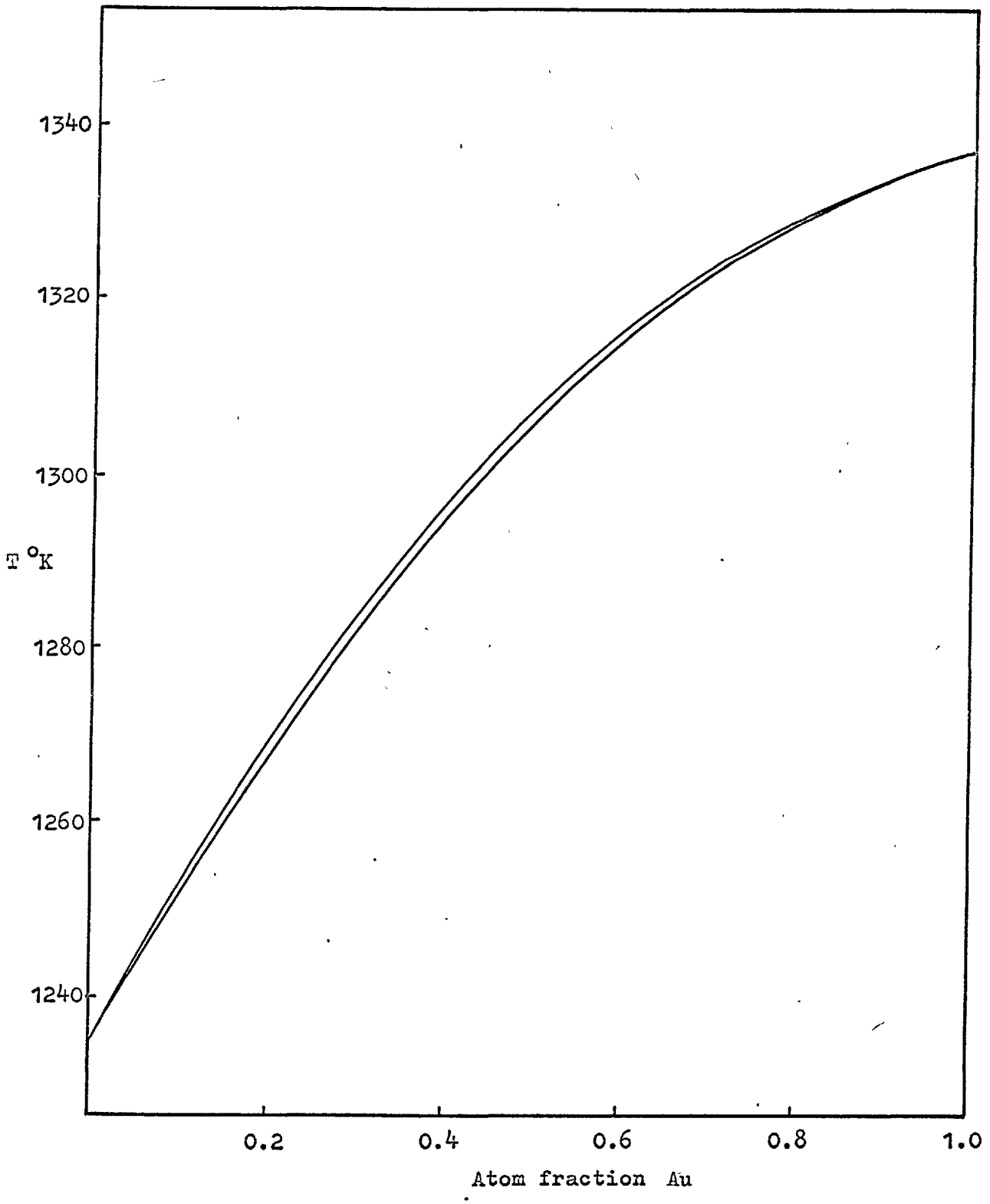

Fig. 29 . The solidus and liquidus of the gold-silver system.

Table 20

Heats of fusion of gold-silver alloys

Alloys	Melting points °C (at 1 atm.) (O_2 press)	Sieverts' constant* at 1050°C	ΔH_f from Sieverts' k	ΔH_f from exp.46	Phase contour values of N_O at 1 atm. from calcd. ΔH_f
10% Au-Ag	960.5	0.012	2781	2861	0.0126
20% Au-Ag	976.0	0.009	2877	2867	0.0092
40% Au-Ag	1004	0.003	3546	2881	0.0028

* Limiting slopes obtained from N_O vs $p^{\frac{1}{2}}$ plots at 1 atm.

Table 21

Activity coefficients of oxygen in gold-silver alloys at 1050°C

% gold	Dissolved oxygen N_O	f_O	log f_O	Dissolved oxygen Wt. %	f_O'	log f_O'
0	0.019	1.000	0.0000	0.2865	1.000	0.0000
5	0.015	1.238	0.0927	0.2307	1.243	0.0942
10	0.012	1.583	0.1995	0.1798	1.5934	0.2023
20	0.009	2.112	0.3247	0.1345	2.1301	0.3284
40	0.003	5.939	0.7738	0.0448	6.3951	0.8058

contents obey Sieverts' law, the heat of fusion of the alloy can be calculated from the relation,

$$N_O = \frac{\Delta H_f \text{ (alloy)}}{R} \left(\frac{1}{T} - \frac{1}{T_o} \right) \qquad (44)$$

where N_O is the atom fraction of oxygen dissolved in the liquid alloy at the phase contour temperature T and T_o is the melting point of the alloy.

In the case of pure liquid silver, a change of 100^0 C alters the Sieverts' constant by about 10%. Since at an oxygen pressure of 1 atm., the phase contour temperature for any of the three alloys differ from 1050^0 C by less than 100^0, the values of Sieverts' constant for the three aloys at 1050^0 C and 1 atm. pressure are not expected to be very much different from those at the phase contour temperatures. Therefore, substituting these values for N_O in expression (44), approximate heats of fusion for the three alloys are obtained. These values are given in Table 20.

However, estimates of the heats of fusion of the alloys, at given compositions, can be made from the heats of fusion of pure silver and gold by using the following relation:

$$\Delta H_f \text{ (alloy)} = N_{Ag}\Delta H_f(Ag) + N_{Au}\Delta H_f(Au) + (\Delta H^M(l) - \Delta H^M(s)) \qquad (45)$$

In view of the degree of thermodynamic deviation in the solid and liquid alloys being almost the same, the contribution due to the difference in heats of mixing can be considered negligible. Expression (45), then, becomes,

$$\Delta H_f \text{ (alloy)} = N_{Ag}\Delta H_f(Ag) + N_{Au}\Delta H_f(Au) \qquad (46)$$

The heats of fusion thus calculated are also given in Table 20.

The two sets of heats compare well except those for 40% Au-Ag; a very small error in composition measurements could easily result in such a descrepancy. To verify this, a reverse calculation was made, that is, from the estimated heats of fusion of the alloys, the solubilities of oxygen at the phase contour temperatures and 1 atm. pressure were calculated. These are given in the last column of the Table 20. It is seen again that while the phase contour values of N_O for 10% and 20% Au-Ag are slightly higher than the corresponding values at 1050° C (and which is expected), the phase contour value of N_O for 40% Au-Ag is slightly lower than the value obtained from the limiting slope at 1 atm. and 1050° C.

B. The Interaction Parameter

In a dilute, multicomponent solution of several elements in the solvent, component 1, the activity coefficient of component 2 is expressed by the equation[112],

$$\ln f_2 (N_2, N_3, N_4 \ldots) = \ln f_2^0 + N_2 \epsilon_2^2 + N_3 \epsilon_2^3 + N_4 \epsilon_2^4 \ldots \qquad (47)$$

where $\epsilon_2^3 = \left(\frac{\partial \ln f_2}{\partial N_3}\right)_{N_1 \longrightarrow 1}$ etc. and the derivatives are taken from the limiting case of infinitely dilute solution. The ϵ_i^j's are called interaction parameters.

For convenience, common logarithms are frequently used and concentrations are expressed in weight percentages; this gives the more conventional[113] form of the interaction parameters. For example,

$$\log f_2\ (\%2, \%3, \%4 \ldots) = e_2^2\ \%2 + e_2^3\ \%3 + e_2^4\ \%4 + \ldots \quad (48)$$

where $e_2^3 = \left(\frac{\partial \log f_2}{\partial\ \%3}\right)_{\%1 \rightarrow 100}$ etc.

Neglecting the secondary effects which are usually small, and adopting the infinitely dilute solution as the reference state so that $f_2^0 = 1$, the following expression is obtained:

$$\ln f_2 (N_2, N_3, N_4 \ldots) = N_2 \epsilon_2^2 + N_3 \epsilon_2^3 + N_4 \epsilon_2^4 + \ldots \quad (49)$$

Also, if component 2 obeys Sieverts' Law in the liquid multicomponent alloys, the activity of component 2 in an alloy of fixed composition is proportional to its concentration and $\epsilon_2^2 = 0$. Therefore, for a solution of three components, as considered here,

$$\ln f_2\ (N_2, N_3) = N_3 \epsilon_2^3 \quad (50)$$

$$\text{i.e., } \ln f_0\ (N_0, N_{Au}) = N_{Au} \epsilon_0^{Au} \quad (51)$$

Fig. 30* shows the plots of log f_0 against both weight percentages and atom fractions of gold in the gold-silver alloys. From the limiting slopes the interaction parameters are obtained. These are:

$$\epsilon_0^{Au} = 7.83$$

$$e_0^{Au} = 0.019$$

---

* see Table 21

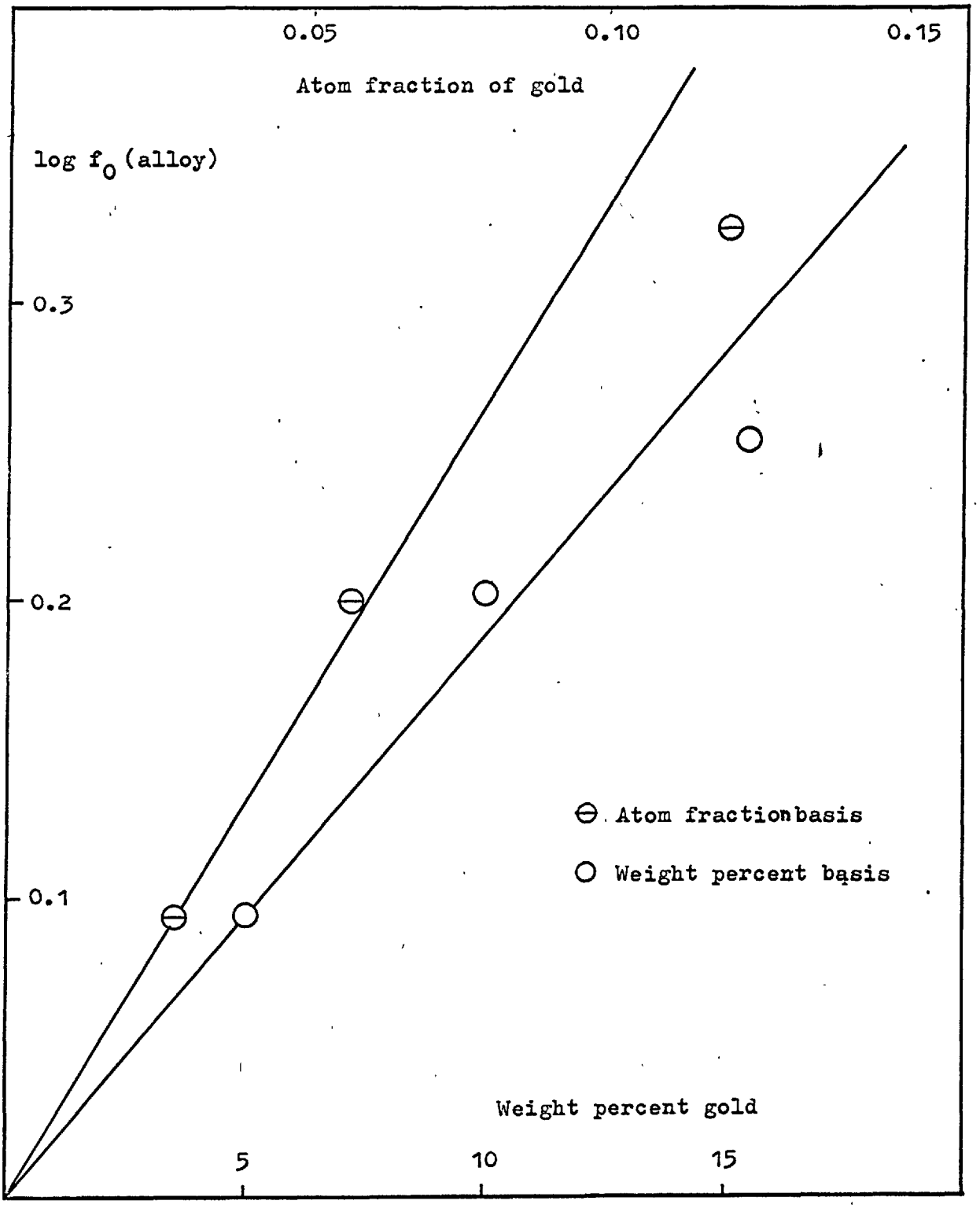

Fig.30 . Plot for the estimation of the interaction parameter.

The interaction parameters reflect both the extra enthalpy and entropy of solution. The positive interaction parameter found here may be attributed to the possible clustering of the two metallic species to the exclusion of the oxygen. The opposite is the case when metallic atoms cluster around those of the non-metal. The interaction parameter $e_O^{Cu} = -0.267$, at 1050^0 C for Cu-Ag-O system[114] illustrate this.

C. The Extra Free Energy of Solution of Oxygen

The standard free energy of solution of oxygen in silver, for the process,

$$\tfrac{1}{2}O_2 = \underline{O} \qquad (52)$$

is given by

$$\Delta G^0 = -3380 + 10.44T \text{ cals.}$$
$$= -RT \ln K = -RT \ln \frac{N_O}{p^{\frac{1}{2}}}.$$

Now if the dissolution of oxygen in the liquid gold-silver alloys is represented as

$$\tfrac{1}{2}O_2 = \underline{O} \text{ (in alloy)} \qquad (53)$$

$$K^a \quad \frac{N_O^a}{p^{\frac{1}{2}}} \qquad (54)$$

and ΔG^a represents the free energy of solution of half a mole of oxygen in the 1 atom per cent solution of oxygen in the alloy, then,

$$\Delta G^a = -RT \ln K^a = -RT \ln \frac{N_O^a}{p^{\frac{1}{2}}} \qquad (55)$$

The extra free energy of solution of oxygen due to the presence of the alloying element is given by

$$G^{xtr} = \Delta G^a - \Delta G^o \qquad (56)$$

$$= -RT \ln \frac{N_O^a}{p^{\frac{1}{2}}} + RT \ln \frac{N_O}{p^{\frac{1}{2}}}$$

$$= -RT \ln \frac{N_O^a}{N_O}$$

$$= RT \ln \frac{N_O}{N_O^a} \qquad (57)$$

Now with the dilute solution as the reference state, the atom fraction of oxygen in silver is equal to its activity and at a given temperature and partial pressure of oxygen, the activity is the same in the Ag-O and in the Ag-Au-O alloys. The expression (57), then, takes the form,

$$G^{xtr} = RT \ln f_O \text{ (in alloy)} \qquad (58)$$

By putting the values of the activity coefficients in expression (58), the extra free energy of solution of oxygen in the three alloys have been calculated. These are given in Table 22.

Table 22

Extra free energies of solution of oxygen in gold-silver alloys at 1 atm. and 1050°C.

N_{Au}	log f_O	Extra free energy (cal.) $G^{xtr.} = RT \ln f_O$
0.0280	0.0927	- 570
0.0574	0.1995	- 1208
0.1205	0.3247	- 1965
0.2674	0.7738	- 4683

Table 23

Heats of solution of oxygen in gold-silver alloys at 1 atm. and 1050°C

N_{Au}	$-\bar{\Delta H}_{Ag(Au-Ag)}$ (cals.)	$-\bar{\Delta H}_{O(Au-Ag)}$ (cals.)
0.0000	0	3380
0.0280	140	3360
0.0574	260	3240
0.1205	480	3020
0.2674	865	2635

D. The Heat of Solution of Oxygen in the Alloy

The heat of solution of oxygen in the alloy, $\Delta\bar{H}^{a}$ and the entropy of solution, ΔS^{a}, can only be obtained with certainly, if measurements are available at a number of temperatures. There are, however, some models[105,115,116] on the basis of which the thermodynamics of solution of a non-metallic solute, X, in a binary metallic solvent, M_1-M_2, can be estimated from the thermodynamic properties of the three binary solutions, namely, M_1-X, M_2-X and M_1-M_2.

One of these models is due to Belton and Tankins[105] and has been applied particularly to the solutions of oxygen in binary metallic solvents. The main assumption in this model is that the dissolved oxygen forms compound species of the type MO and that the amount of the species formed by each metal is proportional to the mole fraction of that metal present in the solution. According to this model, the heat of solution of oxygen in the alloy, for example, is calculated as follows

$$\Delta\bar{H}^{a}_{O(M_1-M_2)} = \frac{N_{M_1O}}{N_O}\left(\Delta\bar{H}_{O(M_1)} - \Delta\bar{H}_{M_1(M_2)}\right) + \frac{N_{M_2O}}{N_O}\left(\Delta\bar{H}_{O(M_2)} - \Delta\bar{H}_{M_2(M_1)}\right) \qquad (59)$$

Where N_O is the total atom fraction of oxygen dissolved in the alloy, N_{M_1O} and N_{M_2O} are the mole fractions of the compound species and are equal to $N_{M_1}N_O$ and $N_{M_2}N_O$ respectively. $\Delta\bar{H}_{O(M_1)}$ and $\Delta\bar{H}_{O(M_2)}$ are the

heats of solution of oxygen in the pure metals and $\Delta\overline{H}_{M_1\,(M_2)}$ and $\Delta\overline{H}_{M_2\,(M_1)}$ are the partial molar heats of mixing in the binary metallic solution at a given composition.

Since oxygen solubility in gold is negligible, for the present Au-Ag-O system, $N_{Au\text{-}O}/N_O$ is zero. Also since, the interactions are only between silver and oxygen, it is assumed that all the dissolved oxygen goes to form compound (Ag_2O) with silver. Therefore expression (59) becomes,

$$\Delta\overline{H}_{O(Au\text{-}Ag)} = \frac{N_{Ag_2O}}{N_O}\left(\Delta\overline{H}_{O(Ag)} - \Delta\overline{H}_{Ag(Au)}\right) \qquad (60)$$

In view of the fact that N_{Ag_2O}/N_O is almost equal to unity when the oxygen content is small, the heat of solution of oxygen in the alloy will be increased by an amount $\Delta\overline{H}_{Ag(Au)}$. The heats of solution calculated from this expression are given in Table 23.

In the absence of data on the effect of temperature on the interaction parameter, ϵ_O^{Au} it is not possible to specify the separate contribution of the extra heat and entropy to the extra free energy of solution of oxygen in the gold-silver alloys. It is, therefore, difficult to comment on the magnitudes of the heats of solution obtained by the use of expression (60). However, Belton and Tankins' model itself has some basic weaknesses. For example, it is difficult to see how two metals having different affinities towards oxygen will form compound species with dissolved oxygen in amounts directly in proportion to their mole fractions. In addition, it suffers from the

limitation that it takes no account of an equilibrium between Ag_2O and free O atoms in the alloy. In these alloys, the effect of preferential "squeeze in" of gold into the silver quasi-lattice would be expected not only to reduce the total oxygen content but also to tend to break up compounds such as Ag_2O.

The above calculations of the heats of solution of oxygen in gold-silver alloys must be considered approximate. Owing to the experimental difficulties even in the case of pure silver the heats of solution of oxygen are approximate (cf. page153) so that it is unlikely that thermogravimetric measurements at different temperatures with the alloys would yield values of $\Delta\overline{H}_O$ of satisfactory precision.

APPENDIX

Appendix 1

Ancillary studies on the effect of nitrogen pressure on the melting point of silver, and oxygen pressure on the melting point of gold :

In contrast to the behaviour with silver, oxygen dissolves to a negligible extent in liquid gold. This is confirmed by the results shown in Table 24 for the effect of oxygen pressure on the melting point of a thin strip of gold. The gold strip was welded to two platinum wires, and the melting temperature was detected electrically by the method described earlier (cf. p. 64). After allowance for an average error of 1.5°, the melting temperatures correspond roughly to those expected from the elevating effect of the mechanical pressure exerted by the gas; any solubility of oxygen is thus exceedingly small. Analogous results for the effect of notrogen pressure on the melting point of silver are also shown in Table 24 and confirm a negligible solubility of nitrogen.

Table 24

Effect of gas pressure on the melting points of gold and silver

Gold		Silver	
Oxygen pressure (atm.)	Temp. (°C)	Nitrogen pressure (atm.)	Temp. (°C)
0	1063	0	961
86.5	1062	365	963.5
139	1065	450	967
228	1067.5		

Appendix 2

Properties of 'high duty' alloys used in the present high pressure equipment.[117]

1. K-Monel (Compressor head, cf. page 48)

Chemical Composition

Ni - 66%

Cu - 30%

Al - 3.5%

Fe - 1.5%

C - 0.20 max.

Other metals - 5% max.

Physical Properties

	Y.S.	Y.P.	% El.	% R.A.	Brin. No.
Heat treated	120,000 to 160,000	80,000 to 120,000	40 to 15	50 to 20	325 to 350

Remarks: Corrosion resistant.

2. Inconel (Inco Chrome Nickel) ['Header' and electrode pin, cf. p. 57]

Chemical Composition

Cr - 11-15%

Ni - 70% maximum

Fe - 10% maximum

Si - 0.5% maximum

C - 0.15% maximum.

Physical Properties

	Y.S.	Y.P.	% l.	% R.A.	Brin. No.
Annealed	80,000 to 95,00	30,000 to 40,000	55 to 45	75 to 65	140 to 140
Cold drawn	100,000 to 115,000	80,000 to 95,000	30 to 20		270 to 280

Remarks: Corrosion resistant; heat and oxidation resistant.

3. Phosphor Bronze (Power input assembly, cf. page 57)

Chemical composition :

Cu	94%
Sn	5.75%
P	0.1%

Physical properties :

	Y. S.	% El.
Hard	80,000	10
Annealed	48,000	60

Remarks :

Wear and abrasion resistant.

Appendix 3

Table 25 a

Detailed data on buoyancy corrections

At 950°C

Press. (p atm.)	Weight of crucible g.	Weight of silver g.	Vol. of cruc. c.c.	Vol. of silver c.c.	Total volume v.cc.	Apparent weight increase W_a g.10^3
16	3.9210	5.0268	0.9850	0.4790	1.464	51.43
25	3.2585	5.0045	0.8187	0.4766	1.295	60.00
40	3.9420	5.0002	0.9905	0.4762	1.467	74.89
60	3.7650	5.0003	0.9460	0.4762	1.422	84.10
100	3.6547	5.0055	0.9183	0.4767	1.395	99.48

At 1050°C

9	3.7200	5.0230	0.9347	0.4784	1.413	35.07
16	3.7200	5.0230	0.9347	0.4784	1.413	46.45
25	3.2585	5.0045	0.8187	0.4766	1.295	53.33
40	4.3070	5.0270	1.0820	0.4788	1.561	66.82
60	3.2812	5.1654	0.8244	0.4919	1.316	80.00

Table 25 b

Detailed data on buoyancy corrections

At 950°C

Press. p atm.	Temp.* t°C	Oxygen density d_t x10³	Oxygen density d_{950} x 10³	$(d_t - d_{950})$ x 10³	Δd . v x 10³	True weight increase $(W_a - \Delta d.v)$ g. x 10³
16	850	5.562	5.107	0.455	0.67	50.76
25	840	8.770	7.980	0.790	1.00	59.00
40	820	14.270	12.770	1.500	2.20	72.69
60	780	22.200	19.200	3.000	4.30	79.80
100	740	38.540	31.960	6.580	9.20	90.28

At 1050°C

p atm.	t°C	d_t. x 10³	d_{1050} x 10³	$(d_t - d_{1050})$ x10³	Δd. v x 10³	$(W_a - \Delta d.v)$ g. x10³
9	880	3.047	2.656	0.391	0.55	34.52
16	850	5.562	4.721	0.841	1.20	45.25
25	840	8.770	7.377	1.390	1.80	51.53
40	820	14.270	11.800	2.470	3.80	63.02
60	780	22.200	17.700	4.500	5.90	74.10

* Temperature at which the initial spring reading was taken.

d = density of oxygen, g./c.c. v = Tptal volume from Table 25a.

Appendix 4

A typical calculation of composition from the spring extension.

i) Basic data:

weight of silver = 5.000 g.

sensitivity of the quartz spring = 1.930cm/g.

spring constant = $\frac{1}{1.93}$ = 0.51813 g/cm.

extension of the spring

= Final spring reading - Initial spring reading

= 11.540 - 11.416

= 0.124 cm.

ii) Total oxygen dissolved = 0.124 x 0.51813 g.

= 0.06425 g.

iii) Weight of oxygen dissolved per g. Ag

= $\frac{0.06425}{5.000}$ = 0.01285 g.

iv) Weight percent oxygen dissolved

= $\frac{0.01285}{1.01285}$ x 100

= 1.269

v) Atom fraction, N_O, of oxygen dissolved is given by

$$N_O = \frac{n_O}{n_{Ag} + n_O}$$

where n. is the number of moles.

Now taking 1 g. Ag

$$n_{Ag} = \frac{1}{108.77} = 9.2696.10^{-3}$$

$$n_O = \frac{0.01285}{16} = 0.8031.10^{-3}$$

$$N_O = \frac{0.8031}{9.2696 + 0.8031} = 0.07973$$

vi) Conversion to N_{Ag_2O} from N_O

$$\frac{1}{N_O} - 2 = \frac{1}{N_{Ag_2O}} \quad .$$

$$N_{Ag_2O} = 0.09484$$

REFERENCES

References

1. Canton, J. : Trans. Roy. Soc. 640 (1762)
2. Hall, J. : Trans. Roy. Soc. Edin. 6, 71 (1812)
3. Perkins, J. : Trans. Roy. Soc. 324 (1819-1820)
4. Amagat, E. H. : C. R. 68, 1170 (1869)
5. Parsons, C. A. : Proc. Roy. Soc. 44, 320 (1888)
6. Parsons, C. A. : Proc. Roy. Soc. 79, A 532 (1907)
7. Tammann, G. : Z. Phys. Chem. 11, 676 (1893)
8. Bridgman, P. W. : 'The Physics of High Pressure', Bell and Sons, London. (1931)
9. Paul, W. and Warschauer, D.M. (ed.) : 'Solids under pressure', Mc Graw-Hill (1963)
10. Bradley, R.S. (ed.) : 'High Pressure Physics and Chemistry', Acad. Press,Lond. (1963)
11. Gschneider, K.A., Hepworths, M.T. and Parlee, N.A.D. (ed.) : 'Metallurgy at High Pressures and High Temperatures', Gordon and Breach Sci.Publishers, London (1964)
12. Weale, K.E. : 'Chemical Reactions at High Pressures', Spon, London. (1967)
13. Richardson, F. D. and Jeffes, J.H.E. : J.Iron Steel Inst. 160, 261 (1948)
14. (i) Elliott, J.F. : 'The Physical Chemistry of Steelmaking', The Technology Press, The M.I.T. and John Wiley and Sons, New York (1958)

14. (ii) Elliott, J.F. and Gleiser, M. (ed.) 'Thermochemistry for Steelmaking', Vol. I, Addison-Wesley Pub. Co. (1960)

(iii) Elliott, J.F., Gleiser, M. and Ramakrishna, V. : 'Thermochemistry for Steelmaking' Vol. II, Addison-Wesley Pub. (1963)

15. Derge, G. (ed.): 'Basic Open Hearth Steelmaking', Am. Inst. Min. Met. Pet. Engineers, New York (1964)

16. Smithells, C.J. : 'Gases and Metals', Chapman and Hall, p - 175 (1937), p- 175

17. Hanson, D., Marrayat, C. and Ford, G.W.: J. Inst. Met. 30, 197 (1923)

18. Vogel, P. and Pocher, W. : Z. Metallk. 21, 333 (1929)

19. Allen, N.P. and Street, A.C. : J. Inst. Met. 51, 233 (1933)

20. Rhines, F.N. and Mathewson, C.H. : Trans. A.I.M.E. 111, 337 (1934)

21. Phillips, A. and Skinner, E.N. : Trans. A.I.M.E. 143, 301 (1941)

22. Clasing, M. and Sauerwald, F. : Z. anorg. u. allegem. Chem. 271, 81 (1952)

23. Lucas, M.S. : Ann. Chemie et Phys. 12(11), 402 (1819)

24. Chevillot, M. : Ann.Chemie et Phys. 13(11), 299 (1820)

25. Graham, T. : Phil. Meg., (london). 32, 503 (1861)

26. Hamp. W. : Chem. Centralblatt 378 (1875)
: Polytech. Jnl. 489 (1875)

27. Heyn, E. : Z. anorg. Chem. 39, 1 (1904)

28. Slade, R.E. and Farrow, F.D. : Proc. roy. Soc. 87 A , 524 (1912)

29. Roberts, H.S. and Smith, F.H. : J. Am. Chem Soc. 137 , 1061 (1921)

30. Stockdale, D. : J. Inst. Met. 43, 159 (1930)

31. Randall, M., Nielsen, R.F. and West, G.H. : Ind. Eng. Chem. 23, 3881 (1931)

32. Girardi, D.J. and Siebert, C.A. : Trans. A.I.M.E. 188, 1168 (1950)

33. Sano, K. and Sakao, H. : J. Japan Inst. Met. 19 , 431 (1955)

34. Sano, K. and Sakao, H. : ibid 19 , 435 (1955)

35. Young, D.R.: London University Ph. D. Thesis (1965)

36. Toop, G.W. : Lond. Univ. Ph.D. Thesis (1963)

37. Hofmann, W. and Schneider, H.J. : Giesserei Tech. - Wiss. Beih. Giesserei w. u. Metallk. 28, 1567 (1960)

38. Belton, G.R. and Tankins, E.S. : Private communication

39. Mcdonald, D. : ' The History of Silver' in 'Silver : Economics, Metallurgy and Use', edited by A. Butts and C.D. Coxe, D. Van Nostrand Co. (1967)

40. Dumas : Compt. rend. 86 , 68 (1878)

41. Steacie , E.W.R. and Johnson, F.M.G. : Proc. Roy. Soc. A 112, 542 (1926)

42. Simons, J.H. : J. Phys. Chem. 36, 652 (1932)

43. Domański, W. : Arch. Hutnictwa 3 , 81 (1958)

44. Eichenauer, W. and Muller, G. : Z. Metallk. 53 , 321 (1962)

45. Podgurski, H.H. and Davies, F.N. : Trans. Met. Soc. A.M.I.E. 230 , 731 (1964)

46. Chaston, J.C. : J.Inst. Metals 71 , 23 (1945)

47. Klein, M.J. and Huggins, R.A. Trans. Met. Soc. A.M.I.E. 224 , 903 (1962)

48. Le Chatelier : Z. physic. Chem. 1 , 516 (1887)

49. Lewis, G.N. : J. Am. Chem. Soc. 28 , 139 (1906)

50. Keyes, F.G. and Hara, H. : J. Am. Chem. Soc. 44 , 479 (1922)

51. Benton, A.F. and Drake, L.C. : J. Am. Chem. Soc. 54 , 2186 (1932)

52. Otto, E.M. : J. Electrochem. Soc. 113(7),643(1966)

53. Chevillot, M. : Ann. chim. Phys. 13 , 299 (1820)

54. Gay Lussac : Ann. chim. Phys. 45 , 221 (1830)

55. Sieverts, A. and Hagenacker, J. : Z. phys. Chem. 68 , 115 (1909)

56. Donnan, F.G. and Shaw, T.W.A. : J. Soc. Chem. Ind. 29 , 987 (1910)

57. Parlee, N.A.D. and Sacris, E.M. : Trans. Am . Inst. Min. Engrs. 233, 1918(1965)

58. Diaz, C.M., Masson, C . R. and Richardson, F.D. : Trans. Instn. Min. Metall. 75, C 183 (1966)

59. Allen, N.P. : J. Inst. Metals 49 , 317 (1932)

60. Vacher, H.C. : 'Metals Handbook' (1948) p.1151

61. Chaston, J.C. : 'Oxygen in Silver' in 'Silver : Economics, Metallurgy and Use', edited by A. Butts and C.D. Coxe ; D. Van Nostrand and Co. (1967) p. 304

62. Baker, E. H. and Johnstone, J.K. : Nature 205 , 65 (1966)

63. Report of the Committee on Gas Cylinders : H. M. S. Office (1921)

64. Luth, W. C. and Tuttle, O.F. : American Mineralogist 48 , 1401 (1963)

65. 'Symposium on the effect of temperature on the properties of materials'. American Soc. Mech. Eng. and Am. Soc. for Testing Materials (1932)

66. Morley, A. : 'Strength of Materials', Longmans Green (1913) p. 303

67. Newitt, D.M. : 'Design of High Pressure Plant and the Properties of Fluids at High Pressures'; Clarendon Press,Oxford (1940)

67 a. Dodge, B.F. :'High Pressure Technique' in Chemical Engineers' Hand Book edited by J. H. Perry; Mc Graw Hill (1950) p. 1234

68. Hamann, S.D. : 'Physico-Chemical Effects of Pressure'; Butterworth Sci. Pub. (1957) p. 9

69. Macrae : 'Overstrain of Metals and its application to Autofrettage Process of Cylinder and Gun construction'; H.M.S. Office, London (1930)

70. Bridgman, P.W. : 'The Physics of High Pressure'; Bell and Sons, London. (1958)

71. Adams, L.H., Williamson, E.D. and Johnston, J. : J. Am. Chem. Soc. 41 , 12 (1919)

72. Goranson, : Am. J. Sci. 222 , 481 (1931)

73. Birch, : Physical Review 41 , 641 (1932)

74. Lazarre, F., Saurel, J.R. and Voder, B. J. Res. C. N. R. S. Bellevue 5 (26), 320 (1954)

75. Gugan, D. : J. Sci. Instr. 33 , 160 (1956)

76. Paul, W., Benedek, G.B. and Warschauer, D.M. : Rev. Sci. Instr. 30 , 874 (1959)

77. Balain, K.S. and Bergeron, C.J. : Rev. Sci. Instr. 30 , 1058 (1959)

78. Smyth, F.H. and Adams, L.H. : J. Am. Chem. Soc. 45, 1167 (1923)

79. Honda, K. : Sci. Rept. Tohoku Univ. 4 , 97 (1915)

80. Coats, A.W. and Redfern, J.P. : Analyst 88 , 906 (1963)

81. Bartlett, E.S. and Williams, D.N. : Rev. Sci. Instr. 28 , 919 (1957)

82. Holley, J.G. : Can. J. Chem. 35 , 374 (1957)

83. Pope, M.I. : J. Sci. Instr. 34 , 229 (1957)

84. Rbatin, J.G. and Card, C.S. : J. Am. Chem. Soc. 31 , 1689 (1959)

85. Biermann, W.J. and Heinrichs, M. : Can. J. Chem. 40 , 1361 (1962)

86. Baker, E.H. : J. Chem.Soc. 339 (1963)

87. McKewan, W. and Martin Fassel (Jr.),W.: Trans. A.I.M.E. 197, 1127 (1953)

88. Emich, F. : Monatsh 36 , 436 (1915)

89. McBain,J.and Bakr,A.: J.Am.Chem.Soc. 48 , 690 (1926)

91. Madorsky, S.L., in 'Vacuum Microbalance Techniques, Vol. 2', edited by R.F. Walker; Plenum Press, New York (1962) p. 47

92. Anderson, P.G. and Horloch, R.F. : Trans. Farad. Soc. 58, 1993 (1962)

93a. Baker, E.H. : J. Chem. Soc. 464 , (1962)

b. Baker, E.H. : ibid. 339 , (1963)

94. Alcock, C.B. : Platinum Metals Rev. 134 , (1961)

95. Fox, E.G. and Esdaile, R.J. : Acta Met. 11 , 1363 (1963)

96. Lowe, R.M. : Acta Met. 12 , 1111 (1964)

97. Esser, H. and Eusterbrock, H. : Arch Eisenhüttenw 14 , 341 (1941)

98. Kirschenbaum, A.D., Cahill, J.A. and Grosse, A.V. : J. Inorg. Nucl. Chem. 24 , 333 (1962)

99. Hilsenrath, J., Beckett, C.W., Benedict, W.S., Fano, L., Hoge, H.J., Masi, J.F., Nuttall, R.L., Touloukian, Y.S. and Woolley, H.W. : 'Tables of Thermal Properties of Gases'; N.B.S. Circular, 564. (1955) p. 388

100. Hennig, H. : Erjmetall 8 , 117 (1955)

101. Kordes, E. : Z. Anorg. Chem. 154, 93 (1926)

102. Baker, E.H. and Richardson, F.D. : Trans. Instn. Min. Metall. 75 , C 147 (1966)

103. Oriani, R.A. and Alcock, C.B. : Trans. Met. Soc. A.I.M.E. 224 ,1104 (1962)

104. Erimenko, V.M. and Naidich, Yu. V. : Report of the Institute of Metalceramics and Special Alloys, Acad. Sci.,Ukr.SSR (1961) p. 100

105. Belton, G.R. and Tankins, E.S. : Trans. Met. Soc. A.I.M.E. 233 , 1892 (1965)

106. Libowitz, G.G. on 'Nonstoichiometry in Chemical Compounds' in 'Progress in Solid State Chemistry - Vol. 2', edited by H. Reiss; Pergamon Press (1965) p. 216

107. Heikes, R.R. and Johnston, W.D. : J. Chem. Phys. 26 , 582 (1957)

108. van Daal , H.J. and Bosman, A.J. : Phys. Rev. 158(3),736(1967)

109. O'Keeffe, M. and Moore, W.J. : J. Chem. Phys. 35 , 1324 (1961)

110. Hultgren, R., Orr, R.L., Anderson,P.D. and Kelley, K.K. : 'Selected Values of Thermodynamic Properties of Metals and Alloys'; John Wiley and Sons, N.Y. (1963) p. 341

111. Wagner, C. : Acta Met. 2 , 242 (1954)

112. Wagner, C. : 'Thermodynamics of Alloys'; Addison-Wisley Pub. Co., Mass. (1952) p. 51

113. Sims, C.E. (ed.) : 'Electric Furnace Steelmaking - Vol. II'; Intersci. Pub. (1963) p. 120

114. Parlee, N.A.D. and Sacris, E.N. : Trans. Met. Soc. A.I.M.E. 239, 2005 (1967)

115. Alcock, C.B. and Richardson, F.D. : Acta Met. 6 , 385 (1958)

116. Alcock, C.B. and Richardson, F.D. : Acta Met. 8 , 882 (1960)

117. Woldman, N.E. and Metzler, R.J. : 'Engineering Alloys'; Am. Soc. for Metals. (1936), Revised ed.1945